The behaviour of metamorphic apatite in mid-amphibolite to granulite facies metapelites and metapsammites: insights from the Stafford Member of the Arunta Region, Australia

Thesis submitted in accordance with the requirements of the University of Adelaide for an Honours Degree in Geology

Thomas William Baggs

November 2017

THE UNIVERSITY of ADELAIDE

THE BEHAVIOUR OF METAMORPHIC APATITE FROM MID-AMPHIBOLITE TO GRANULITE FACIES METAPELITES AND METAPSAMMITES: INSIGHTS FROM THE STAFFORD MEMBER FROM THE ARUNTA REGION, AUSTRALIA

RUNNING TITLE: THE BEHAVIOUR OF METAMORPHIC APATITE

ABSTRACT

The chemical behaviour of metamorphic apatite was investigated in a quasi-unchanging rock composition to gain insight into the stability of apatite and distribution of heat production in the continental crust. Samples of two rock types were collected from the Stafford Member: metapelites and metapsammites, that record calculated metamorphic conditions from mid-amphibolite facies (~ 2.1 kbar, 590 °C) to granulite facies (~ 3.9 kbar, 800 °C) conditions. The chemical compositions, petrographic relationships and abundances of accessory phosphate minerals were investigated as a function of metamorphic grade, with a focus on the relationship between apatite and monazite, both of which increase in abundance with metamorphic grade. At mid-amphibolite facies metamorphic conditions, apatite growth is driven by the partial consumption of accessory xenotime and complete consumption of low-grade allanite and detrital apatite (Reaction 4). At upper-amphibolite facies conditions, apatite growth is driven by the partial breakdown of xenotime and plagioclase (Reaction 5). Additionally, apatite was found to be intimately linked with the breakdown of biotite and muscovite micas at all metamorphic conditions (Fig. 3 & 5), as they supply the F, Cl and OH component required for apatite growth. Granulite facies monazite growth is facilitated by the dissolution of apatite (Fig. 9) and the breakdown of xenotime (Reaction 2). However, as the major reservoir for P_2O_5 in the samples, the stability and high abundance of apatite at granulite facies conditions (Figures 10, 5e, 5f, 3c, 3d) is enhanced by the enrichment of P_2O_5 in residual samples (Table 2). Furthermore, during partial melting, heat producing elements U + Th preferentially remain in monazite relative to apatite and the melt, therefore the melt and apatite is relatively depleted in HPEs. Consequently, melt loss of HPE depleted segregates could enrich HPEs in the residual, partially melted monazite bearing rocks of the Stafford Member.

KEYWORDS

apatite, monazite, HPEs, REEs, metamorphism, geochemistry

TABLE OF CONTENTS

LIST OF FIGURES AND TABLES

INTRODUCTION

Apatite [$(Ca,Y,REE,Th,U)_5(PO_4)_3(F,Cl,OH)$] is an abundant accessory phosphate mineral found in metamorphic rocks of all grades and most compositions (Spear and Pyle, 2002). Apatite and other common accessory minerals such as monazite, xenotime and zircon typically contain 80 to 90% of total rock rare earth elements (REEs), uranium, thorium and yttrium (Bea and Montero, 1999; Rubatto et al., 2006). In addition, apatite typically incorporates a significant amount of F and Cl in its crystal structure (Marks et al., 2012). U and Th are commonly and widely used for geochronology and are two of the major radiogenic heat producing elements in Earth's crust (Korenaga, 2011) and halogens F and Cl are key complexing agents for ore genesis (e.g. Aiuppa et al., 2009; Mathez and Webster, 2005). Therefore, apatite and other U–Th–bearing accessory minerals are essential to quantifying the timing of tectonic events, the vertical distribution of crustal heat production and the distribution of REEs, F and Cl with metamorphic grade. Quantification of these characteristics requires knowledge of how common accessory minerals distribute Y + REE + Th + U + F + Cl as a function of depth, temperature (i.e. metamorphic grade) and rock composition. To that end, apatite and other accessory minerals have been studied extensively in numerous metamorphic systems to develop a better understanding of their parageneses and textural relationships (e.g. Bea and Montero, 1999; Gasser et al., 2012; Kim et al., 2009; Kohn and Malloy, 2004; Spear, 2010; White et al., 2003). However, studies focused on the compositional variation of apatite through changing metamorphic grade are few; even fewer are studies that investigate apatite composition in a single quasi-unchanging rock composition (Spear and Pyle, 2002). Variable rock composition across metamorphic grade has the potential to mask changes to the solid

solution composition of accessory minerals as a function of metamorphic grade, particularly if the changes are subtle. For this reason, studying the changes to apatite composition within a quasi-unchanging rock composition is ideal.

Mount Stafford, Australia, is a rare location that preserves metamorphosed metasediments of quasi-unchanging composition (Greenfield et al., 1996) and is thus suited for investigating the impact of metamorphism on the composition of apatite and other accessory minerals. The region outcrops a low-pressure, high-temperature sequence of metasediments—the Stafford Member—that transitions from mid-amphibolite to granulite facies metamorphic grade over a horizontal distance of ~10km (Rubatto et al., 2006). More importantly, the Stafford Member is characterised as a metamorphosed sequence of interbedded pelites and psammites that occurs through and defines the entire metamorphosed zone (Claoue´-Long et al., 2008). In the context of investigating the chemical changes that occur to accessory minerals, this is useful in two ways: 1) the protolith composition in the granulite facies zone is effectually identical to the protolith composition of the mid-amphibolite facies zone (Greenfield et al., 1996) and 2) the interbedded nature of the protolith provides two different compositions to study (see Table 2).

The goal of this project is to quantify the abundance and composition of apatite in the Stafford Member samples of varying peak metamorphic grade, in order to constrain the reaction relationships and thus the metamorphic response of apatite in the context of other accessory minerals such as monazite and xenotime. Mineral composition data will be collected by means of MLA, EPMA and LA–ICP–MS analysis. Ultimately, the outcomes of this project are several apatite and monazite

involving mineral reactions, implications for the distribution of crustal heat production and implications for the overall stability of apatite in the continental crust.

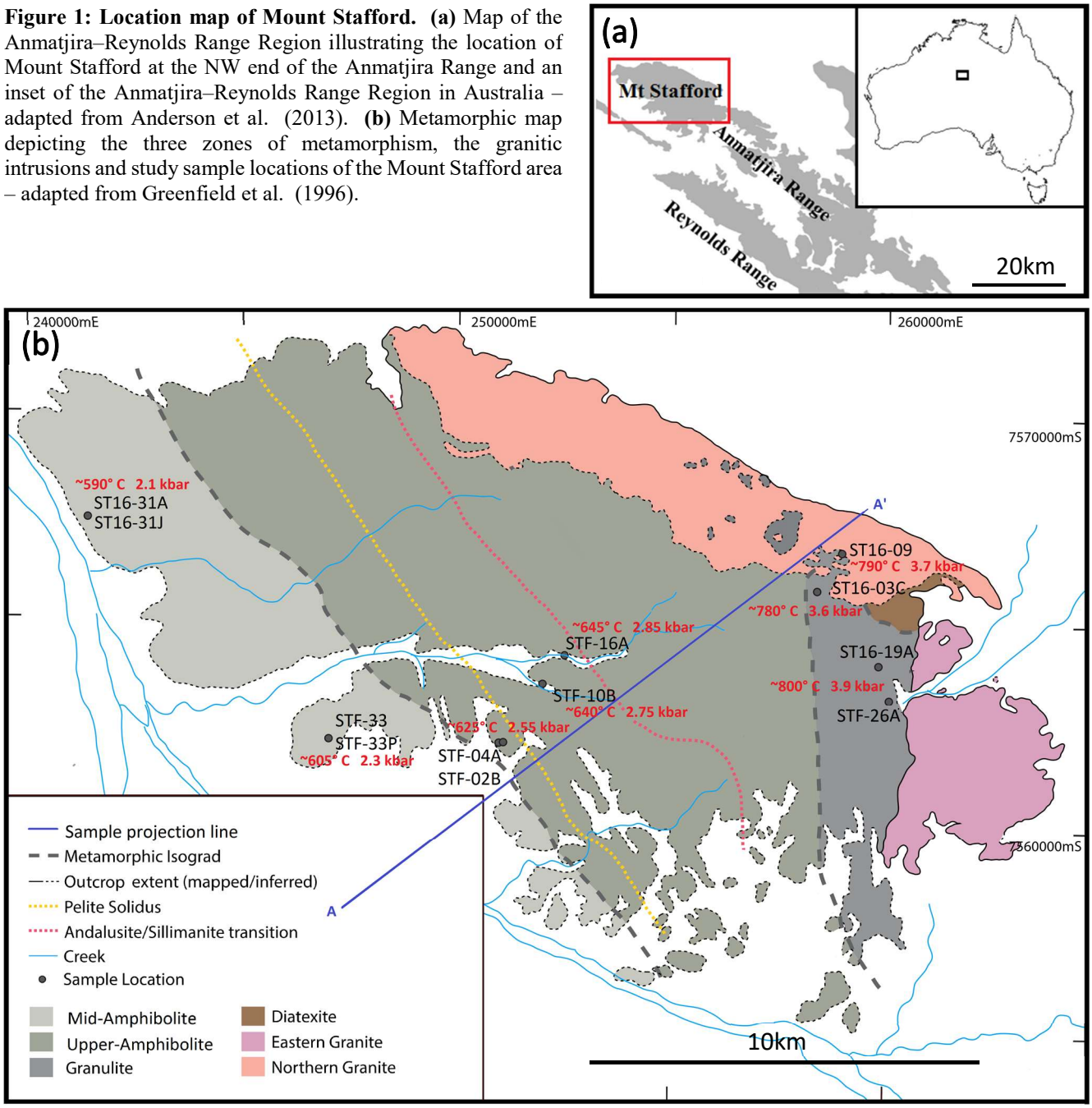

Figure 1: Location map of Mount Stafford. **(a)** Map of the Anmatjira–Reynolds Range Region illustrating the location of Mount Stafford at the NW end of the Anmatjira Range and an inset of the Anmatjira–Reynolds Range Region in Australia – adapted from Anderson et al. (2013). **(b)** Metamorphic map depicting the three zones of metamorphism, the granitic intrusions and study sample locations of the Mount Stafford area – adapted from Greenfield et al. (1996).

GEOLOGICAL SETTING

Mount Stafford is located at the NW end of the Anmatjira–Reynolds Range in the Arunta region of central Australia (Fig. 1). This region comprises outcrop of the oldest sedimentary sequence in the Arunta Inlier: The Lander Formation (Scrimgeour, 2013), which is separated from the overlying Reynolds Range Group by an unconformity (Greenfield et al., 1996; Vry et al., 1996, Stewart et al., 1984). The Lander Formation has a maximum deposition age of c. 1868 Ma (Claoué-Long et al., 2008) and was intruded by granitic and mafic rocks during the c. 1810–1790 Ma Stafford and c. 1790–1770 Ma Yambah events (Howlett et al., 2015). Mount Stafford comprises outcrop of three major rock types: metamorphosed interbedded psammites and pelites, granitic intrusions and mafic amphibolites and granulites, primarily consisting of the former, named the Stafford Member (Greenfield et al., 1996). The Stafford Member is considered part of the Lander Formation due to similar ages of detrital zircons, with a maximum deposition age of c. 1858 Ma (Claoué-Long et al., 2008). Large intrusive bodies to the north and east of the Stafford Member are respectively named northern and eastern Stafford Granites (Greenfield et al., 1998; 1996) with crystallisation ages of c. 1805–1802 Ma (Rubatto et al., 2006).

The metamorphic sequence at Mount Stafford increases from mid-amphibolite facies (~ 2.1 kbar, 590 °C) to granulite facies (~ 3.9 kbar, 800 °C) over approximately 10 km from the SW to NE of the region (White et al., 2003). Such a thermal gradient (~75 °C per vertical kilometre) is characteristic of a high metamorphic gradient where temperature is the dominant control (Wang et al., 2014). This notion coupled with the estimated ages of the Stafford Granite suggests that a contact metamorphic aureole

formed during the Stafford event because of the intruding Stafford Granites and therefore is proposed to be responsible for local metamorphism of the Stafford Member (Howlett et al., 2015; Hand and Buick, 2001; Vernon et al., 1990). Heating during this event was argued to have occurred relatively quickly (in less than 20 m.y.) because the ages between peak metamorphism in sub-solidus and supra-solidus rocks are indistinguishable within uncertainty (Rubatto et al., 2006). Because the exposed beds show mid-amphibolite through to granulite facies metamorphism there are also concomitant variations in the metamorphic mineral assemblages through metamorphic grade (Table 1). However, the protolith itself was proposed to be compositionally homogeneous across the study area (Greenfield et al., 1996). Consequently, the Stafford Member is ideal for the purposes of this project.

ANALYTICAL METHODS

Samples and Petrography

Twelve representative samples from Mount Stafford (Fig. 1b) were selected from a larger sample set for an equal contribution (six each) of metapelite and metapsammite from mid-amphibolite, upper-amphibolite and granulite facies conditions. Thin sections were prepared by Adelaide Petrographics and Continental Instruments (India) for each sample, then carbon coated at Adelaide Microscopy in preparation for imaging with a scanning electron microscope and mineral analyses with an electron microprobe. A Nikon optical microscope was used for petrographic analyses. Full methods detailed in Appendix A.

Whole Rock Geochemistry (WRG)

The whole-rock geochemistry for each sample was obtained from Franklin and Marshall College in Pennsylvania, USA. Samples were powdered then elements were analysed by fusing a 0.4 g portion of the powdered sample with lithium tetraborate for analysis by X-Ray Fluorescence following methods of Boyd and Mertzman (1987).

Mineral Liberation Analysis (MLA)

Back scattered electron (BSE) image maps and mineral liberation analysis (MLA) maps (Appendix D) of each polished thin section were acquired using a FEI Quanta 600 scanning electron microscope at Adelaide Microscopy. BSE maps were acquired for reference in petrography, LA–ICP–MS and EPMA. BSE and MLA maps show the location of accessory minerals and were used to estimate their abundance in thin section. Full methods detailed in Appendix A.

Electron Probe Micro-analysis (EPMA)

Major element data was collected using electron probe microanalysis (EPMA) on monazite, apatite, Fe–Ti oxides and silicate minerals in each sample using a Cameca SXFive electron microprobe with an accelerating voltage of 15 kV and beam current of 20 nA. Elements that were measured for apatite and monazite include: Ca, Mg, Ti, Si, Al, Fe, Mn, Cl, F, La, Ce, Nd, K, P, Na, S, As, Sr and Y (+ U and Th in monazite). Elements measured for silicates and Fe–Ti oxides were: Ca, Mg, Ti, Si, Al, Fe, Mn, Cr, Cl, F, K, P, Na, Ba, V, Zn, Zr and Sr. Xenotime, thought present in the samples were not analysed by EPMA due to time limitations. Data calibration and reduction was carried out in Probe for EPMA, distributed by Probe Software Inc. Poor and contaminated analyses were found and removed from the dataset by using cation calculation spreadsheets and monitoring K, Mg, Al and Si concentrations for apatite and monazite. Full methods detailed in Appendix A.

LA–ICP–MS, Trace Element Chemistry and U–Pb Geochronology

Laser Ablation–Inductively Coupled Plasma–Mass Spectrometry (LA–ICP–MS) isotopic and trace element analyses were undertaken on apatite, monazite, Fe–Ti oxides and various silicate minerals using an ASI M-50-LR 193 nm excimer laser in a He ablation atmosphere coupled to an Agilent 7700cx ICP–MS. Isotopes measured for geochronology were ^{202}Hg, ^{204}Pb, ^{206}Pb, ^{207}Pb, ^{208}Pb, ^{232}Th and ^{238}U. Trace element isotopes measured concurrently with the geochronology isotopes were ^{29}Si, ^{31}P, ^{43}Ca, ^{89}Y, ^{90}Zr, ^{139}La, ^{140}Ce, ^{141}Pr, ^{146}Nd, ^{147}Sm, ^{153}Eu, ^{157}Gd, ^{159}Tb, ^{163}Dy, ^{165}Ho, ^{166}Er, ^{169}Tm, ^{172}Yb and ^{175}Lu. Each analysis was pre-ablated with five laser pulses to remove any surface contamination. Apatite was ablated for 40 seconds after a hold time of 30 seconds using a spot size of 13 microns and fluence of 2.0 J/cm^2. Monazite was ablated

for 30 seconds after a hold time of 30 seconds using a spot size of 13 microns and fluence of 2.0 J/cm^2. Silicate minerals and Fe–Ti oxides were ablated for 50 seconds after a hold time of 30 seconds, using a spot size of 29 microns and fluence of 3.5 J/cm^2. Data reduction for both trace elements and geochronology was carried out by utilizing the Iolite software package (v3.31) (Paton et al., 2011). Instrument drift was corrected by standard–sample bracketing every 15 (monazite) to 20 (silicate and apatite) analyses. Element fractionation bias was corrected by calibration performed on certified synthetic and natural mineral standards from Astimex Ltd and P&H Associates, specifically MAdel standard for monazite. Geochronology calibration accuracy was determined on monazite using internal Ambat and 94-222/Bruna-NW standards. NIST610 and NIST612 glass were used as a standard for the trace element composition of monazite, apatite and silicates. Age data were plotted using Isoplot 3.75 (Ludwig, 2012). Trace element concentrations for each mineral analysis were measured and tabulated in parts per million (ppm) by using major element data from electron probe microanalyses as an internal standard. Full methods detailed in Appendix A.

RESULTS & OBSERVATIONS

Samples and Petrography

All twelve samples of the Stafford Member (Fig. 1b) have unique mineralogical and microstructural characteristics that are linked directly to the protolith composition and the *P–T* conditions at which metamorphism was recorded. Grain size is the major difference between the metapelite and metapsammite samples, which are distinguished based on the whole rock SiO_2 - Al_2O_3 ratio. Whereas the abundance of k-feldspar and the presence of plagioclase are the major variances between mid-amphibolite and granulite facies samples. The metamorphic grade of each sample was determined based on *P–T* values calculated from a study by White et al (2003) by using a projection line on Figure 1b.

Table 1: Primary mineralogy and inferred peak metamorphic grade of all Stafford Member samples. *Peak metamorphic grade inferred from P–T values calculated by White et al. (2003) and preserved mineralogy (presented below). ^Andalusite highly fractured and rare. Mineral abbreviations as per Holland & Powell (2011).

Sample Number	Mineralogy (relative abundance) Highest to Lowest	Unit	Metamorphic Grade*	
ST16-31J	bi–q–and–mu–ilm	Pelite	Mid-amphibolite	Increasing Metamorphic Grade ↓
STF-33P	mu–bi–q–ksp–mt	Pelite	Mid-amphibolite	
STF-02B	ksp–bi–and–q–mu–ilm	Pelite	Upper-amphibolite	
STF-16A	ksp–cd–bi–q–and–sill–ilm	Pelite	Upper-amphibolite	
ST16-09	ksp–sill–cd–bi–pl–q–ilm ± saph	Pelite	Granulite	
ST16-19A	ksp–cd–sill–bi–q–pl–ilm	Pelite	Granulite	
ST16-31A	q–bi–ksp–mu	Psammite	Mid-amphibolite	Increasing Metamorphic Grade ↓
STF-33	q–bi–mu–ilm	Psammite	Mid-amphibolite	
STF-04A	q–mu–bi–ksp–ilm	Psammite	Upper-amphibolite	
STF-10B	q–ksp–cd–pl–bi–sill–ilm	Psammite	Upper-amphibolite	
ST16-03C	q–ksp–bi–pl–sill–ilm ± and^	Psammite	Granulite	
STF-26A	ksp–cd–bi–sp–g–q–ilm	Psammite	Granulite	

METAPELITES

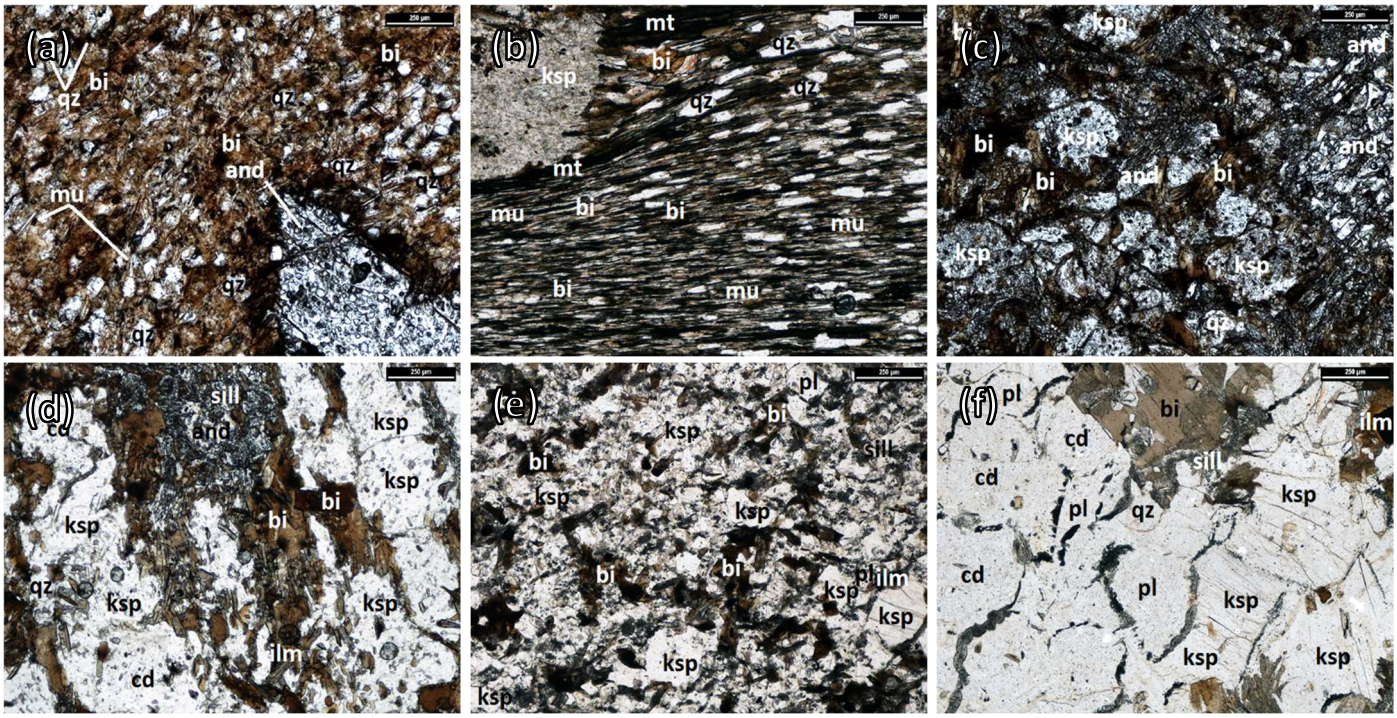

Figure 2: Representative petrographic photomicrographs of the metapelite thin sections (PPL). Scalebar is 250µm in all photomicrographs. Preserved mineralogy detailed in Table. 1. (a) ST16-31J. (b) STF-33P. (c) STF-02B. (d) STF-16A. (e) ST16-09. (f) ST16-19A.

Sample ST16-31J

Sample ST16-31J is very fine-grained, comprised of co-dominant quartz and biotite, sub-dominant muscovite, and very large poikiloblasts of andalusite (Fig. 2a). Biotite and muscovite are generally fine-grained and define a strong fabric, but when in direct contact with the margins of andalusite are coarser-grained and un-oriented. Inclusions contained within andalusite are predominantly very fine-grained quartz. Apatite is quite scarce in this sample and is only found as tiny (<10 µm) inclusions in porphyroblastic andalusite. Monazite is quite abundant in this sample commonly as inclusions in poikiloblastic andalusite. Ilmenite is present in low abundance and occurs together with coarse biotite on the edges of andalusite porphyroblasts.

Sample STF-33P

Sample STF-33P is very fine-grained, comprised of dominant muscovite and biotite, sub-dominant quartz with large porphyroblasts of k-feldspar (Fig. 2b). Fine-grained biotite and muscovite comprise ~80% of the rock and define a strong fabric. The k-feldspar is uncharacteristically poikiloblastic with minor inclusions of quartz and magnetite. Apatite is virtually non-existent in this sample with very few (<5 μm) inclusions in k-feldspar (too small to analyse by LA–ICP–MS). Monazite is relatively scarce in this sample. This is the only sample in the set that contains magnetite rather than ilmenite, commonly observed as euhedral, rectangular shaped grains.

Sample STF-02B

Sample STF-02B is fine-grained with co-dominant k-feldspar and biotite, sub-dominant quartz and accessory muscovite and andalusite (Fig. 2c). There is a lack of observable fabric in this sample as the micas are un-oriented. K-feldspar is present as both microcline and anorthoclase. Andalusite is present as skeletal poikiloblasts with abundant quartz inclusions. Muscovite is mantled by biotite grains. Apatite is more abundant in this sample and commonly occurs in contact with biotite and muscovite. Monazite is quite scarce and often located in the proximity of fractured andalusite. Ilmenite is common in this sample, but very fine-grained and is commonly in contact with k-feldspar or andalusite.

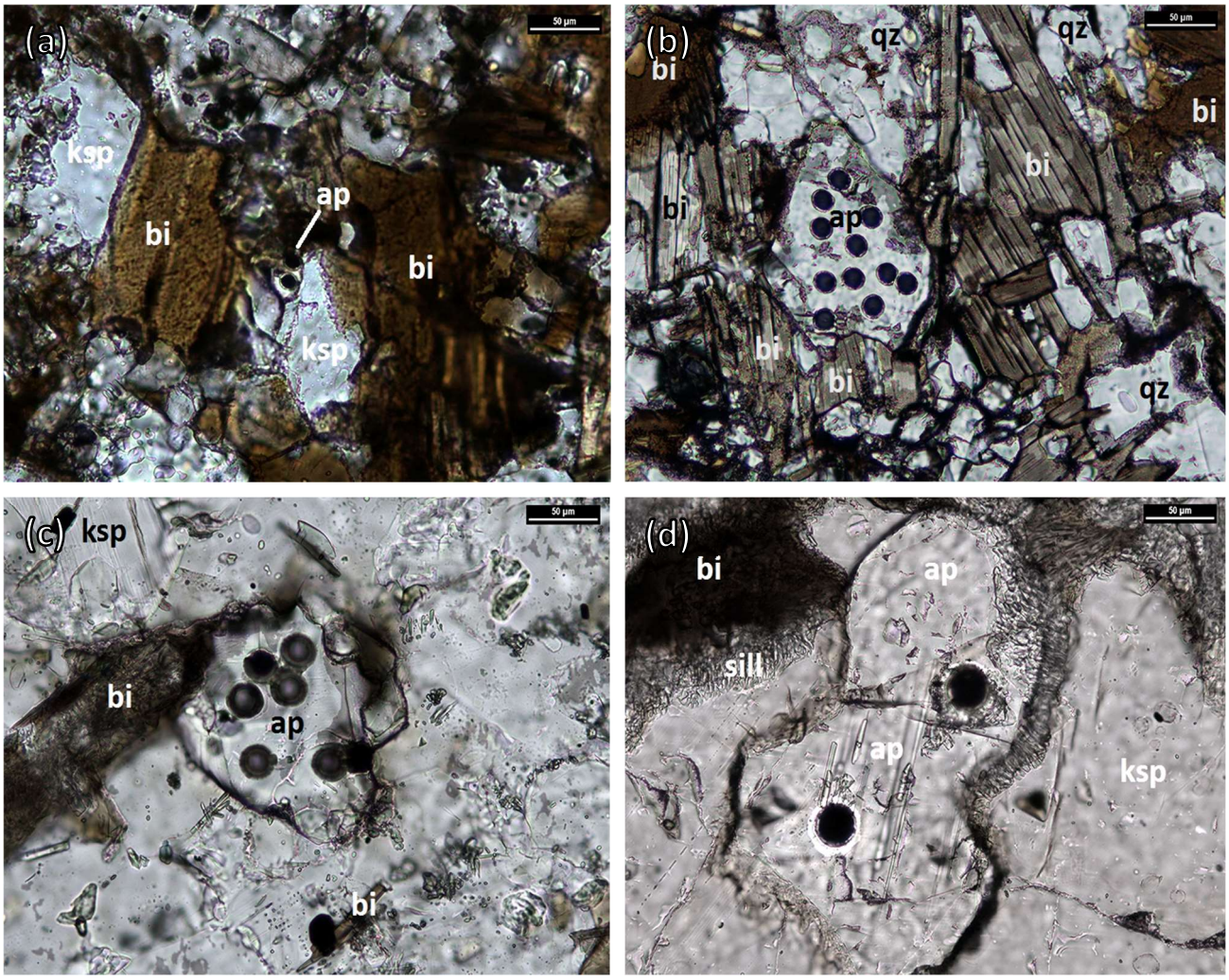

Figure 3: Photomicrographs of key petrographic relationships between accessory apatite and other minerals in metapelite samples. Scalebar is 50µm in all photomicrographs. Photomicrographs for ST16-31J and STF-33P are not presented as apatite within these samples were not analysed due to their size of <5 µm. In these photomicrographs, apatite is in contact with biotite or muscovite in all four samples. (a) STF-02B. (b) STF-16A. (c) ST16-09. (d) ST16-19A.

Sample STF-16A

Sample STF-16A is fine to medium-grained, comprised of dominant k-feldspar, sub-dominant biotite and cordierite and accessory sillimanite and andalusite (Fig. 2d). No fabric is observed. Andalusite poikiloblasts are mantled by fine-grained, acicular sillimanite and the cordierite and k-feldspar matrix. Accessory apatite is relatively abundant in this sample, commonly surrounded by and in direct contact with biotite. Monazite is scarce and commonly occurs in proximity to sillimanite-andalusite complexes. Ilmenite occurs as coarse-grained inclusions in biotite.

Sample ST16-09

Sample ST16-09 is fine-grained and comprised of dominant k-feldspar, sub-dominant cordierite and biotite, accessory sillimanite, plagioclase and quartz and trace sapphirine (Fig. 2e). Sapphirine occurs rarely in between k-feldspar or sillimanite grains. Lens-shaped, optically continuous sillimanite and k-feldspar occur throughout the sample. Plagioclase occurs in the centre of quartz grains throughout the sample and is identified by its characteristic simple twinning. Apatite abundance is far higher in this sample than in the lower grade samples and commonly occurs within the optically continuous sillimanite and k-feldspar zones. Monazite is abundant in this sample and commonly occurs on the grain boundaries of apatite. Ilmenite is relatively abundant as euhedral, rectangle shaped grains.

Sample ST16-19A

Sample ST16-19A is coarse-grained and dominated by k-feldspar with sub-dominant cordierite and biotite and accessory sillimanite, plagioclase and quartz (Fig. 2f). There is no observable fabric in this sample. Quartz and plagioclase are more abundant in this sample than ST16-09. This sample contains the highest abundance of apatite of all metapelitic samples. Diamond shaped grains of apatite are commonly observed in contact with plagioclase or between k-feldspar crystals. Monazite is abundant and tiny grains are commonly observed on apatite grain boundaries. Ilmenite is relatively abundant in this sample, commonly occurring in contact with biotite or between k-feldspar.

METAPSAMMITES

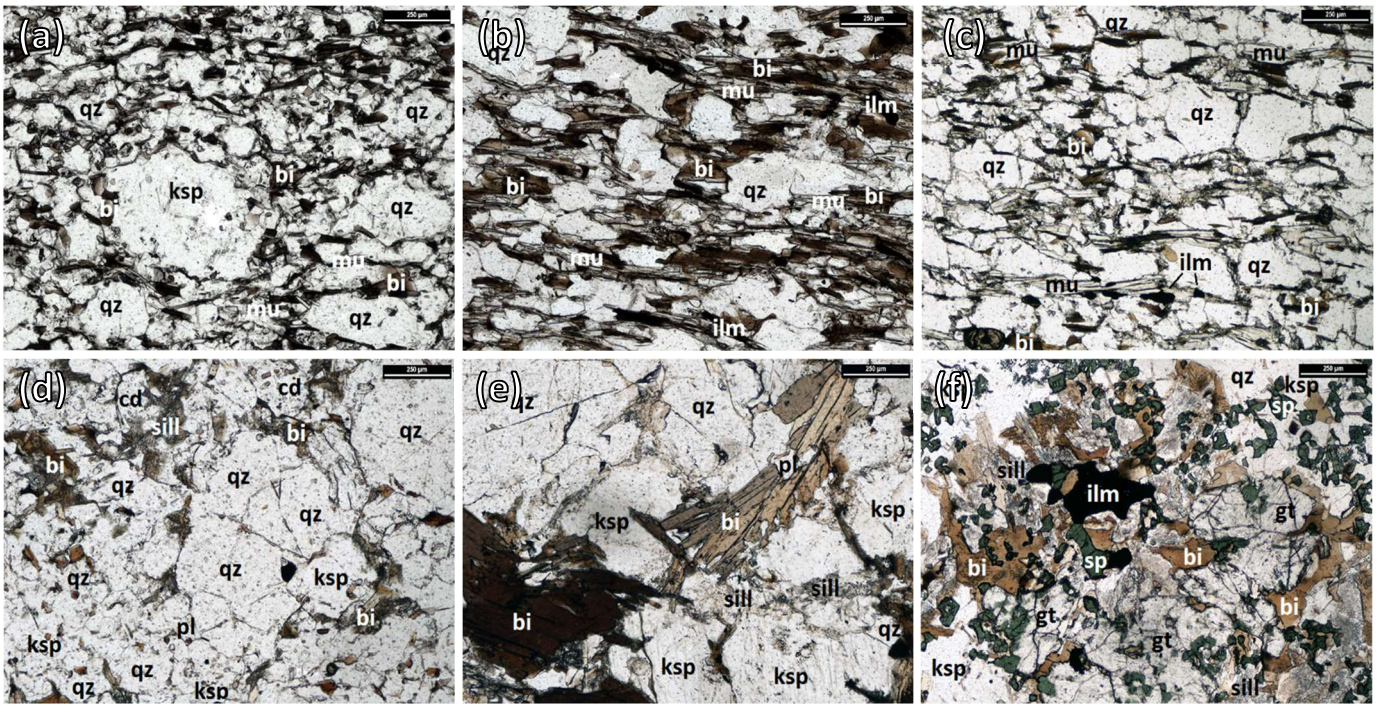

Figure 4: Representative petrographic photomicrographs of the metapsammite thin sections (PPL). Scalebar is 250µm in all photomicrographs sections. Descriptions of each sample given below. Preserved mineralogy detailed in Table. 1. (a) ST16-31A. (b) STF-33 (c) STF-04A (d) STF-10B (e) ST16-03C (f) STF-26A

Sample ST16-31A

Sample ST16-31A is fine-grained and is comprised of dominant quartz and sub-dominant matrix biotite, coarse k-feldspar and trace matrix muscovite (Fig. 4a). Biotite and muscovite define a weak to moderately strong fabric. Apatite is more abundant than in the metapelite equivalent (ST16-31J) and commonly occurs in contact with muscovite. Monazite is very scarce and only forms as tiny inclusions within k-feldspar. There are no visible occurrences of Fe–Ti oxides.

Sample STF-33

Sample STF-33 is fine-grained and is comprised of dominant quartz and sub-dominant biotite and muscovite (Fig. 4b). Biotite and muscovite define a moderately strong foliation. Apatite is far more abundant than in the metapelite equivalent (STF-33P) and

occurs as diamond-shaped crystals in contact with muscovite. Monazite is scarce, commonly occurring in contact with biotite. Ilmenite occurs predominantly within the matrix, commonly aligned with the foliation.

Sample STF-04A

Sample STF-04A is a medium-grained psammite comprised of dominant quartz and sub-dominant k-feldspar, matrix biotite and muscovite (Fig. 4c). Biotite and muscovite define a moderate foliation in the sample, and biotite seems to be partially replacing muscovite. Apatite is quite abundant and is significantly coarser in upper-amphibolite samples. Apatite commonly occurs within or in contact with muscovite and/or biotite. Monazite is scarce and commonly occurring in contact with biotite. Ilmenite is aligned with the foliation of the matrix.

Sample STF-10B

Sample STF-10B is medium-grained and is comprised of dominant quartz, sub-dominant k-feldspar and cordierite and accessory biotite, plagioclase and sillimanite (Fig. 4d). There is no preferential orientation of biotite. Apatite is relatively coarse-grained, many grains are occurring in contact with biotite, some are surrounded by rims of plagioclase and some occur rarely as small inclusions in coarse-grained k-feldspar. Monazite is relatively abundant and is commonly in contact with apatite or sillimanite. Ilmenite is relatively coarser-grained and occurs randomly scattered throughout the sample.

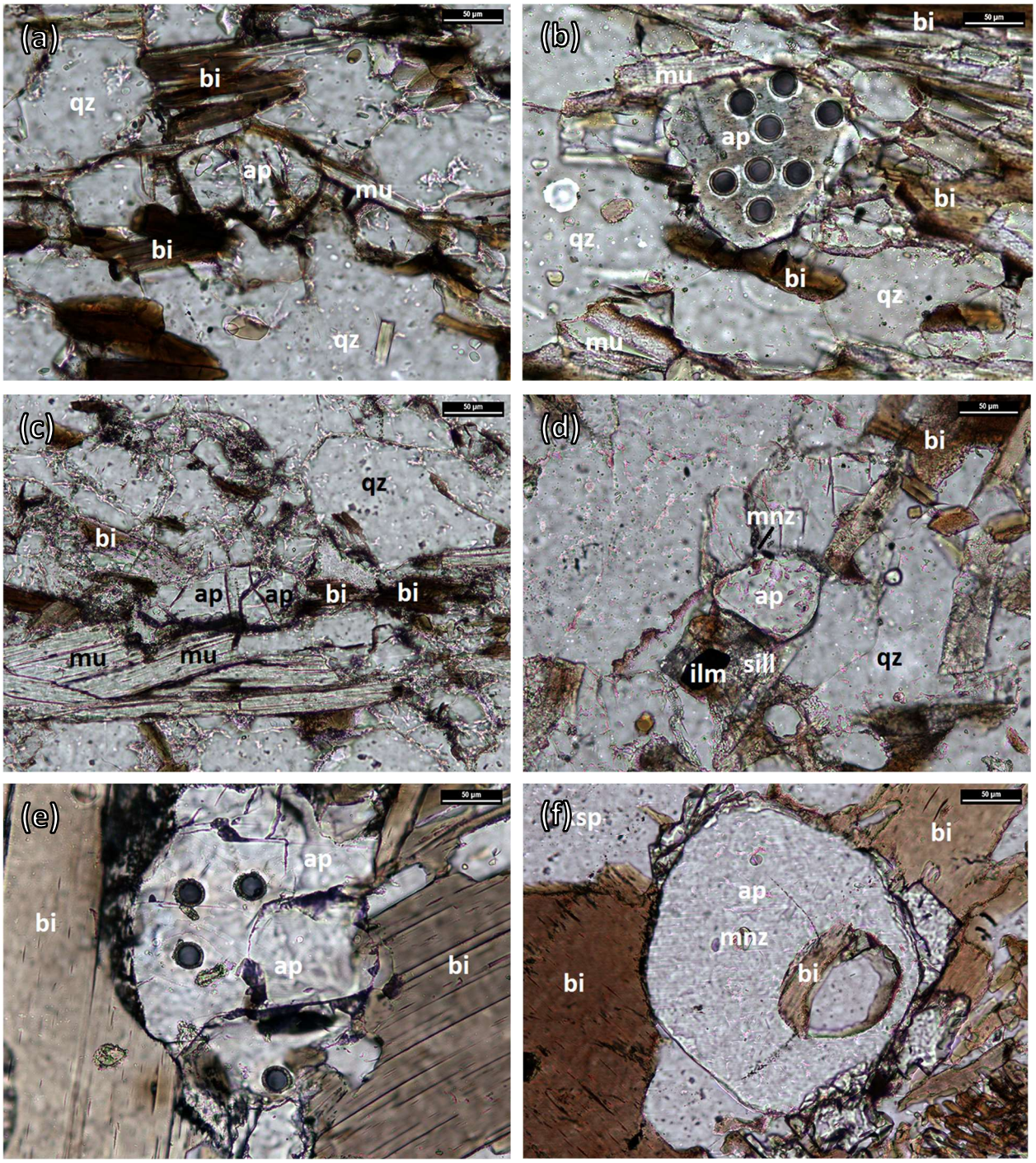

Figure 5: Metapsammite Photomicrographs of key petrographic relationships between accessory apatite and other minerals. Scalebar is 50µm in all photomicrographs. Biotite and/or muscovite are in contact with apatite crystals in all photomicrographs. The transition from amphibolite to granulite facies represents a significant increase in apatite grain size to very-coarse >150 µm apatites. (a) ST16-31A. (b) STF-33. (c) STF-04A. (d) STF-10B. (e) ST16-03C. (f) STF-26A.

Sample ST16-03C

Sample ST16-03C is coarse-grained and is comprised of co-dominant quartz and biotite, sub-dominant k-feldspar and trace plagioclase and sillimanite (Fig. 4e). Andalusite occurs in this high-grade sample as skeletal poikiloblasts. Sillimanite occurs as fibrous crystals surrounding biotite and andalusite. This sample contains the lowest apatite abundance of all metapsammitic samples; however, the grain size of the apatites are much larger (up to 0.5 mm). Monazite is abundant in this sample and commonly occurs on the grain boundaries of apatite. Ilmenite is only present as large inclusions in biotite grains.

Sample STF-26A

Sample STF-26A is coarse-grained and is comprised of dominant k-feldspar, sub-dominant cordierite and biotite and coarse accessory spinel, garnet and quartz (Fig. 4f). There is no preferential alignment or foliation present. This sample is comprised of four main zones: a quartz dominant with very little k-feldspar; a k-feldspar dominant with very little quartz; a garnet–biotite dominant with abundant accessory apatite and a spinel–garnet–biotite dominant. This sample comprises the highest apatite abundance of all samples, which commonly occurs as coarse crystals in contact with biotite within the garnet–biotite zone. Monazite is abundant in this sample and commonly occurs on the grain boundaries of apatite or as inclusions of apatite. Ilmenite is present as un-oriented, euhedral rectangle shaped grains.

Whole Rock Geochemistry

Whole rock major and trace element geochemistry for the samples is provided in Table 2. The ratio of SiO_2 to Al_2O_3 is greater in the metapsammites than the metapelites.

Table 2: Whole rock geochemistry of samples. Values presented as weight percent values of whole rock for major elements and mean ppm for trace elements. Psam = metapsammites. Pel = metapelites.

	ST16 31J	STF 33P	STF 02B	STF 16A	ST16 09	ST16 19A	ST16 31A	STF 33	STF 04A	STF 10B	ST16 03C	STF 26A
Major (wt%)	Pel	Pel	Pel	Pel	Pel	Pel	Psam	Psam	Psam	Psam	Psam	Psam
SiO_2	56.90	58.92	55.39	55.53	56.38	54.78	82.18	76.73	83.20	75.16	73.92	73.69
TiO_2	0.58	0.54	0.61	0.59	0.52	0.74	0.31	0.37	0.32	0.47	0.49	0.55
Al_2O_3	25.15	21.06	24.43	24.73	25.13	25.18	9.26	11.17	8.84	13.17	13.74	12.78
Fe_2O_3T	7.68	7.13	8.06	7.83	6.90	9.55	2.63	4.20	1.77	4.48	4.57	6.61
MnO	0.07	0.07	0.13	0.06	0.10	0.11	0.05	0.04	0.06	0.13	0.07	0.11
MgO	2.33	1.89	2.60	2.03	2.31	3.20	0.75	1.32	0.48	1.35	1.48	1.83
CaO	0.03	0.10	0.34	0.21	0.36	0.33	0.64	0.44	0.66	0.71	0.84	0.47
Na_2O	0.68	0.44	0.62	1.23	1.37	1.17	1.24	0.98	1.05	0.74	1.49	0.59
K_2O	6.26	6.04	6.64	6.62	6.66	4.58	2.76	2.97	2.41	3.25	3.63	2.36
P_2O_5	0.05	0.10	0.13	0.13	0.15	0.20	0.10	0.09	0.11	0.11	0.07	0.10
LOI	4.42	3.94	2.06	0.72	1.16	0.75	0.70	1.82	1.11	0.89	0.95	1.25
Total	**96.40**	**100.2**	**101.0**	**99.68**	**94.04**	**90.93**	**97.94**	**100.1**	**100.0**	**100.5**	**96.61**	**100.3**
Trace (ppm)												
Rb	448.0	409.0	380.7	407.7	284.4	228.9	128.4	199.0	96.4	161.8	187.6	119.4
Sr	74	61	106	49	134	148	105	85	57	121	117	57
Y	24.7	13.6	34.2	28.5	32.1	22.7	19.8	22.2	24.7	24.1	19.6	23.5
Zr	118	117	118	92	120	166	265	224	335	251	273	260
V	90	81	92	69	135	113	40	43	27	60	57	64
Ni	54	55	42	38	43	66	18	29	16	31	27	38
Cr	86	78	70	60	75	94	56	54	25	59	78	81
Nb	16.6	15.7	16.6	16.7	15.4	16.6	10.2	12.4	10.0	13.5	13.4	13.8
Ga	35.0	32.2	34.2	34.5	35.9	35.3	14.5	17.2	12.6	20.2	20.5	20.1
Cu	34	34	37	41	17	25	13	9	8	16	49	7
Zn	107	118	111	115	93	117	45	73	27	73	65	134
Co	17	19	17	18	17	29	2	9	1	11	8	21
Ba	1011	884	913	1060	1014	956	587	567	487	521	852	516
La	36	26	45	42	41	53	47	43	46	41	34	40
Ce	78	163	108	109	93	132	80	75	80	84	74	83
U	0.3	0.80	0.50	0.25	0.3	0.3	2.5	0.70	3.20	1.20	1.2	0.25
Th	32.5	33.6	33.5	35.2	25.1	38.1	30.4	27.2	37.0	33.7	29.6	25.3

Accessory forming P_2O_5 and CaO increase with metamorphic grade and the metapelite samples show a strong HPE + LREE enrichment at granulite facies conditions (samples ST16-09 and ST16-19A) as Th is the dominant HPE. Spider diagrams of trace and major element data are presented in Appendix B.

U-Pb Geochronology

In-situ monazite U-Pb geochronology was undertaken on the Stafford Member samples. Samples STF-33 and STF-33P were totally excluded from the results because all analyses performed exceeded the 95-105% concordance threshold or contained significant $_{204}$Pb contamination. Table 3 summarises the monazite ages determined on each sample. Concordia diagrams for monazite standards Ambat (c. 520 Ma) and 94-222/Bruna-NW (c. 450 Ma) are presented below in Figure 6. The concordia ages of both standards fall within 5 m.y. of the referenced ages (see Payne et al., 2008). All U-Pb Concordia ages of the monazites centre around c. 1770 - 1800 Ma (Table 3) except

Table 3: Summary of *In-Situ* monazite U-Pb geochronology for all samples. Concordia ages presented range from c. 1714 – 1804 Ma. Includes mean square weighted deviation (MSWD) and concordia age error bars for all samples.

Sample Number	Unit	Metamorphic Facies	Concordia Age (Ma)	Age Error (Ma)	MSWD
ST16-31J	Pelite	Mid-amphibolite	1782	± 10	0.06
STF-33P	Pelite	Mid-amphibolite	–	–	–
STF-02B	Pelite	Upper-amphibolite	1804	± 38	1.50
STF-16A	Pelite	Upper-amphibolite	1794	± 11	0.30
ST16-09	Pelite	Granulite	1784	± 7.4	0.09
ST16-19A	Pelite	Granulite	1776	± 10	1.50
ST16-31A	Psammite	Mid-amphibolite	1714	± 38	1.80
STF-33	Psammite	Mid-amphibolite	–	–	–
STF-04A	Psammite	Upper-amphibolite	1715	± 140	5.10
STF-10B	Psammite	Upper-amphibolite	1766	± 10	0.68
ST16-03C	Psammite	Granulite	1778	± 8.7	3.10
STF-26A	Psammite	Granulite	1777	± 9.2	8.70

samples ST16-31A and STF-04A, each of which yielded two concordant analyses. *In-situ* monazite U-Pb geochronology probability density plots and full description are in Appendix C.

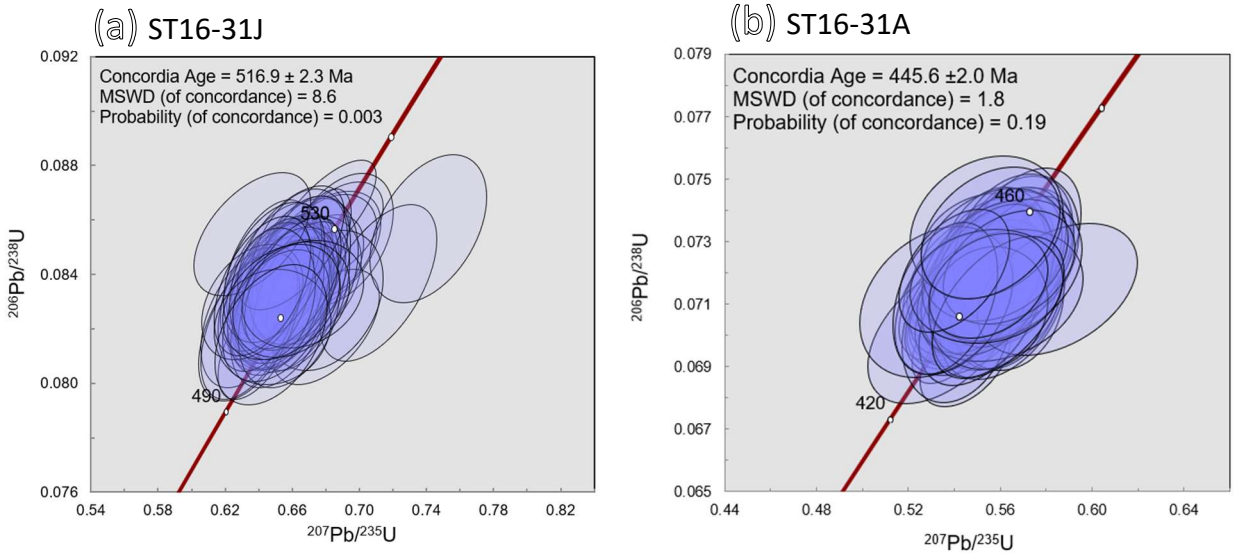

Figure 6: *In Situ* monazite geochronology concordia diagrams for monazite standards. (a) Ambat monazite standard with a U-Pb concordia age of 516.9 ± 2.3 Ma. (b) 94-222/Bruna-NW monazite standard with a U-Pb Concordia age of 445.6 ± 2 Ma.

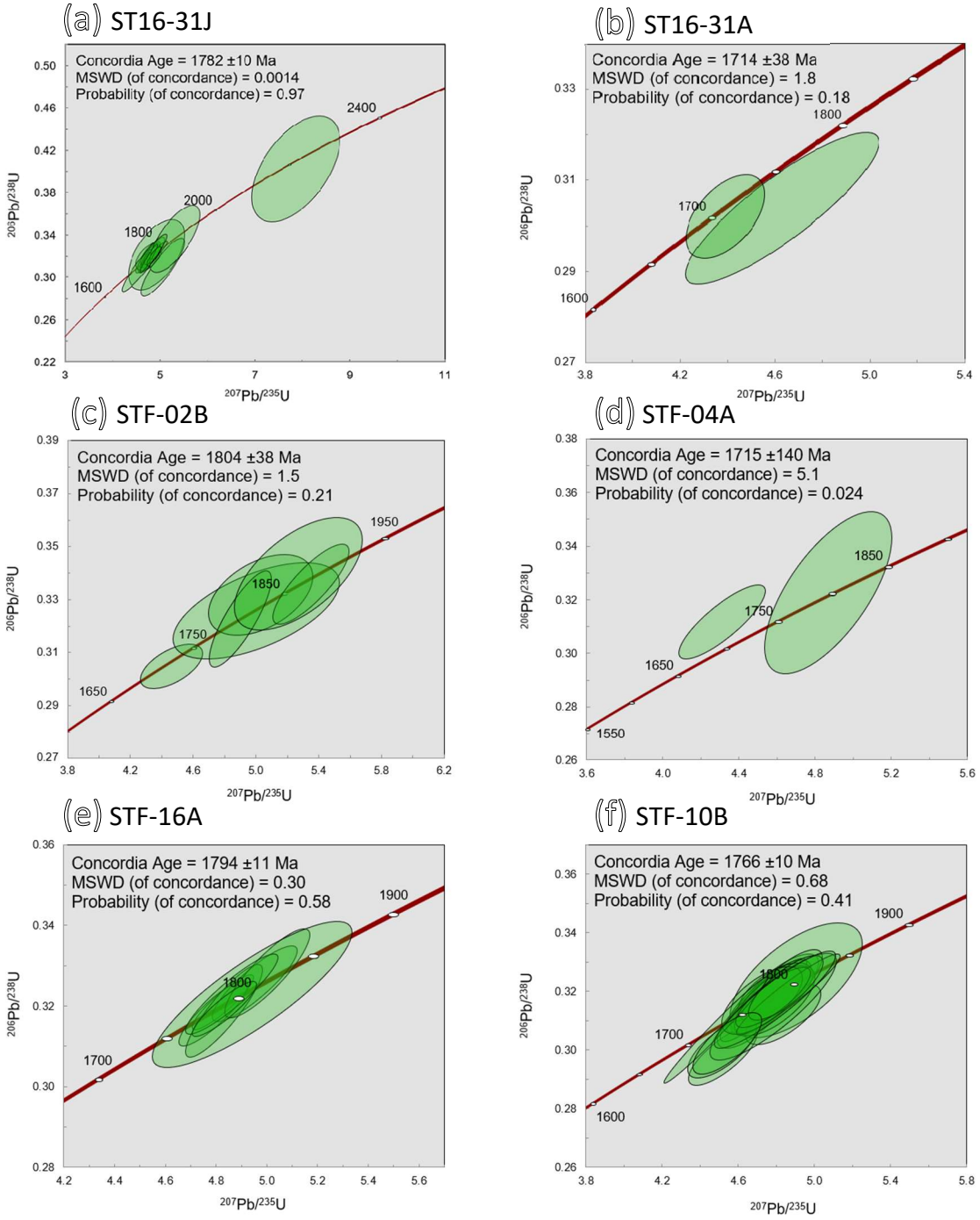

Figure 7: *In-situ* monazite U-Pb geochronology Concordia diagrams for amphibolite facies samples. All data presented herein are concordant (>95%, <105% concordance). (a) ST16-31J. (b) ST16-31A. (c) STF-02B. (d) STF-04A. (e) STF-16A. (f) STF-10B.

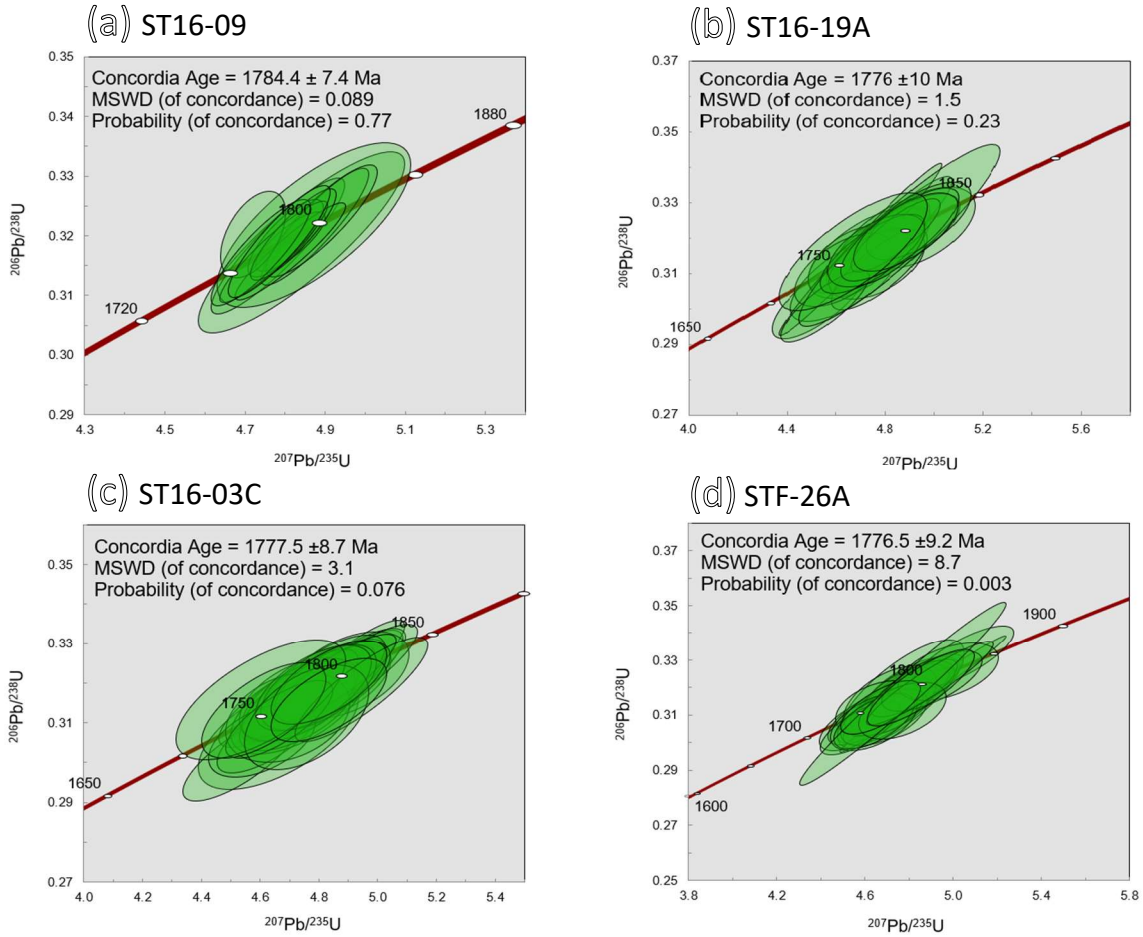

Figure 8: *In-situ* monazite U-Pb geochronology Concordia diagrams for granulite facies samples. All data presented herein are concordant (>95%, <105% concordance). (a) ST16-09. (b) ST16-19A. (c) ST16-03C. (d) STF-26A.

Mineral Liberation Analysis (MLA)

Estimated modal proportions of accessory minerals apatite and monazite were determined for each sample through mineral liberation analysis (MLA maps in Appendix D) to examine the influence of metamorphic grade on the growth of accessory minerals (particularly apatite). Monazite is commonly observed in contact with the grain edges of apatite in granulite facies samples (Fig. 9).

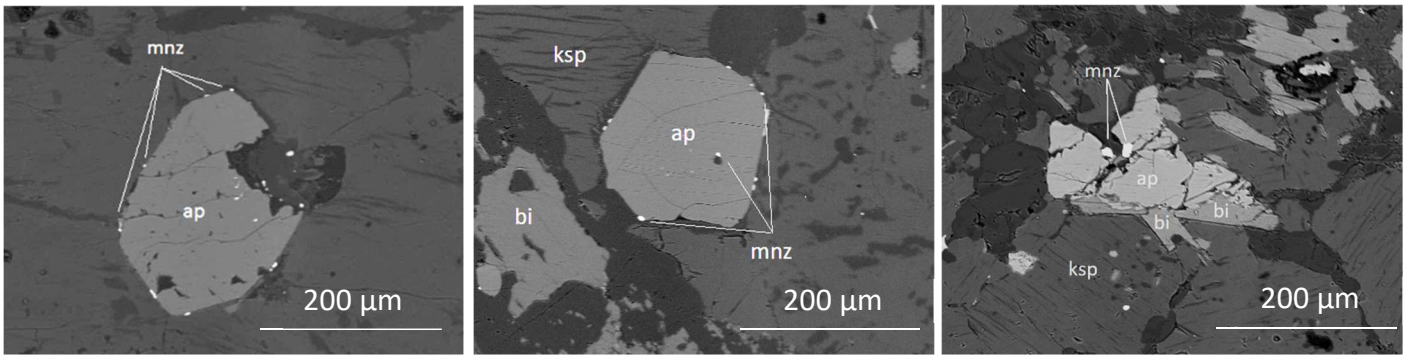

Figure 9: Back scattered electron (BSE) maps of granulite facies samples depicting monazite on the grain boundaries of apatite. (a) STF-26A. (b) ST16-19A. (c) ST16-03C.

APATITE MINERAL LIBERATION ANALYSIS

The modal proportion of apatite was estimated from the mineral liberation maps by performing a pixel count in photoshop (Appendix A). These values were then plotted

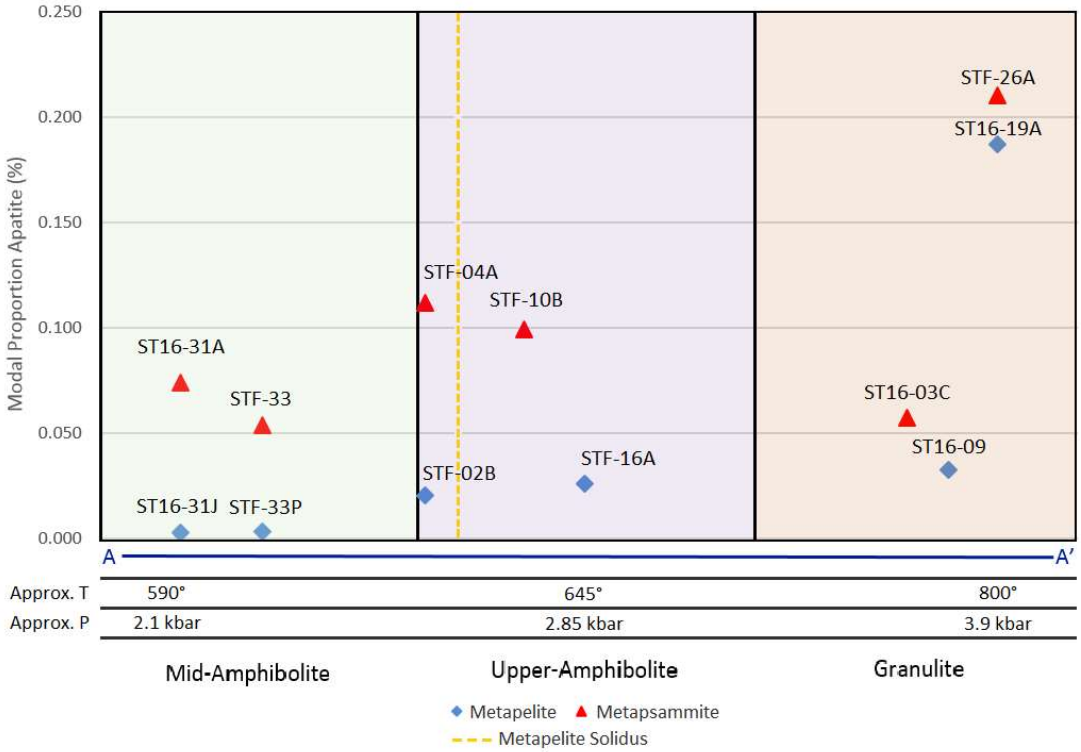

Figure 10: Apatite abundance with metamorphic grade: The modal proportion of apatite increases with higher P–T conditions. Mid-amphibolite samples typically contain few, small apatite grains, whereas granulite samples typically contain many coarse grains of apatite. The presented range is the highest and lowest modal proportion of sample pairs (samples taken within ~1 km proximity in the field).

against the location of the sample, as determined by the projection line in Figure 1. In general, the modal proportion of apatite increases with increasing *P–T* (Fig. 10), except for ST16-03C and ST16-09 which have significantly lower apatite abundances.

MONAZITE MINERAL LIBERATION ANALYSIS

The modal proportion of monazite was estimated by the same method detailed in the above section. These values were also plotted against the *P–T* conditions of the samples, as determined by the projection line in Figure 1. There is a general trend for the modal proportion of monazite to increase with increasing *P–T* conditions for both metapelite and metapsammite samples.

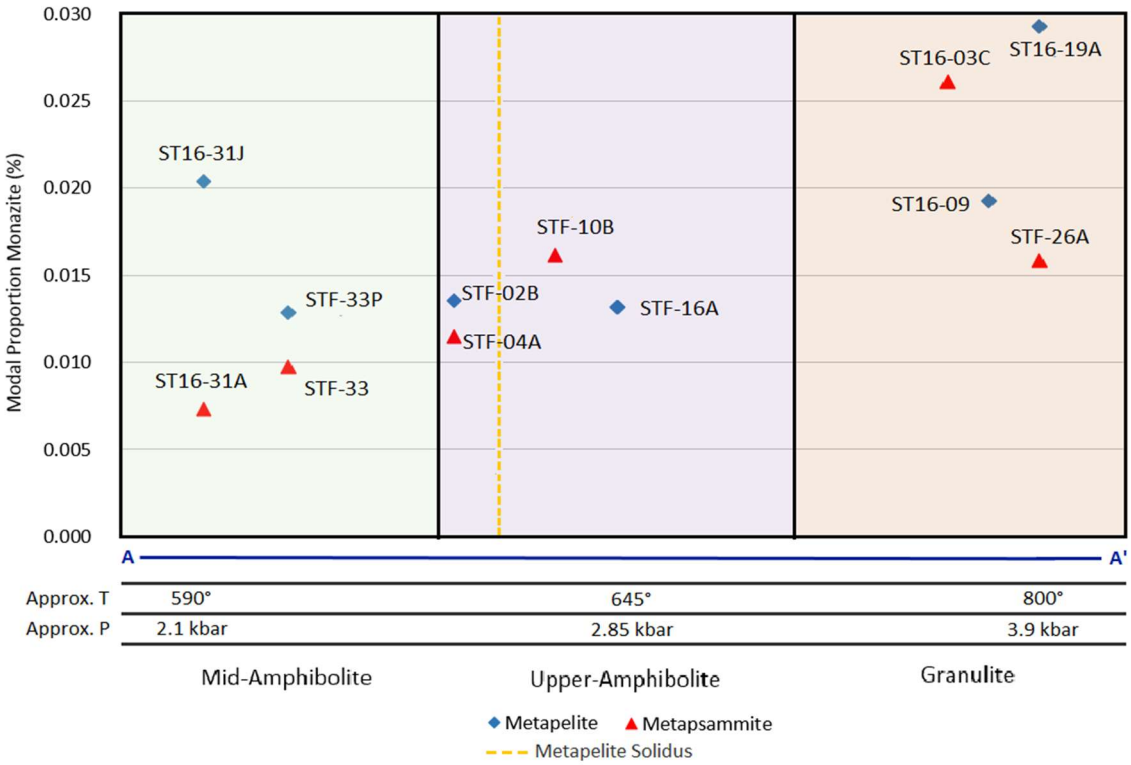

Figure 11: Monazite abundance with metamorphic grade: The modal proportion of monazite increases with higher P–T conditions. ST16-31J and ST16-31A (the two lowest grade samples) have a significant difference in monazite abundance, despite being sampled within a few metres in the field. The presented range is the highest and lowest modal proportion of sample pairs (samples taken within ~1 km proximity in the field).

Apatite and Monazite Chemistry

Averaged and raw major and trace element data for apatite, monazite and silicates are all presented in the same format in Appendix E. Of the 343 individual LA–ICP–MS trace-element analyses performed on apatite across all samples, 102 were excluded from the presented results. 94 were excluded due to silicon or aluminium contamination of greater than 10,000 ppm. The remaining 8 were excluded due to zirconium contamination of greater than 200 ppm. Of the 232 individual LA-ICP-MS trace-element analyses performed on monazite across all samples, 19 were excluded from the presented results. 16 were excluded due to silicon contamination of greater than the combination of U and Th concentration. 3 were excluded due to silicon contamination of greater than 100,000 ppm. Trace element compositional data is presented as chondrite-normalised (McDonough and Sun, 1995) spider diagrams (Fig. 12 / 13).

The spider diagram for apatite in metapelites shows significant spread in composition in the mid-amphibolite facies sample and less spread (except Th) in higher grade samples. Although there is significant overlap in upper-amphibolite and granulite facies apatite compositions, (Fig. 12a / 12b) there is an overall trend to lower REE, Zr, Y and Th content in upper-amphibolite facies apatite. Light rare earth elements (LREEs) (e.g. La, Ce) and heavy rare earth elements (HREEs) (e.g. Tm, Yb, Lu) are heavily depleted in supra-solidus apatite, whereas middle rare earth elements (MREEs) (e.g. Sm, Eu, Gd, Tb, Dy) show a moderate preference for the supra-solidus, granulite facies apatite in the middle of the chondrite normalised REE plots (Fig. 12a / 12b). Similarly, the

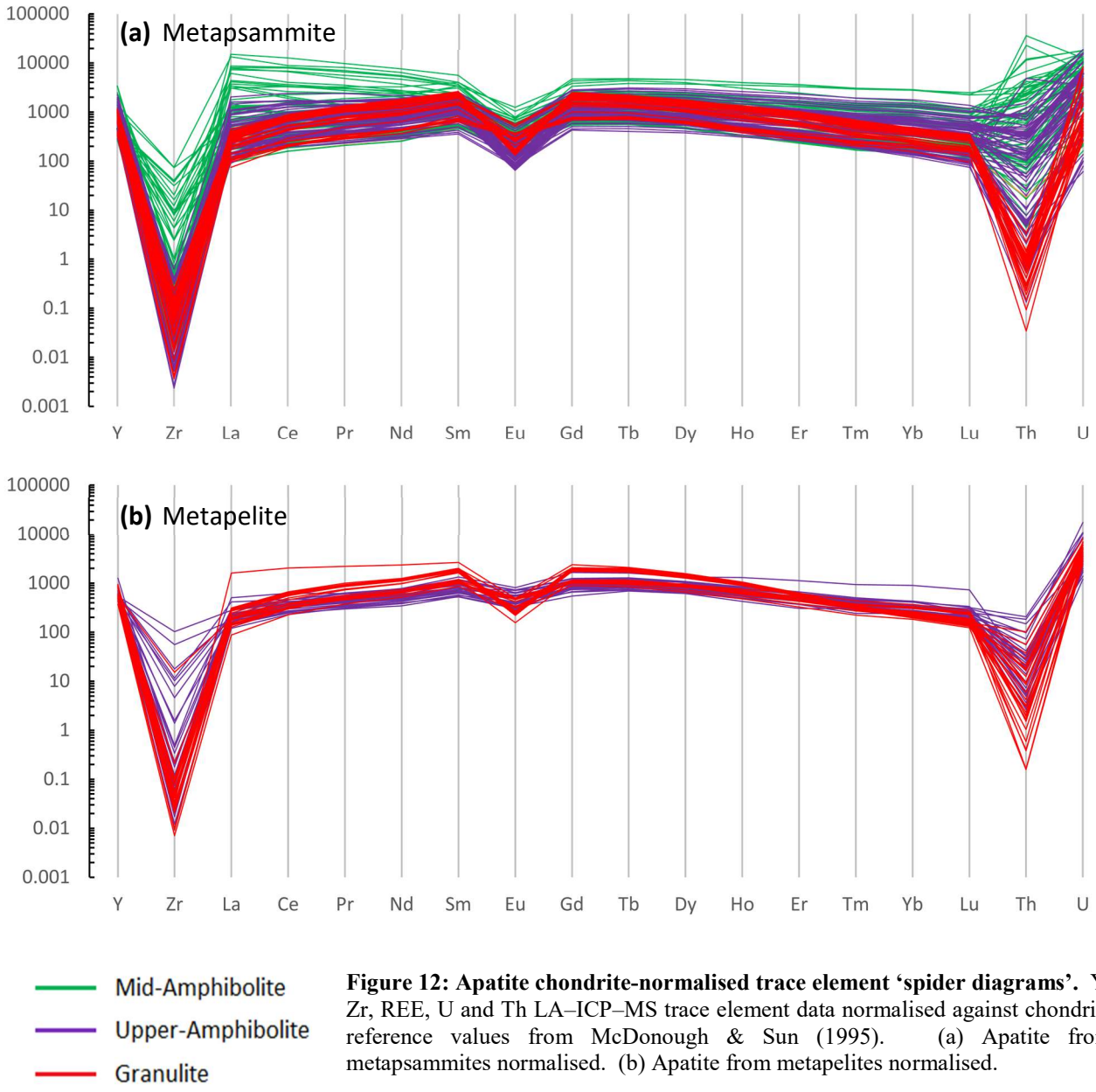

Figure 12: Apatite chondrite-normalised trace element 'spider diagrams'. Y, Zr, REE, U and Th LA–ICP–MS trace element data normalised against chondrite reference values from McDonough & Sun (1995). (a) Apatite from metapsammites normalised. (b) Apatite from metapelites normalised.

europium of apatite in metapsammites expresses a slightly higher concentration at granulite facies, whereas europium in the metapelite apatite expresses a slight preference for upper-amphibolite conditions (e.g. Bea and Montero, 1999).

The spider diagrams for monazite in metapelites also show significant spread in composition in the mid and upper-amphibolite facies samples and less spread (except

Th and Zr) in higher grade samples. Th in metapsammite monazite has a large spread and no apparent trend with metamorphic grade. There is an apparent depletion of REEs in granulite facies, metapelite monazites (Fig. 13b), however, in the granulite facies metapsammites, there is no discernible trend with varying metamorphic grade due to the large spread (Fig. 13a). Eu is an exception to this, as it is clearly depleted in supra-solidus monazites.

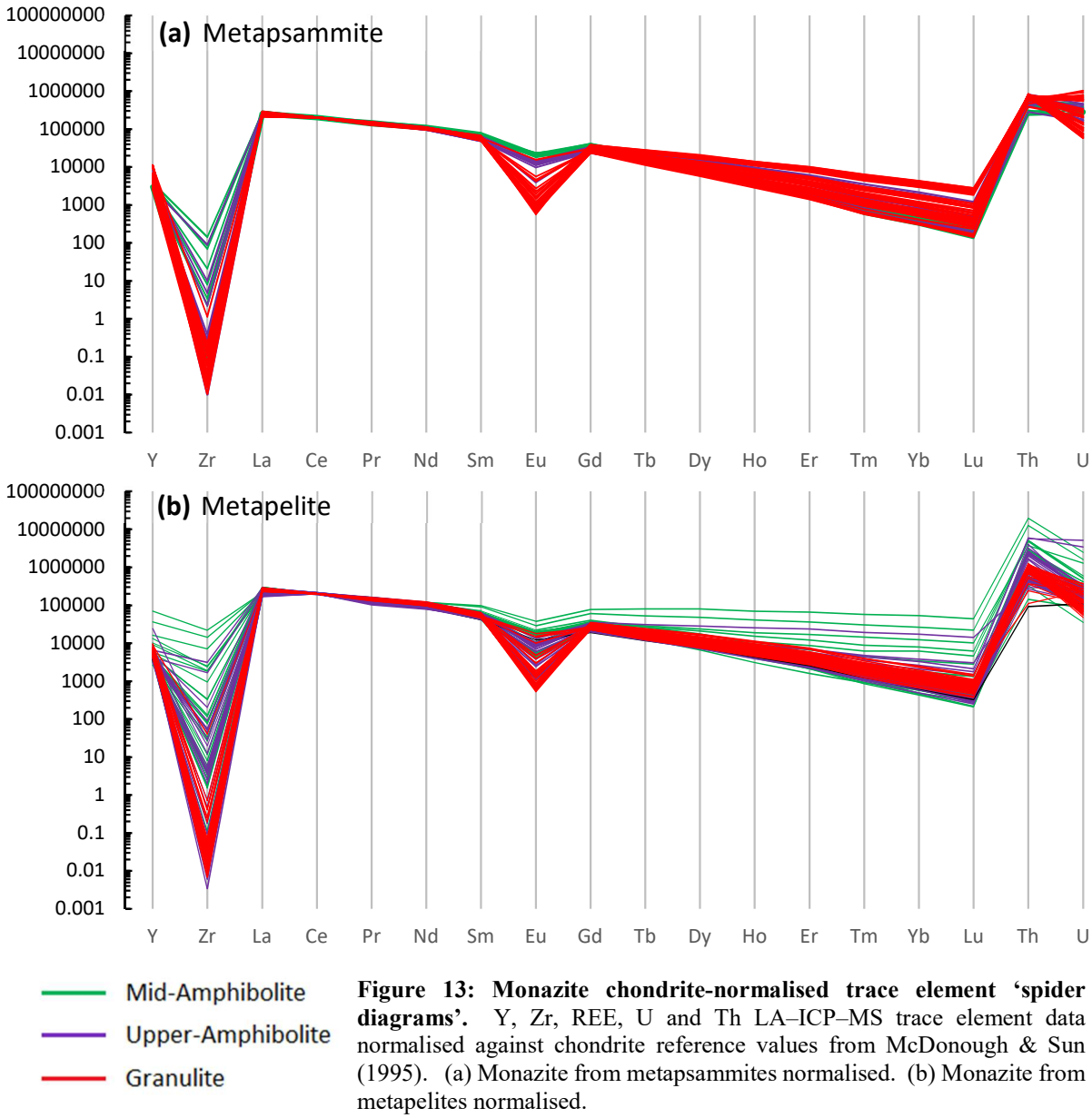

Figure 13: Monazite chondrite-normalised trace element 'spider diagrams'. Y, Zr, REE, U and Th LA–ICP–MS trace element data normalised against chondrite reference values from McDonough & Sun (1995). (a) Monazite from metapsammites normalised. (b) Monazite from metapelites normalised.

Generally, monazite contains up to an order of magnitude higher U and Th than apatite (Fig. 12 & 13). Despite the fact monazite contains far higher concentrations of both HPEs, within individual accessory minerals it is clear apatite prefers uranium relative to thorium (Fig. 12) whereas monazite prefers thorium relative to uranium (Fig. 13).

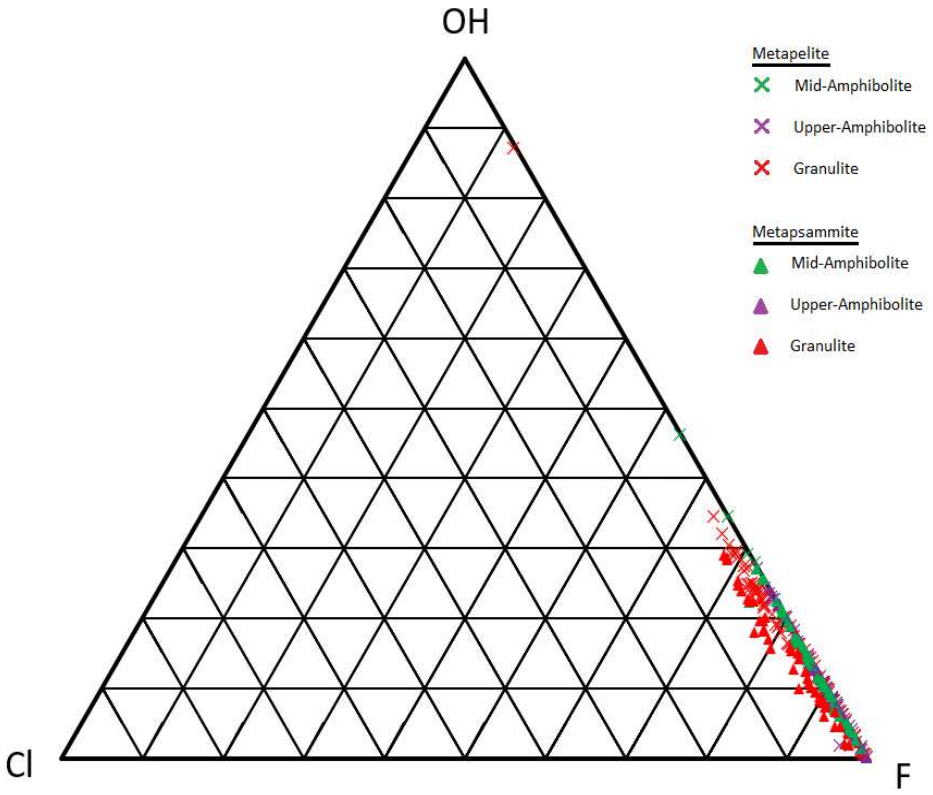

Figure 14: Apatite F–Cl–OH Ternary Diagram. Anion proportion for the F-Cl-OH site in apatite was calculated for each sample and plotted on a ternary diagram that records the relative proportion of each component. Hydroxide occupies the same site as F and Cl in apatite.

F, Cl and OH anion EPMA data of apatite (see Appendix E for raw data) were calculated for the average proportion within the halogen site in apatite's crystal structure (Fig. 14). On average, F occupies greater than 70% of the F-Cl-OH site in the apatite crystal structure. Cl occupies less than 6% of the F-Cl-OH site in apatite and is slightly more abundant in granulite facies apatite relative to amphibolite. OH occupies around 25 to 30% of the crystal structure.

DISCUSSION

Interpretation of U–Pb Monazite Geochronology

Before apatite and monazite compositional data can be discussed, it will be determined whether the accessory minerals are detrital or metamorphic in origin. Monazite growth has been recognized at mid-amphibolite, upper-amphibolite and granulite facies conditions, and therefore it is a widely and commonly used metamorphic geochronometer (Kohn and Malloy, 2004). Conversely, apatite is not typically used as a metamorphic geochronometer in high grade rocks, as it has a closure temperature of ~450° C (Flowers et al., 2005) and commonly contains relatively high concentrations of common lead ($_{204}$Pb) (Gelcich et al., 2005). The lowest grade samples in this study record temperatures of ~590 °C (Fig. 1b), which is above the closure temperature of apatite. Therefore, apatite within the Stafford Member samples would record the age of cooling rather than the age of metamorphism. Consequently, the geochronology of monazite was used to determine the nature of accessory mineral growth.

The lowest recorded temperature at Mount Stafford is above the biotite-in reaction isograd, which was described by several studies to correspond with the consumption of low-grade metamorphic monazite (e.g. Budzyń et al., 2011; Wing et al., 2003; Smith and Barreiro 1990). Metamorphic monazite was stated by Gasser et al. (2012) to be produced about the andalusite-in and garnet-in isograds, which in the Stafford Member is to higher temperatures than the mid-amphibolite samples. Therefore, detrital monazite is likely to be present in the lowest grade samples (e.g. Catlos et al., 2001; Suzuki et al., 1994) and may also persist in higher grade samples even where andalusite is present (e.g. Wing et al., 2003). Some of the spread in the compositional data for

monazite (Fig. 13b) may be due to detrital monazite within the lower-grade, mid-amphibolite samples. Concordant U-Pb age data show a spread from 2180 to 1714 Ma in mid-amphibolite samples (Figures 7a and 7b). The age of deposition of the Stafford Member is c. 1858 Ma (Claoue´-Long et al., 2008) and the age of metamorphism of the Stafford Member is c. 1810 Ma – 1770 Ma. On this basis, monazite grains older than c. 1810 Ma can be considered detrital. According to this classification, there are only a few monazite grains that are both detrital and concordant (Fig. 7a), and these are restricted as inclusions in andalusite or cordierite. Conversely, monazite grains corresponding to the age of metamorphism are considered metamorphic in origin and tend to be located on the grain boundaries of biotite and apatite, particularly in the granulite facies samples (e.g. Fig. 9).

A lot has been written about metamorphic monazite (e.g. Smith and Barreiro, 1990; Wing et al., 2003; Kohn and Malloy, 2004; Corrie and Kohn, 2008; Gasser et al., 2012) and very little about metamorphic apatite, yet in all these studies, apatite is ubiquitously present. Detrital apatite is known to occur in metasedimentary rocks (Spear and Pyle, 2002), therefore, it is likely at least some of the samples contain detrital apatite. Low-grade, mid-amphibolite samples also have the largest spread in terms of apatite Y + Zr + REE + Th + U concentration (Fig. 12), perhaps due to the presence of both detrital and metamorphic grains. Numerous studies in addition to this concur that apatite is required as a reactant in the growth of monazite since both minerals contain phosphorous (e.g. Budzyń et al., 2011; Spear and Pyle, 2010; Janots et al., 2008), thus it would seem likely detrital apatite is preserved in the Stafford Member samples.

Trace Element Distribution with Metamorphic Grade

Understanding the distribution of trace elements with increasing metamorphic grade is a vital component to proposing apatite involving mineral reactions. In addition, information about the changes to apatite abundance with increasing metamorphic grade, its microstructural location in samples and information about major silicate mineral reactions (e.g. Vernon et al., 1990; White et al., 2003) is utilised.

DISTRIBUTION COEFFICIENTS

Considering existing literature describes the two-way reaction link between apatite and monazite (e.g. Budzyń et al., 2011; Janots et al., 2011) and the link between biotite and apatite (e.g. Broska et al., 2005; Bingen et al., 1996), distribution coefficients were calculated for the mineral pairs: apatite/monazite and apatite/biotite in order to determine the partitioning behaviour of elements with changing metamorphic grade. Raw EPMA and LA–ICP–MS data were used to calculate these coefficients.

$$D = \frac{Element\ concentration\ (Mineral\ A)}{Element\ concentration\ (Mineral\ B)}$$

If D > 1 the element has a preference for Mineral A.

If D < 1 the element has a preference for Mineral B.

Although the compositional data for xenotime was not collected in this study, the partitioning of elements for apatite/xenotime are expected to be greater than 1 for Y + HREEs and less than 1 for LREEs + MREEs (e.g. Pyle et al., 2001). The partitioning of elements in the apatite/melt pair is greater than 1 for all REEs + Y and less than 1 for

Th, U, Zr (Prowatke and Klemme, 2006). The partitioning of elements in the monazite/melt pair is greater than 1 for all REEs + Y + Th + U, with a significantly stronger Th than REE preference for monazite (Stepanov et al., 2012). This would imply Th and U will preferentially partition to monazite during partial melting. Distribution coefficients calculated in this study also support this notion, as there is a distinct preference of U + Th for monazite relative to apatite, that only improves with metamorphic grade (Fig. 15).

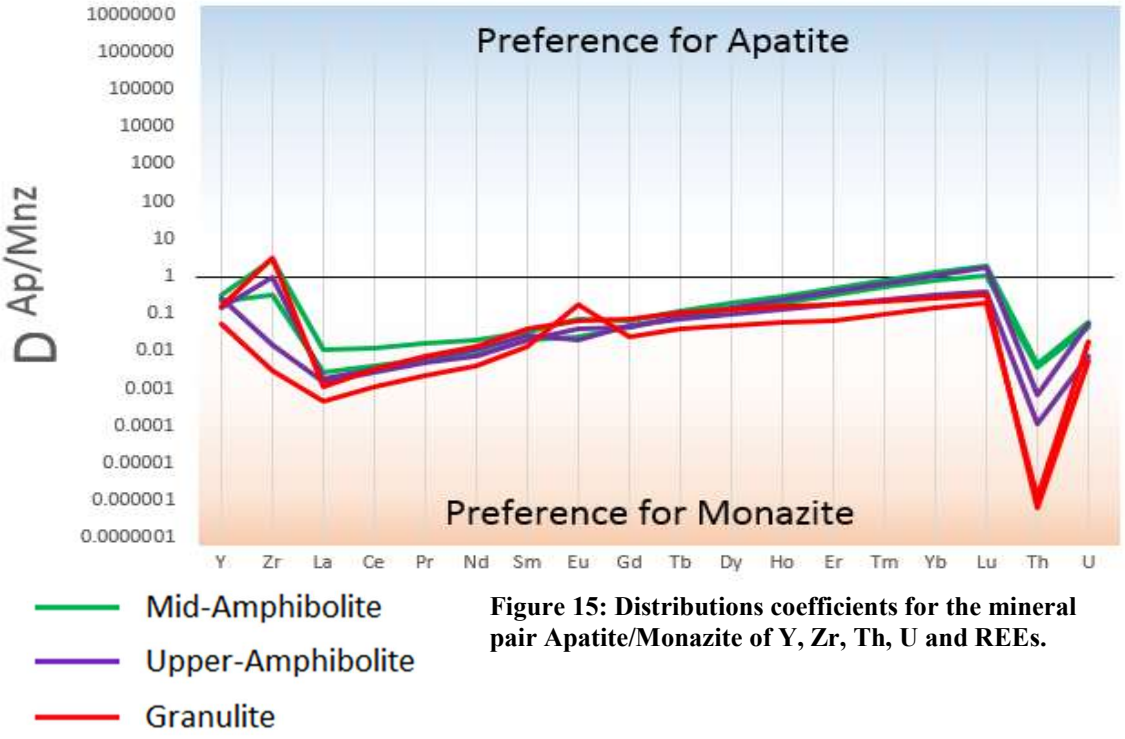

Figure 15: Distributions coefficients for the mineral pair Apatite/Monazite of Y, Zr, Th, U and REEs.

LREEs also have a strong preference for monazite over apatite, particularly as metamorphic grade increases. This likely suggests a prograde metamorphic exchange of REEs from apatite to monazite (e.g. Wing et al., 2003). However, MREEs do not follow this trend with grade and instead show a slightly lower preference for monazite

with increasing metamorphic grade (Fig. 15). HREEs such as Yb and Lu have a slight preference for apatite in sub-solidus samples, but a preference for monazite in supra-solidus samples. There is no discernible trend for Zr and Y. Th has a strong preference for monazite, with a clear intensification of this preference with higher grade *P–T* conditions. U has a slight to moderate preference for monazite (Fig. 15) (e.g. Stepanov et al., 2012).

In the apatite/biotite pairing (Fig. 16), F has a preference for apatite. However, as metamorphic grade increases, the preference for apatite decreases. There is no clear preference trend of Cl for biotite or apatite with increasing metamorphic grade, and this likely reflects the low Cl concentrations in both biotite (Appendix E) and apatite (Fig. 14) in this study. Th and U both have a strong preference for apatite relative to biotite under mid-amphibolite facies conditions. At granulite conditions, the U preference for

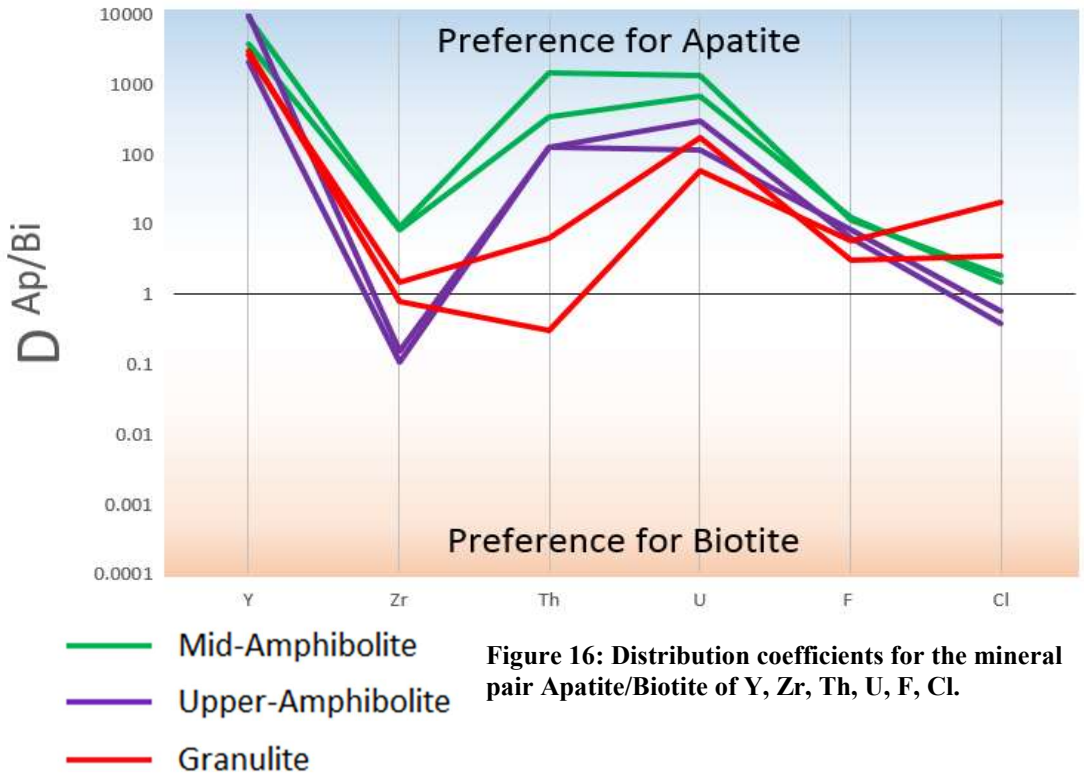

Figure 16: Distribution coefficients for the mineral pair Apatite/Biotite of Y, Zr, Th, U, F, Cl.

apatite is reduced and Th has a slight preference for biotite, though will preferentially partition into monazite. There is no discernible grade trend for Y between apatite and biotite, but Y partitions strongly into apatite. Zr preferentially partitions into mid-amphibolite apatites and upper-amphibolite biotites in this binary system.

SPIDER DIAGRAMS (RARE EARTH ELEMENTS)

REEs (particularly LREEs) are up to two orders of magnitude lower in apatite relative to monazite (Fig. 12 and 13) because when apatite coexists with monazite in metapelites, LREEs are preferentially enriched in monazite (Spear and Pyle, 2002). MREE enrichment in granulite facies apatite relative to the upper-amphibolite facies apatite would suggest MREEs tend to remain in apatite during partial melting. Experimental work by Ayers and Watson (1993) found the distribution coefficients between apatite and partial melt were higher than 15 for Sm and Dy (MREEs), which indicates a propensity for MREEs to remain in apatite during partial melting. In general, the apatite spider diagrams (Fig. 12) demonstrate there is a relative depletion of HREEs and LREEs in apatite in supra-solidus, partially melted samples, likely because high field strength elements (HFSEs) such as REEs are 'incompatible elements' and thus have a higher tendency to fractionate into the melt during partial melting (Francis, 2003). A preferential enrichment (or lack of depletion) of MREEs in supra-solidus samples is possibly due to a preference for MREEs to remain in apatite, as evidenced by the abnormally high distribution coefficient between apatite and partial melt for MREEs (Bingen et al., 1996) and the enrichment of MREEs relative to HREEs and LREEs (Fig. 12). An alternative possibility is another mineral rich in MREEs is in reaction with apatite at upper-amphibolite and granulite conditions.

Granulite facies monazites tend to be depleted in REEs relative to mid-amphibolite monazites (Fig. 13), partly due to the incompatibility of REEs (Francis, 2003). The large spread of granulite REE concentrations in metapsammite monazites can be explained by the exchange of REEs to monazite during the growth of monazite on the edges of granulite facies apatite crystals (see Fig. 9) (Krenn et al., 2012; Budzyń et al., 2011), where MREE rich apatite is incongruently broken down to form monazite under high *P–T* conditions (Johnson et al., 2015; Krenn et al., 2012; Wolf and London, 1995). Oppositely, the low-grade Stafford Member samples rarely exhibit accessory monazite growth on the edges of apatite. These two outcomes may be indicative of apatite's relatively high solubility at higher *P–T* conditions (Wolf and London, 1995; Pichavant et al., 1992). This proposed high-grade breakdown of apatite to monazite explains both the large spread of REE concentration in supra-solidus monazite as well as the depletion of LREEs relative to MREEs in supra-solidus apatite, i.e. the 'bell shape' of the apatite REE chondrite normalised plot (Bea and Montero, 1999). The increase in modal abundance of monazite with metamorphic grade (Fig. 11), the lower than 1 distribution coefficient $D^{ap/mnz}$ of REEs (Fig. 15) and the relatively high solubility of apatite and tendency for incongruent breakdown as per (Wolf and London, 1995) also support this proposition.

SPIDER DIAGRAMS (HEAT PRODUCING ELEMENTS)

Uranium and thorium are two of the major heat producing elements (HPEs) in" continental crust (Korenaga, 2011) and are mainly contained within monazite and apatite (Rubatto et al., 2006). Therefore, the retentivity of U and Th in monazite and apatite during partial melting is of paramount importance to understanding the overall distribution of heat production in partially melted continental crust. Stepanov et al.

(2012) found that the distribution coefficients for both U and Th between monazite and melt ($D^{mnz/melt}$) decreased with increasing temperature. Notably, this observation is also true for all REEs + Y, but particularly for LREEs. Initially this would tend to suggest that as partial melting progresses with increasing temperature, radiogenic HPEs U and Th are less stable in monazite. However, the distribution coefficients were found to be greater than 1 for $D^{mnz/melt}$ even at temperatures of ~1200 °C. $D^{mnz/melt}$ values calculated for temperatures most comparable to the maximum temperature calculated for the Stafford Member (~800 °C; Fig. 1) were up to ~1600 for Th and ~200 for U, which indicates even at granulite facies conditions, U and Th have a strong preference for monazite over partial melt.

In the metapelite samples, depletion of U and Th in monazites at granulite conditions relative to mid-amphibolite conditions (Fig. 13b) can be at least partially explained by the presence of U and Th enriched detrital monazite grains (see Fig. 7a) in the lower grade samples. These results agree with the data presented in Stepanov et al. (2012), suggesting U and Th remain in monazite during partial melting and therefore the partial melt is depleted in both U and Th relative to monazite. Melt loss would remove this HPE depleted silicate melt from the system, while HPE enriched monazite remains in the residual crust (Fig. 11), potentially increasing heat production in the residual crust with sufficient monazite growth. Furthermore, because apatite (as the major reservoir for P_2O_5) is required for the growth of monazite (Johnson et al., 2015), it is a key component for residual crust HPE enrichment. However, it is likely this would only be possible if the granulite rocks were increasingly enriched in monazite, because whole rock geochemistry suggest there is no enrichment or depletion in the mid-amphibolite

vs granulite facies crust (Table 2). This is likely because the study only investigated compositional changes over a narrow range of metamorphic conditions of ~200 °C (mid-amphibolite to granulite). Extending this range in a new study location,

The notion that residual granulites can have a higher heat production than shallower crustal rocks is not widely recognised. However, there are examples of high-heat producing granulites, in India (Kumar et al. 2007; Roy et al., 2008), Brazil (Iyer et al., 1984), South Africa (Andreoli et al., 2006; Ballard et al 1987) and Finland (Jõeleht and Kukkonen 1998). The results from this study also indicate the residual granulite facies rocks of the Stafford Member *could* have a slightly higher heat production than the lower grade rocks.

Metamorphism Driven Accessory Mineral Reactions

Based on the petrographic analyses, the continuous reaction changes that occur to the major silicate mineralogy with increasing metamorphic grade for the metapelites and metapsammites are presented in Table 4 (see also: Table 1; Vernon et al., 1990; White et al., 2003). Corrie and Kohn (2008) invoke plagioclase and garnet as LREE sources involved in reaction with accessory minerals. However, in contrast to almost all other studies that have investigated monazite growth in the context of silicate minerals and accessory minerals (cf. Tomkins and Pattison, 2007), the Stafford Member is almost entirely garnet absent. Therefore, there is no sufficient Y sink (e.g. garnet) to consume

and remove Y-bearing accessory phases such as xenotime from the assemblage during prograde metamorphism (e.g. Pyle and Spear, 2003). The Stafford member is also almost entirely plagioclase absent (Table 1), particularly in the low-grade samples where a source of Ca is required for the growth of metamorphic apatite at low grades. These outcomes suggest that apart from biotite, no other silicate mineral directly

Table 4: Continuous reaction changes for major silicate minerals in the Stafford Member. Reactions interpreted from petrographic analysis of the Stafford Member samples.

Continuous reaction series:
Metapelites:
muscovite + biotite + andalusite + ilmenite + quartz ± plagioclase
↓
muscovite + biotite + andalusite + k-feldspar + ilmenite + quartz ± plagioclase
↓
biotite + andalusite + cordierite + k-feldspar + ilmenite + quartz ± plagioclase
↓
biotite + sillimanite + cordierite + k-feldspar + ilmenite + quartz ± plagioclase
↓
biotite + sillimanite + cordierite + k-feldspar + ilmenite + quartz + melt ± plagioclase
Metapsammites:
muscovite + biotite + k-feldspar + quartz + ilmenite ± plagioclase
↓
biotite + cordierite + k-feldspar + quartz + ilmenite
↓
biotite + cordierite + sillimanite + k-feldspar + quartz + ilmenite + plagioclase ± melt
↓
biotite + cordierite + sillimanite + k-feldspar + quartz + melt + ilmenite
↓
biotite + cordierite + k-feldspar + quartz + melt
↓
biotite + cordierite + garnet + k-feldspar + quartz + spinel + melt

participated in reactions involving accessory minerals, at least in terms of the exchange of trace elements.

Additionally, it was recognised by some studies that there is no obvious accessory mineral source for all the Th that is typically contained within monazite (e.g. Corrie and Kohn, 2008; Kohn and Malloy, 2004). In the case of the Wing et al. (2003) study, rare grains of $ThSiO_4$ (huttonite or thorite) were identified and argued to be the Th source for monazite. In other studies, the breakdown of detrital monazite was argued to supply Th for growth of metamorphic monazite via recrystallization and/or reaction (e.g. Kohn and Malloy, 2004; Pyle and Spear, 2003). Unfortunately, no mineral chemistry data was collected for xenotime, therefore it is difficult to investigate any Th exchange between xenotime and monazite. However, the modal proportion data for apatite and monazite in combination with the element partitioning behaviour suggests that as metamorphic grade increases, the ratio of the abundances of apatite/monazite decreases, apatite/xenotime increases and monazite/xenotime increases. Given these ratios and knowledge that the abundance of xenotime decreases and the abundance of monazite and apatite increases with increasing *P–T*, it would seem likely monazite grows at the expense of xenotime and apatite. It is therefore conceivable that the source of Th for monazite growth is at least partly supplied by the breakdown of xenotime and apatite. Two silicate mineral involving *unbalanced* reactions are considered here to produce monazite at upper-amphibolite facies conditions (1) and granulite facies conditions (2).

(1)

$$\text{Xenotime} + \text{Apatite} + \text{Andalusite} + \text{Quartz} = \text{Monazite} + \text{Plagioclase} + \text{Sillimanite} + \text{Liq}$$

$$[Y/REE/U/Th(PO_4)] + [Y/REE/U/Th_3/Ca_2(PO_4)_3F/OH] + 3[Al_2SiO_5] + 5[SiO_2]$$

$$\downarrow$$

$$[Y/REE/U/Th(PO_4)] + [CaAl_2Si_2O_8] + [Al_2SiO_5] + Liq$$

In (1) the Ca component of apatite is replaced in plagioclase while the Y + REE + U + Th component of apatite and xenotime is replaced in the monazite. The Al component of andalusite is shared with plagioclase and sillimanite in polymorphic reaction. Monazite growth on the edges of apatite grains appeared when sillimanite and plagioclase first appeared in the samples, therefore it is assumed these reactions occurred simultaneously.

(2)

$$Xenotime + Apatite + Biotite = Monazite + Plagioclase + Garnet + K-feldspar + Liq$$

$$[Y/REE/U/Th(PO_4)] + [Y/REE/U/Th_3/Ca_2(PO_4)_3F] + [K(Mg/Fe)_3AlSi_3O_{10}F]$$

$$\downarrow$$

$$[Y/REE/U/Th(PO_4)] + 2[CaAl_2Si_2O_8] + [(Mg/Fe)_3Al_2Si_3O_{12}] + [KAlSi_3O_8] + Liq$$

In (2) the Y component of xenotime is shared by garnet and monazite; the Ca component of apatite is shared by garnet and plagioclase products and the K component of biotite is replaced in the k-feldspar.

The presence of F and Cl in biotite and apatite, the preference for F and Cl to partition to apatite (Fig. 16) and the observed petrographic relationships between these minerals (Figures 3 and 5) strongly suggest involvement of biotite in accessory mineral reactions. Almost all metamorphic apatite is dominated by the F end member (i.e. fluor-apatite) and contain significantly more OH than Cl (Fig. 14). Biotite is the major supply of F

for the growth of fluor-apatite (Budzyń et al., 2011; Broska et al., 2005; Finger et al., 1998; Zhu and Sverjensky, 1992), consequently biotite is intimately linked with any occurrence of accessory metamorphic fluor-apatite. Bingen et al. (1996) proposed the release of F from the breakdown of biotite under granulite conditions may increase the stability of apatite into higher temperatures. In addition to biotite, silicate minerals that contain calcium must also be involved in apatite producing mineral reactions. Garnet and plagioclase are unlikely to be the only supply of Ca for apatite growth in the Stafford Member samples as they are not present at lower grade. Allanite $[Ce/Ca/Y/La)_2(Al,Fe^{+3})_3(SiO_4)_3(F/OH)]$ is a Ca-bearing accessory mineral common in low-grade metamorphic rocks (e.g. Budzyń et al., 2011; Krenn et al., 2012; Finger et al., 1998; Tomkins and Pattison, 2007) and commonly is consumed by other accessory phases at mid-amphibolite conditions (e.g. Janots et al., 2008). Allanite consumption at lower temperatures in the Stafford Member may have promoted the growth of apatite and monazite at lower grade conditions. The following unbalanced reaction (4) is proposed to produce apatite at low grades of metamorphism.

(4)

$$Muscovite + Biotite + Allanite + Xenotime = K-feldspar + Cordierite + Apatite + Monazite + \text{Liq}$$

$$[KAl_2(AlSi_3O_{10})(F/OH)] + [K(Mg/Fe)_3AlSi_3O_{10}(F/OH)] + [Ce/Ca/Y/La)_2(Al,Fe+3)_3(SiO_4)_3(F/OH)] + [Y(PO_4)]$$

$$\downarrow$$

$$[KAlSi_3O_8] + [(Mg/Fe)_2Al_4Si_5O_{18}] + [Y/REE/U/Th(PO_4)] + [Y/REE/U/Th_3/Ca_2(PO_4)_3(F/OH)] + \text{Liq}$$

In (4) biotite and muscovite supply the F, Cl and OH for apatite, and are clearly frozen in reaction in thin section (Fig. 3 and 5). Allanite supplies the Ca for apatite, however is not observed in the Stafford Member samples likely because it has been completely

consumed at lower-amphibolite facies conditions. REEs + U + Th and PO_4 are sourced from the breakdown of xenotime.

(5)

$$Biotite + Xenotime + Plagioclase = K-feldspar + Apatite + Monazite + Garnet + Liq$$

$$[K(Mg/Fe)_3AlSi_3O_{10}(F/OH)] + [Y(PO_4)] + [CaAl_2Si_2O_8]$$

$$\downarrow$$

$$[KAlSi_3O_8] + [Y/REE/U/Th_3/Ca_2(PO_4)_3(F/OH)] + [Y/REE/U/Th(PO_4)] + [(Mg/Fe)_3Al_2Si_3O_{12}] + Liq$$

(5) is considered to provide both the F and Ca components in to provide the stability for growth of metamorphic apatite at granulite facies metamorphic conditions (e.g. Bingen et al., 1996). Here, biotite, xenotime and plagioclase are broken down to produce apatite and monazite. The reaction is similar to (4) only plagioclase is broken down in place of allanite to supply Ca for the growth of apatite and garnet as the abundance of plagioclase decreases at granulite facies conditions.

Ultimately, apatite growth is driven by the breakdown of silicate minerals, whereas monazite is almost completely dependent on the breakdown of accessory phosphate minerals such as apatite and xenotime.

The Stability of Apatite During Metamorphism of the Continental Crust

The Ivrea–Verbano region of Italy hosts a metamorphosed, garnet–bearing metasedimentary package, and like the Stafford Member, this prograde metamorphic sequence ranges from upper-amphibolite to granulite facies peak metamorphism with evidence of substantial partial melting (Redler et al., 2013). A study by Bea and Montero (1999) on the Ivrea–Verbano zone metasediments found that the modal proportion of apatite decreased markedly with metamorphic grade. Similarly, a study of

the Rogaland metamorphic complex, Norway, by Finch and Tomkins (2017) found the modal proportion of apatite was lower in higher temperature samples of metapelitic migmatites compared to lower-grade samples. However, within the Stafford Member a contradictory trend is evident; the modal proportion of apatite increases steadily and consistently with metamorphic grade and remains abundant at supra-solidus conditions (Fig. 10). Petrographic and MLA analysis of the Stafford Member revealed the average grain size of the metamorphic apatite also generally increased with metamorphic grade (Fig. 5e / 5f), whereas the number of individual grains decreased (e.g. Bea and Montero, 1999). Additionally, petrographic analyses revealed significant supra-solidus partial melting in the higher-grade samples of the Stafford Member. Partial melting of the major silicates prior to melting of accessory phosphates would remove major rock forming silicate elements from the system via melt loss, and therefore increase the relative elemental budget of accessory forming elements within the system, i.e. phosphate and calcium (Table 2). Recent work by Yakymchuk (2017) presents plots of the stability of metamorphic apatite as a function of pressure, temperature and whole rock P_2O_5 concentration using apatite dissolution equations from Harrison and Watson (1984) and Wolf and London (1995). Low P_2O_5 concentrations of 0.1 wt% in Yakymchuk (2017) accurately represent the Stafford Member whole rock geochemistry for supra-solidus and sub-solidus samples. Given the highest *P–T* conditions recorded for the samples at Mount Stafford (~ 3.9 kbar, 800° C) and 0.1 wt% P_2O_5, the solubility equations predict between 10% (Harrison and Watson, 1984) and 30% (Wolf and London, 1995) apatite dissolution in a closed monazite-melt-apatite system, which is well below the conditions for total apatite dissolution. In an open system scenario at 6 kbar with an initial whole rock 0.1% P_2O_5 amount, P_2O_5 becomes increasingly

concentrated in the residual rock with increasing temperature, as also seen in the whole rock geochemistry of this study (Table 2), suggesting apatite preservation is enhanced by melt loss, as the major P_2O_5 reservoir. These outcomes imply apatite should still be abundant in supra-solidus, granulite facies samples and the ratio of apatite to monazite discussed earlier in addition to the observed growth of monazite on the grain boundaries of apatite (Fig. 9) suggests some dissolution of apatite to produce monazite ensues at granulite facies conditions (Johnson et al., 2015).

CONCLUSIONS

(1) Metamorphic apatite growth at mid-amphibolite facies is driven by the complete consumption of low-grade allanite and detrital apatite and the partial consumption of muscovite, biotite and xenotime. Whereas metamorphic apatite growth at granulite facies is driven by the breakdown of biotite, plagioclase and xenotime (Reactions 4 and 5). Therefore, apatite growth is primarily dependent on the breakdown of silicate minerals.

(2) Metamorphic monazite growth at amphibolite facies metamorphism is primarily driven by the breakdown of xenotime and some apatite, while new monazite growth at granulite facies is primarily driven by the dissolution of apatite. (Reactions 1 and 2). Therefore, monazite breakdown is primarily dependant on the breakdown of other accessory minerals, particularly apatite.

(3) During partial melting, heat producing elements U + Th preferentially remain in monazite relative to apatite and the melt, therefore the melt and apatite is relatively depleted in HPEs. Consequently, melt loss of HPE depleted segregates would enrich the residual, partially melted, monazite-bearing rocks of the Stafford Member in HPEs and increase heat production.

(4) As the major reservoir for P_2O_5 in the continental crust, the stability and high relative abundance of apatite is sustaine at granulite facies conditions (Figures 10, 5e, 5f, 3c, 3d) by melt loss driven enrichment of P_2O_5 in residual samples (Table 2).

Although apatite was the focus of this study, it is clear from the conclusions and established literature that monazite is the more important reservoir for HPEs and therefore more relevant to the conclusions concerning heat production. Future work including xenotime compositional data and calculated *P–T* pseudosections would gain further insight into the heat production of the continental. More emphasis should be placed on investigating the whole rock distribution of U and Th (and therefore crustal heat production) by extending their minimum and maximum metamorphic conditions. The data and reactions presented herein may also prove useful for further study given the close link between metamorphic monazite and apatite.

ACKNOWLEDGEMENTS

I would like to thank my supervisor David Kelsey for his enthusiastic guidance and support throughout the course of my project. I would also like to thank Megan Williams (PhD candidate) for her continued support, advice and assistance throughout the year. The assistance provided by Benjamin Wade, Sarah Gilbert, David Kelsey and other staff at Adelaide Microscopy is also greatly appreciated. Laura Morrissey and Naomi Tucker are thanked for running the THERMOCALC tutorials and assistance with Cation Calculation from EPMA.

REFERENCES

AIUPPA, A., BAKER, D. R., & WEBSTER, J. D. (2009). Halogens in volcanic systems. *Chemical Geology*, **263**, 1-18. doi:10.1016/j.chemgeo.2008.10.005

ANDERSON, J. R., KELSEY, D. E., HAND, M., & COLLINS, W. J. (2013). Conductively driven, high-thermal gradient metamorphism in the Anmatjira Range, Arunta region, central Australia. *Journal of Metamorphic Geology*, **31**, 1003-1026. doi:10.1111/jmg.12054

ANDREOLI, M. A. G. (2006). Correlations between U, Th Content and Metamorphic Grade in the Western Namaqualand Belt, South Africa, with Implications for Radioactive Heating of the Crust. *Journal of Petrology,* **47**, 1095-1118. doi:10.1093/petrology/egl004

AYERS J. C. AND WATSON E. B. (1993) Apatite/Fluid partitioning of rare-earth elements and strontium: experimental results at 1.0 GPa and 1000°C and application to models of fluid-rock interaction. *Chem. Geol*. **110**, 299-314.

BALLARD, S., & POLLACK, H. N. (1987). Diversion of heat by Archean cratons: a model for southern Africa. *Earth and Planetary Science Letters,* **85**, 253-264.

BEA, F. (2012). The sources of energy for crustal melting and the geochemistry of heat-producing elements. *Lithos,* **153**, 278-291. doi:10.1016/j.lithos.2012.01.017

BEA, F., & MONTERO, P. (1999). Behavior of accessory phases and redistribution of Zr, REE, Y, Th, and U during metamorphism and partial melting of metapelites in the lower crust: An example from the Kinzigite Formation of Ivrea-Verbano, NW Italy. *Geochimica et Cosmochimica Acta,* **63**, 1133-1153.

BINGEN, B., DEMAIFFE, D., & HERTOGEN, J. (1996). Redistribution of rare earth elements, thorium, and uranium over accessory minerals in the course of upper-amphibolite to granulite facies metamorphism: The role of apatite and monazite in orthogneisses from southwestern Norway. *Geochimica et Cosmochimica Acta*, **60**, 1341-1354.

BOYD, F. R., & MERTZMAN, S. A. (1987). Composition and structure of the Kaapvaal lithosphere, southern Africa. In B. O. Mysen (Ed.), Magmatic Processes: Physicochemical Principles **1**, 13-24: Geochemical Society, Washington DC.

BROSKA, I., WILLIAMS, C. T., JANÁK, M., & NAGY, G. (2005). Alteration and breakdown of xenotime-(Y) and monazite-(Ce) in granitic rocks of the Western Carpathians, Slovakia. *Lithos,* **82**, 71-83. doi:10.1016/j.lithos.2004.12.007

BUDZYŃ, B., HARLOV, D. E., WILLIAMS, M. L., & JERCINOVIC, M. J. (2011). Experimental determination of stability relations between monazite, fluorapatite, allanite, and REE-epidote as a function of pressure, temperature, and fluid composition. *American Mineralogist,* **96**, 1547-1567. doi:10.2138/am.2011.3741

CATLOS, E.J., HARRISON, T.M., KOHN, M.J., GROVE, M., RYERSON, F.J., MANNING, C.E., UPRETI, B.N., (2001). Geochronologic and thermobarometric constraints on the evolution of the Main Central Thrust, central Nepal Himalaya. *Journal of Geophysical Research, Solid Earth and Planets,* **106**, 177–204.

CLAOUÉ-LONG, J., EDGOOSE, C., & WORDEN, K. (2008). A correlation of Aileron Province stratigraphy in central Australia. *Precambrian Research,* **166**, 230-245. doi:10.1016/j.precamres.2007.06.022

CORRIE, S. L., & KOHN, M. J. (2008). Trace-element distributions in silicates during prograde metamorphic reactions: implications for monazite formation. *Journal of Metamorphic Geology,* **26**, 451-464. doi:10.1111/j.1525-1314.2008.00769.x

FINCH, E. G., & TOMKINS, A. G. (2017). Fluorine and chlorine behaviour during progressive dehydration melting: Consequences for granite geochemistry and metallogeny. *Journal of Metamorphic Geology,* **35**, 739-757. doi:10.1111/jmg.12253

FINGER, F., BROSKA, I., ROBERTS, M., & SCHERMAIER, A. (1998). Replacement of primary monazite by apatite-allanite-epidote coronas in an upper-amphibolite facies granite gneiss from the eastern Alps. *American Mineralogist,* **84**, 248-258.

FLOWERS, R.M., BOWRING, S.A., TULLOCH, A.J., & KLEPEIS, K.A. (2005). Tempo of burial and exhumation within the deep roots of a magmatic arc, Fiordland, New Zealand. *Geology,* **33**, 17-20.

GASSER, D., BRUAND, E., RUBATTO, D., & STUWE, K. (2012). The behaviour of monazite from mid-amphibolite facies phyllites to anatectic gneisses: An example from the Chugach Metamorphic Complex, southern Alaska. *Lithos,* **135**, 108-122. doi:10.1016/j.lithos.2011.12.003

GELCICH, S., DAVIS, D. W., & SPOONER, E. T. C. (2005). Testing the apatite-magnetite geochronometer: U-Pb and 40Ar/39Ar geochronology of plutonic rocks, massive magnetite-apatite tabular bodies, and IOCG mineralization in Northern Chile. *Geochimica et Cosmochimica Acta,* **69**, 3367-3384. doi:10.1016/j.gca.2004.12.020

GREENFIELD, J. E., CLARKE, G. L., BLAND, M., & CLARK, D. J. (1996). In-situ migmatite and hybrid diatexite at Mt Stafford, central Australia. *Journal of Metamorphic Geology*, **14**, 413-426.

GREENFIELD, J. E., CLARKE, G. L., & WHITE, R. W. (1998). A sequence of partial melting reactions at Mt Stafford, central Australia. *Journal of Metamorphic Geology*, **16**, 363-378.

HARRISON, T. M., & WATSON, E. B. (1984). The behaviour apatite during crustal anatexis: Equilibrium and kinetic considerations. *Geochimica et Cosmochimica Acta*, **48**, 1467-1477.

HAND, M., & BUICK, I. S. (2001). Tectonic evolution of the Reynolds-Anmatjira Ranges: a case study in terrain reworking from the Arunta Inlier, central Australia. Geological Society, London, Special Publications, **184**, 237-260.

HOLLAND, T. J. B., & POWELL, R. (2011). An improved and extended internally consistent thermodynamic dataset for phases of petrological interest, involving a new equation of state for solids. *Journal of Metamorphic Geology*, **29**, 333-383. doi:10.1111/j.1525-1314.2010.00923.x

HOWLETT, D., RAIMONDO, T., & HAND, M. (2015). Evidence for 1808–1770 Ma bimodal magmatism, sedimentation, high-temperature deformation and metamorphism in the Aileron Province, central Australia. *Australian Journal of Earth Sciences*, **62**, 831-852. doi:10.1080/08120099.2015.1108364

IYER, S. S., CHOUDHURI, A. V., M.B.A., & CORDANI, U. G. (1984). Radioactive element distribution in the Archean granulite terrane of Jequi6- Bahia, Brazil. *Contributions to Mineralogy and Petrology,* **85**, 95-101.

JANOTS, E., BERGER, A., & ENGI, M. (2011). Physico-chemical control on the REE minerals in chloritoid-grade metasediments from a single outcrop (Central Alps, Switzerland). *Lithos,* **121**, 1-11. doi:10.1016/j.lithos.2010.08.023

JANOTS, E., NEGRO, F., BRUNET, F., GOFFÉ, B., ENGI, M., & BOUYBAOUÈNE, M. L. (2006). Evolution of the REE mineralogy in HP–LT metapelites of the Sebtide complex, Rif, Morocco: Monazite stability and geochronology. *Lithos,* **87**, 214-234. doi:10.1016/j.lithos.2005.06.008

JANOTS, E., ENGI, M., BERGER, A., ALLAZ, J., SCHWARZ, J. O., & SPANDLER, C. (2008). Prograde metamorphic sequence of REE minerals in pelitic rocks of the Central Alps: implications for allanite–monazite–xenotime phase relations from 250 to 610 °C. *Journal of Metamorphic Geology,* **26**, 509-526. doi:10.1111/j.1525-1314.2008.00774.x

JÕELEHT, A., & KUKKONEN, I. T. (1998). Thermal properties of granulite facies rocks in the Precambrian basement of Finland and Estonia. Tectonophysics, **291**, 195-203.

JOHNSON, T. E., CLARK, C., TAYLOR, R. J. M., SANTOSH, M., & COLLINS, A. S. (2015). Prograde and retrograde growth of monazite in migmatites: An example from the Nagercoil Block, southern India. *Geoscience Frontiers*, **6**, 373-387. doi:10.1016/j.gsf.2014.12.003

KIM, Y., YI, K., & CHO, M. (2009). Parageneses and Th-U distributions among allanite, monazite, and xenotime in Barrovian-type metapelites, Imjingang belt, central Korea. *American Mineralogist,* **94**, 430-438. doi:10.2138/am.2009.2769

KOHN, M. J., & MALLOY, M. A. (2004). Formation of monazite via prograde metamorphic reactions among common silicates: implications for age determinations. *Geochimica et Cosmochimica Acta,* **68**, 101-113. doi:10.1016/s0016-7037(03)00258-8

KORENAGA, J. (2011). Earth's heat budget: Clairvoyant geoneutrinos. *Nature Geoscience,* **4**, 581-582. doi:10.1038/ngeo1240

KRENN, E., HARLOV, D. E., FINGER, F., & WUNDER, B. (2012). LREE-redistribution among fluorapatite, monazite, and allanite at high pressures and temperatures. *American Mineralogist,* **97**, 1881-1890. doi:10.2138/am.2012.4005

KUMAR, P. S., MENON, R., & REDDY, G. K. (2007). The role of radiogenic heat production in the thermal evolution of a Proterozoic granulite-facies orogenic belt: Eastern Ghats, Indian Shield. *Earth and Planetary Science Letters,* **254**, 39-54. doi:10.1016/j.epsl.2006.11.018

LUDWIG K.L. (2012). Isoplot 3.75. A geochronological toolkit for Microsoft Excel: Berkeley Geochronology Center Special Publication No. 5, 1-72

MARKS, M. A. W., WENZEL, T., WHITEHOUSE, M. J., LOOSE, M., ZACK, T., BARTH, M., . . . MARKL, G. (2012). The volatile inventory (F, Cl, Br, S, C) of magmatic apatite: An integrated analytical approach. *Chemical Geology,* **291**, 241-255. doi:10.1016/j.chemgeo.2011.10.026

MATHEZ, E. A., & WEBSTER, J. D. (2005). Partitioning behavior of chlorine and fluorine in the system apatite-silicate melt-fluid. *Geochimica et Cosmochimica Acta*, **69**, 1275-1286. doi:10.1016/j.gca.2004.08.035

MCDONOUGH, W., & SUN, S. (1995). The composition of the Earth. *Chemical Geology,* **120**, 223-253.

PATON, C., HELLSTROM, J., PAUL, B., WOODHEAD, J., & HERGT, J. (2011). Iolite: Freeware for the visualisation and processing of mass spectrometric data. *Journal of Analytical Atomic Spectrometry,* **26**, 2508. doi:10.1039/c1ja10172b

PAYNE, J., HAND, M., BAROVICH, K. & WADE, B., 2008. Temporal constraints on the timing of high-grade metamorphism in the northern Gawler Craton: implications for assembly of the Australian Proterozoic. *Australian Journal of Earth Sciences,* **55**, 623-640.

PICHAVANT, M., MONTEL, J., & RICHARD, L. R. (1992). Apatite solubility in peraluminous liquids: Experimental data and an extension of the H~rison-Watson model. *Geochimica et Cosmochimica Acta,* **56**, 3855-3861.

PROWATKE, S., & KLEMME, S. (2006). Trace element partitioning between apatite and silicate melts. *Geochimica et Cosmochimica Acta,* **70**, 4513-4527. doi:10.1016/j.gca.2006.06.162

PYLE, J. M., & SPEAR, F. S. (2003). Four generations of accessory-phase growth in low-pressure migmatites from SW New Hampshire. *American Mineralogist,* **88**, 338-351.

REDLER, C., WHITE, R. W., & JOHNSON, T. E. (2013). Migmatites in the Ivrea Zone (NW Italy): Constraints on partial melting and melt loss in metasedimentary rocks from Val Strona di Omegna. *Lithos,* **175**, 40-53. doi:10.1016/j.lithos.2013.04.019

ROY, S., RAY, L., BHATTACHARYA, A., & SRINIVASAN, R. (2007). Heat flow and crustal thermal structure in the Late Archaean Closepet Granite batholith, south India. *International Journal of Earth Sciences,* **97**, 245-256. doi:10.1007/s00531-007-0239-2

RUBATTO, D., HERMANN, J., & BUICK, I. S. (2006). Temperature and Bulk Composition Control on the Growth of Monazite and Zircon During Low-pressure Anatexis (Mount Stafford, Central Australia). *Journal of Petrology,* **47**, 1973-1996. doi:10.1093/petrology/egl033

SCRIMGEOUR, I.R. 2013 Chapter 12: Aileron Province. IN 'Geology and mineral resources of the Northern Territory', Ahmad M. and Munson T.J. (compilers) Northern Territory Geological Survey. Special Publication 5 12:1-74

SMITH, H., & BARREIRO, B. (1990). Monazite U-Pb dating of staurolite grade metamorphism in pelitic schists. *Contributions to Mineralogy and Petrology*, **105**, 602-615.

SPEAR, F. S. (2010). Monazite–allanite phase relations in metapelites. Chemical Geology, **279**, 55-62. doi:10.1016/j.chemgeo.2010.10.004

SPEAR, F. S., & PYLE, J. M. (2002). Apatite, Monazite, and Xenotime in Metamorphic Rocks. *Reviews in Mineralogy and Geochemistry,* **48**, 293-335. doi:10.2138/rmg.2002.48.7

SPEAR, F. S., & PYLE, J. M. (2010). Theoretical modeling of monazite growth in a low-Ca metapelite. *Chemical Geology,* **273**, 111-119. doi:10.1016/j.chemgeo.2010.02.016

STEPANOV, A. S., HERMANN, J., RUBATTO, D., & RAPP, R. P. (2012). Experimental study of monazite/melt partitioning with implications for the REE, Th and U geochemistry of crustal rocks. *Chemical Geology*, **300**, 200-220. doi:10.1016/j.chemgeo.2012.01.007

STEWART, A. J. SHAW, R. D. BLACK, L. P. (1984). The Arunta Inlier: a complex ensialic mobile belt in central Australia. Part 1: stratigraphy, correlations and origin. *Australian Journal of Earth Sciences,* **31**, 445-455.

SUZUKI, K. A., M, & KAJIZUKA, I. (1994). Electron microprobe observations of Pb diffusion inmetamorphosed detrital monazites. *Earth and Planetary Science Letters,* **128**, 391-405.

TOMKINS, H. S., & PATTISON, D. R. M. (2007). Accessory phase petrogenesis in relation to major phase assemblages in pelites from the Nelson contact aureole, southern British Columbia. *Journal of Metamorphic Geology,* **25**, 401-421. doi:10.1111/j.1525-1314.2007.00702.x

VERNON, R.H., CLARKE, G.L. & COLLINS, WI. (1990). Mid-crustal granulite facies metamorphism: low-pressure metamorphism and melting, Mount Stafford, central Australia. In: Ashworth, J.R. & Brown, M. (editors), High-temperature metamorphism and crustal anatexis. Special Publication of the Mineralogical Society of Great Britain and Ireland, **2**, 272- 319.

VRY, J., COMPSTON, W., & CARTWRIGHT, I. (1996). SHRIMP II dating of zircons and monazites: reassessing the timing of high-grade metamorphism and fluid flow in the Reynolds Range, northern Arunta Block, Australia. *Journal of Metamorphic Geology,* **14**, 335-350.

WANG, W.-R., DUNKLEY, E., CLARKE, G. L., & DACZKO, N. R. (2014). The evolution of zircon during low-Partial melting of metapelitic rocks: theoretical predictions and a case study from Mt Stafford, central Australia. *Journal of Metamorphic Geology,* **32**, 791-808. doi:10.1111/jmg.12091

WHITE, R. W., POWELL, R., & CLARKE, G. L. (2003). Prograde Metamorphic Assemblage Evolution during Partial Melting of Metasedimentary Rocks at Low Pressures: Migmatites from Mt Stafford, Central Australia. *Journal of Petrology,* **44**, 1937-1960. doi:10.1093/petrology/egg065

WING, B. A., FERRY, J. M., & HARRISON, T. M. (2003). Prograde destruction and formation of monazite and allanite during contact and regional metamorphism of pelites: petrology and geochronology. *Contributions to Mineralogy and Petrology,* **145**, 228-250. doi:10.1007/s00410-003-0446-1

WOLF, M. B., & LONDON, D. (1995). Incongruent dissolution of REE- and Sr-rich apatite in peraluminous granitic liquids Differential apatite monazite and xenotime solubilities during anatexis. *American Mineralogist,* **80**, 765-775

YAKYMCHUK, C. (2017). Behaviour of apatite during partial melting of metapelites and consequences for prograde suprasolidus monazite growth. Lithos, **274**, 412-426. doi:10.1016/j.lithos.2017.01.009

ZHU, C., & SVERJENSKY, D. A. (1992). F-Cl-OH partitioning between biotite and apatite. *Geochimica et Cosmochimica Acta.* **56**, 3435-3467

APPENDIX A: METHODS

Sample Collection and Selection
For this study, twelve representative samples were selected from Mount Stafford (six metapelite, six metapsammite) from a much larger set of samples with an equal contribution from each metamorphic facies; mid-amphibolite, upper-amphibolite, granulite. These twelve samples were selected from the larger set as they were thought to be representative of their respective metamorphic grades. There are four samples from each mid-amphibolite, amphibolite and granulite metamorphic facies, with two of each metapelite and two metapsammite. Table 1 below lists the sample names and number and their metamorphic grade.
Figure 1 is a map of the study area that displays the original sample location of each of the twelve samples.

Electron Probe Microanalysis (EPMA)
Electron probe microanalysis was performed on each thin section with a Cameca SXFive electron microprobe at Adelaide Microscopy. This was done for apatite, monazite and silicate/oxide minerals in each polished thin section to determine the wt% of each major element. The data were used in the processing of the LA-ICP-MS data as there needs to be a known wt% value for each mineral analysed in Iolite – which EPMA can supply.
Major element data was collected using electron probe microanalysis (EPMA) on monazite, apatite, Fe–Ti oxides and silicate minerals in each sample using a Cameca SXFive electron microprobe with an accelerating voltage of 15 kV and beam current of 20 nA. Elements that were measured for apatite and monazite include: Ca, Mg, Ti, Si, Al, Fe, Mn, Cl, F, La, Ce, Nd, K, P, Na, S, As, Sr and Y (+ U and Th in monazite). Elements measured for silicates and Fe–Ti oxides were: Ca, Mg, Ti, Si, Al, Fe, Mn, Cr, Cl, F, K, P, Na, Ba, V, Zn, Zr and Sr. Xenotime, thought present in the samples were not analysed by EPMA due to time limitations. Data calibration and reduction was carried out in Probe for EPMA, distributed by Probe Software Inc. Poor and contaminated analyses were found and removed from the dataset by using cation calculation spreadsheets and monitoring K, Mg, Al and Si concentrations for apatite and monazite.

Pre-selecting mineral grains for analysis
1) Minerals that were analysed on the microprobe are also analysed on the laser. Therefore when considering which grains to use, the intended laser spot size must also be considered.
2) Mineral grains large enough for the intended laser spot size (13 microns or greater for monazite, 23 microns or greater for silicates/oxides and X microns or greater for apatite) were selected.
3) The grains were pre-selected using petrography and the BSE images to ensure a balanced measurement between different mineral textural settings in each thin section.
4) Grains were circled and labelled on the BSE images for locating later.

EPMA operational procedure

1)Minerals were located using the assistance of BSE and MLA maps digitally attached to the image mentioned in ***pre selecting mineral grains for analysis***
2) Focus calibration was performed prior to plotting each point.
3) points were plotted for the probe to analyse later, often across large grains, transects were plotted to identify any growth zoning.
4) Once all points were plotted the automatic electron probe procedure was initiated and data compiled in the program.
5) Data reduction was performed in probe for EPMA.

Laser Ablation Inductively Coupled Plasma Mass Spectrometry (LA-ICP-MS)

Laser ablation inductively coupled plasma mass spectrometry was performed on silicates, oxides, monazites and apatites in each thin section with an ASI Resolution Excimer 193 nm laser and an Agilent 7900 ICP mass spectrometer. Back scattered electron images overlain with MLA maps were used in ASI's GeoStar μGIS software to plot points for ablation. Agilent's Masshunter 4.1 software was used to output the mass spectrometry data. Data reduction was performed using the Iolite software package.
Laser Ablation–Inductively Coupled Plasma–Mass Spectrometry (LA–ICP–MS) isotopic and trace element analyses were undertaken on apatite, monazite, Fe–Ti oxides and various silicate minerals using an ASI M-50-LR 193 nm excimer laser in a He ablation atmosphere coupled to an Agilent 7700cx ICP–MS. Isotopes measured for geochronology were 202Hg, 204Pb, 206Pb, 207Pb, 208Pb, 232Th and 238U. Trace element isotopes measured concurrently with the geochronology isotopes were 29Si, 31P, 43Ca, 89Y, 90Zr, 139La, 140Ce, 141Pr, 146Nd, 147Sm, 153Eu, 157Gd, 159Tb, 163Dy, 165Ho, 166Er, 169Tm, 172Yb and 175Lu. Each analysis was pre-ablated with five laser pulses to remove any surface contamination. Apatite was ablated for 40 seconds after a hold time of 30 seconds using a spot size of 13 microns and fluence of 2.0 J/cm2. Monazite was ablated for 30 seconds after a hold time of 30 seconds using a spot size of 13 microns and fluence of 2.0 J/cm2. Silicate minerals and Fe–Ti oxides were ablated for 50 seconds after a hold time of 30 seconds, using a spot size of 29 microns and fluence of 3.5 J/cm2. Data reduction for both trace elements and geochronology was carried out by utilizing the Iolite software package (v3.31) (Paton et al., 2011). Instrument drift was corrected by standard–sample bracketing every 15 (monazite) to 20 (silicate and apatite) analyses. Element fractionation bias was corrected by calibration performed on certified synthetic and natural mineral standards from Astimex Ltd and P&H Associates, specifically MAdel standard for monazite. Geochronology calibration accuracy was determined on monazite using internal Ambat and 94-222/Bruna-NW standards. NIST610 and NIST612 glass were used as a standard for the trace element composition of monazite, apatite and silicates. For geochronology, signal selection was carried out by monitoring the Si and P signal in addition to the live concordia plot feature in Iolite. Age data were plotted using Isoplot 3.75 (Ludwig, 2012). For trace elements, signal selection of individual analyses was carried out by monitoring the Si signal (contamination) and the P signal (expected) in both monazite and apatite. Trace element concentrations for each mineral analysis were measured and tabulated in parts per million (ppm) by using major element data from electron probe microanalyses as an internal standard. As the goal of the study is to identify trends in mineral chemistry to assist with identifying mineral reactions with increasing metamorphic grade, all measured trace element compositions of apatite and monazite were plotted on chondrite normalised spider diagrams (McDonough and Sun 1995).

Pre-selecting mineral grains for analysis
1) Minerals that were analysed on the probe were also analysed on the laser mass spectrometer. These include monazite, apatite and rock forming silicate/oxide minerals.
2) The same mineral grains analysed on the probe (where possible) were analysed on the laser, the grain labels were consistent across use of the two instruments.
3) As with EPMA analysis, silicates were pre-selected using petrography and the BSE images to ensure a balanced measurement between different mineral textural settings in each thin section.
4) Grains were circled and labelled on the BSE images for locating later.

LA-ICP-MS preparatory protocols
1) The environment surrounding the laser was cleaned and set at a constant temperature.
2) A notebook and clean pen was prepared for recording the location of thin sections on the sample tray.

3) Gloves were put on and if the thin section tray was already out, it was placed on a clean paper towel, other samples were removed and the thin sections to be analysed were placed on the tray and secured under the springs.
IF the tray was still in the apparatus, it was removed and the thin sections replaced.
4) Mineral appropriate standard sample sections were also inserted into the tray.
5) The tray was reinserted into the apparatus.
6) Once the tray was re-inserted ***'LA-ICP-MS operating protocols'*** was performed.

LA-ICP-MS operational protocols

1)Minerals were located using the assistance of BSE and MLA maps digitally attached to the image, 2) Focus calibration was performed prior to plotting each point.
3) points were plotted for the laser to ablate and collect data through the MS later.
4) once all points were plotted the automatic ablation procedure was started and mass spectrometry data was collected of the ablated material of each mineral.
5) In preparation for Iolite data reduction, extract just the .csv output files from the LA-ICP-MS data output and place them into a folder – one folder for each mineral (all silicates/oxides can go into one folder, apatite and monazite should be separated)

Iolite data reduction (geochronology)
1) Iolite was opened (from Igor software), data were imported by selecting the folder containing the extracted .csv files for **monazite only**.
2) The baseline signal was extracted from the signal by using the active selections tool, all samples listed were selected and the time range of the spline was the laser 'hold time' that occurred prior to 'cleaning' – in this case the first 30 seconds were 'hold time'. Baseline_1 was selected and a 'step forward' spline type was applied.
3) A spline was applied to the standards used on the laser by using the active selections tool, all standards that needed to be splined were selected and the true signal portion of the data were selected. A smoothed 7 spline type was applied to both MAdel and NIST 610 standards.
4) An unknown selection was applied to all unknown samples by using the active selections tool, all unknown samples were selected and the true signal portion of the data were selected. No spline was needed for unknown samples.
5) The Geochronology data reduction scheme was selected for processing geochronology data.
6) Signal selection was performed on the unknown samples by changing the displayed signals in Iolite to the UPb raw age data and opening the 'VizualAge' tool in Iolite. Pb204 was displayed on the grey axis on the graphic window to identify natural lead contamination. By using a combination of live concordia diagrams, raw age data output and natural lead contamination in the graphic window, the signals of the unknown samples were narrowed to just the cleanest or most concordant part of the signals.
7) The data were then processed by pressing the 'CRUNCH DATA' button in the main iolite window. Down-hole fractionation corrections were produced and were checked for any significant residual variation across the signals. (refer to Iolite Manual v3.4 section 3.4.1 – Downhole Fractionation Correction)
8) The data were then output into excel spreadsheets and concordia diagrams were generated using the ___ excel plugin.

Iolite data reduction (trace element)
1) Iolite was opened (from Igor software), data were imported by selecting the folder containing the extracted .csv files for a mineral (silicate/oxides, monazite or apatite).
2) The baseline signal was extracted from the signal by using the active selections tool, all samples listed were selected and the time range of the spline was the laser 'hold time' that

occurred prior to 'cleaning' – in this case the first 30 seconds were 'hold time'. Baseline_1 was selected and a 'step forward' spline type was applied.
3) A spline was applied to the standards used on the laser by using the active selections tool, all standards that needed to be splined were selected and the true signal portion of the data were selected. A smoothed 7 spline type was applied to both MAdel and ___ standards.
4) An unknown selection was applied to all unknown samples by using the active selections tool, all unknown samples were selected and the true signal portion of the data were selected. No spline was needed for unknown samples.
5) The Trace_Element_IS data reduction scheme was selected for processing trace element data of the minerals (refer to Iolite Manual v3.4 section 3.2 – Trace Element IS DRS).
6) Signal selection was performed on the unknown samples by changing the displayed red and grey axis signals in Iolite to two elements that characterise a mineral (e.g. Ce and La in monazite, or Ca and P in apatite). By using the flattest, most consistent part of the element signal for a given mineral, the data of the unknown samples were narrowed to just the cleanest part of the mineral. This also assisted in determining where the laser may have ablated through a targeted grain into an unwanted grain.
7) The data were then processed by pressing the 'CRUNCH DATA' button in the main iolite window.
8) The data were then output into excel spreadsheets for organisation into different minerals (if silicate) and different samples.

Scanning Electron Microscope Analysis (SEM)
Back scattered electron (BSE) images and MLA maps of each polished thin section were acquired with the use of a FEI Quanta 600 scanning electron microscope + MLA at Adelaide Microscopy, UofA.

SEM preparatory protocols
1) The SEM room was cleaned and set at a constant temperature.
2) A notebook and clean pen was prepared for recording the location of thin sections on the sample tray.
3) Gloves were put on, the thin sections were taken out of their storage box and placed on the table face up in the arrangement they will go into the SEM. This configuration was noted in the prepared notebook.
4) The thin sections were then placed on the sample tray in the configuration written in the notebook, they were secured face-up (polished, exposed side up) with a small piece of carbon tape ~10 x 2.5 mm on the back of the thin section slide attached to the sample tray.
5) The already carbon coated thin sections were then each attached to the frame of the sample tray with another small piece of carbon tape (approx. dimensions as above). The carbon coat was in contact with the carbon tape which was in contact with the frame on EACH thin section. i.e. the carbon coated thin section was connected to be in contact with the sample tray frame via carbon tape.
6) The chamber inside the SEM apparatus was vented to restore normal atmospheric pressure in the chamber.
7) The chamber was opened, the sample tray was placed inside the open chamber and secured with a screwdriver. The chamber was closed carefully to ensure nothing would hit the back-scatter plate located at the top of the chamber.
8) The chamber was then pumped to restore vacuum conditions.
9) The sample tray was then raised to just below the 10mm line on the camera screen to set approximate working distance to 10mm.

Petrographic Analyses
Each sample underwent petrographic analysis to gain a mineralogical understanding and

produce a textural description of each sample. A Nikon optical microscope at the University of Adelaide was used along with the pre-cut thin section samples.

1) Thin sections were observed using a transmitted light microscope fitted with a cross-polarising lens.
2) Each thin section was observed separately to establish the dominant silicate and oxide minerals in each sample.
3) Modal proportions of these silicate and oxide minerals were estimated in each sample to use as evidence for approximate mineral stability.
4) Textural relationships were identified and noted to assist the identification of peak mineral assemblage and solid-state reaction relationships.
5) BSE and MLA images were employed to locate accessory minerals such as apatite, monazite, xenotime and zircon in each thin section.
6) The textural setting and style of accessory minerals (including any mineral contact, overgrowth, inclusion relationships) were identified to propose relationships involved in the growth or consumption of accessory phases.
Initially, abundant silicates, aluminosilicates and oxides were searched for in each sample and described in terms of their spatial and temporal relationship with other minerals. This was done to establish a basic sequence of growth and establish a peak metamorphic assemblage for each sample. Apatite was then examined in each sample, noting what mineral(s) they were in contact with and noting the style of contact (temporal growth relationship). This was done to obtain a general understanding of apatite involving reactions in each sample.
Once a basic understanding of the mineralogy and potential metamorphic reactions were obtained for the samples, a more detailed analysis of the thin sections could be undertaken.

1) Minerals that are chemically similar or possess common elements with accessory minerals were identified for each of the four accessory minerals.
2) EPMA and LA-ICP-MS data on accessory minerals (monazite and apatite) and relevant silicate minerals were compiled for analysis.
3) Literature regarding known metamorphic reactions between accessory and other minerals was searched for, identified and collated.
4) Petrographic analyses were continued in further detail in order to propose reactions involving accessory minerals. This was done in collaboration with published reactions from literature and trace/major element data in both silicate and accessory minerals.

Modal Analyses of Thin Sections
Modal proportion analyses of apatite, monazite, xenotime & zircon were performed on each sample using the MLA and BSE output images and Adobe Photoshop CS6 software package. Back scattered electron (BSE) image maps and mineral liberation analysis (MLA) maps (Appendix D) of each polished thin section were acquired using a FEI Quanta 600 scanning electron microscope at Adelaide Microscopy. BSE maps were acquired for reference in petrography, LA–ICP–MS and EPMA. BSE and MLA maps show the location of accessory minerals and were used to estimate their abundance in thin section.

1) A mineral was selected for modal proportion analysis.
2) MLA images of the relevant minerals along with the original BSE images were loaded into Photoshop.
3) The select tool was used to select the rock within each BSE image.
4) The pixel counting histogram was used to calculate the total number of pixels in the thin section (P_{tn}).
5) Select -> Color Range tool was used on the MLA images to select a particular mineral.
6) The pixel counting histogram was used again to calculate the number of pixels occupied by said mineral (P_{mn}).

7) Modal proportion for said mineral was defined as:
Mod ($_{mineral}$) % = (P_{mn} / P_{tn}) * 100
This gave the measured surface area of a mineral relative to the total mineral surface area. Unfortunately, the method assumes each thin section is representative of the rock and was therefore susceptible to systematic misrepresentation due to variations in the orientation of the thin section slice. For example, some minerals have a preferred orientation and will occur more (or less) frequently on a 2D plane in some orientations. The 'occurrence count' and 'line-intercept count' methods could also estimate modal proportions but they do not consider the size of the grains.
Once the modal proportion analyses were completed, the raw data was processed into excel graph format for presenting.

1) The data for all the minerals with estimated modal proportions was compiled into an excel spreadsheet.
2) The data was subdivided into two categories; metapelitic composition and metapsammitic composition.
2) A standard point scatter plot was selected to present all the data of accessory minerals.
3) Sample name/number was selected for the X-axis and ordered in metamorphic grade (i.e. lowest-grade sample on the left and highest-grade sample on the right). Modal proportion in % units was selected for the Y-axis.
4) Modal proportion data for each mineral in each sample was then applied to the graph, with a different graph for each composition and a different data series for each mineral.
6) Trendlines were given to each series (mineral) to see the trend of a mineral through grade.

APPENDIX B: WHOLE ROCK GEOCHEMISTRY

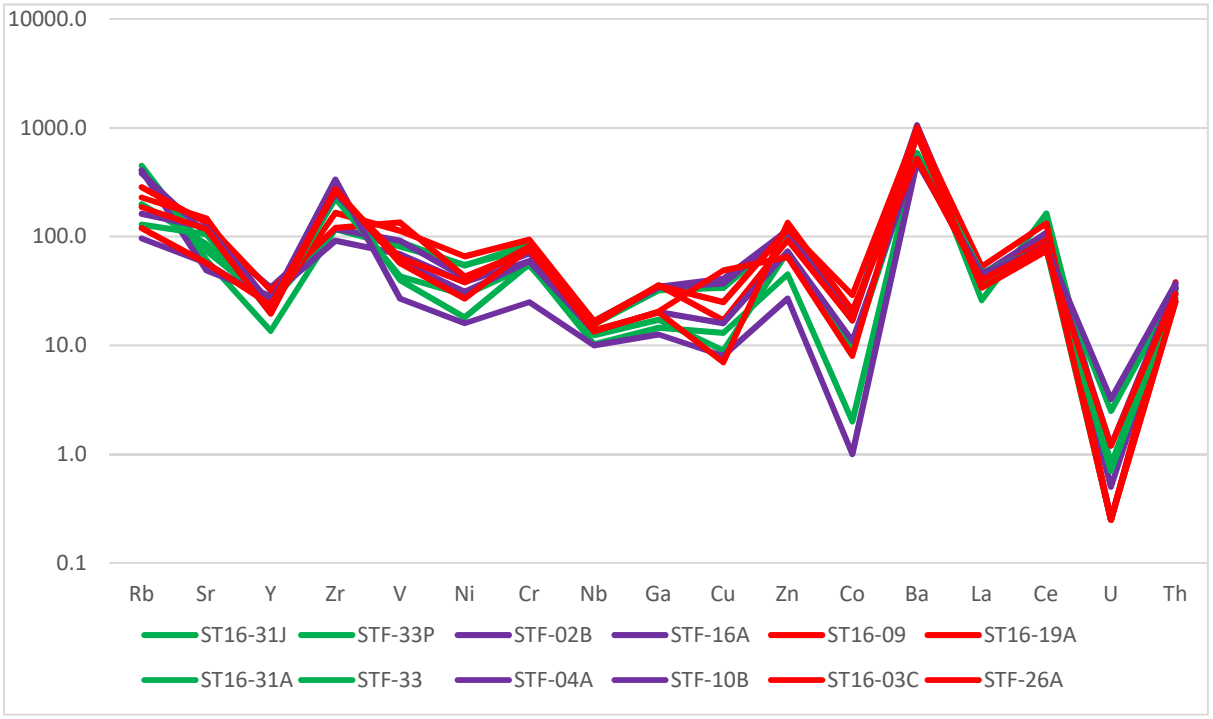

Figure B1: Trace element whole rock geochemistry spider diagram (ppm)

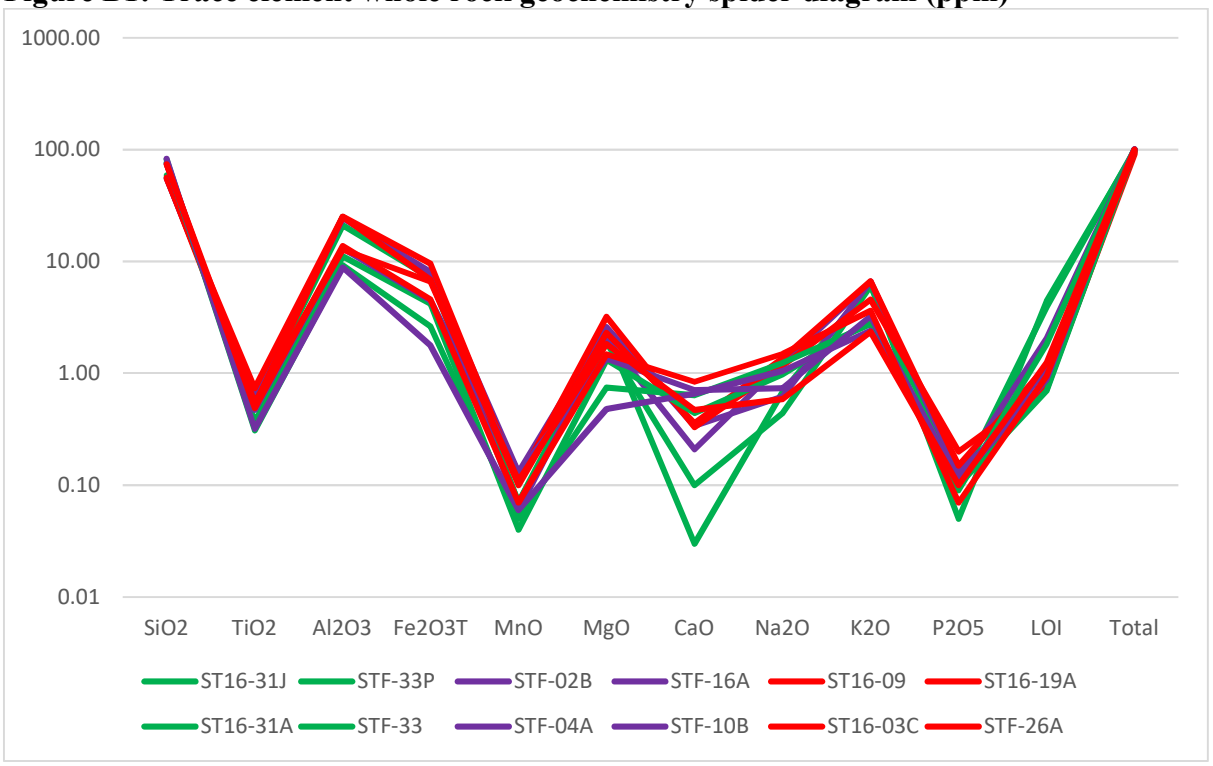

Figure B2: Major element whole rock geochemistry spider diagram (wt%)

APPENDIX C: GEOCHRONOLOGY

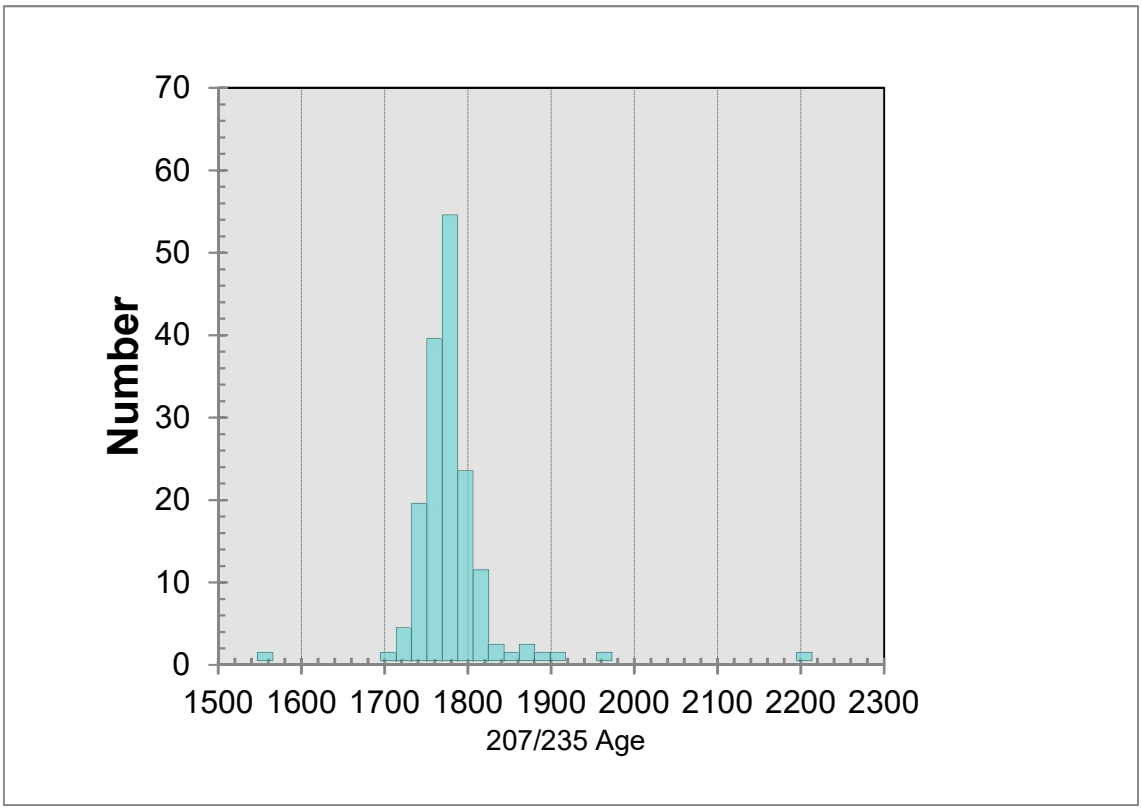

The distribution of all geochronology results on samples (excluding the discordant analyses) are plotted on the above distribution histogram. There are a few > c. 1820 Ma analyses that are concordant and therefore likely detrital, however the majority of these are in the low-grade samples of 31J and 31A. The majority >50 analyses plot around the c. 1775-1785 Ma age results, implying the majority of monazite grains are metamorphic.

APPENDIX D: BSES AND MLAS

STF-33P

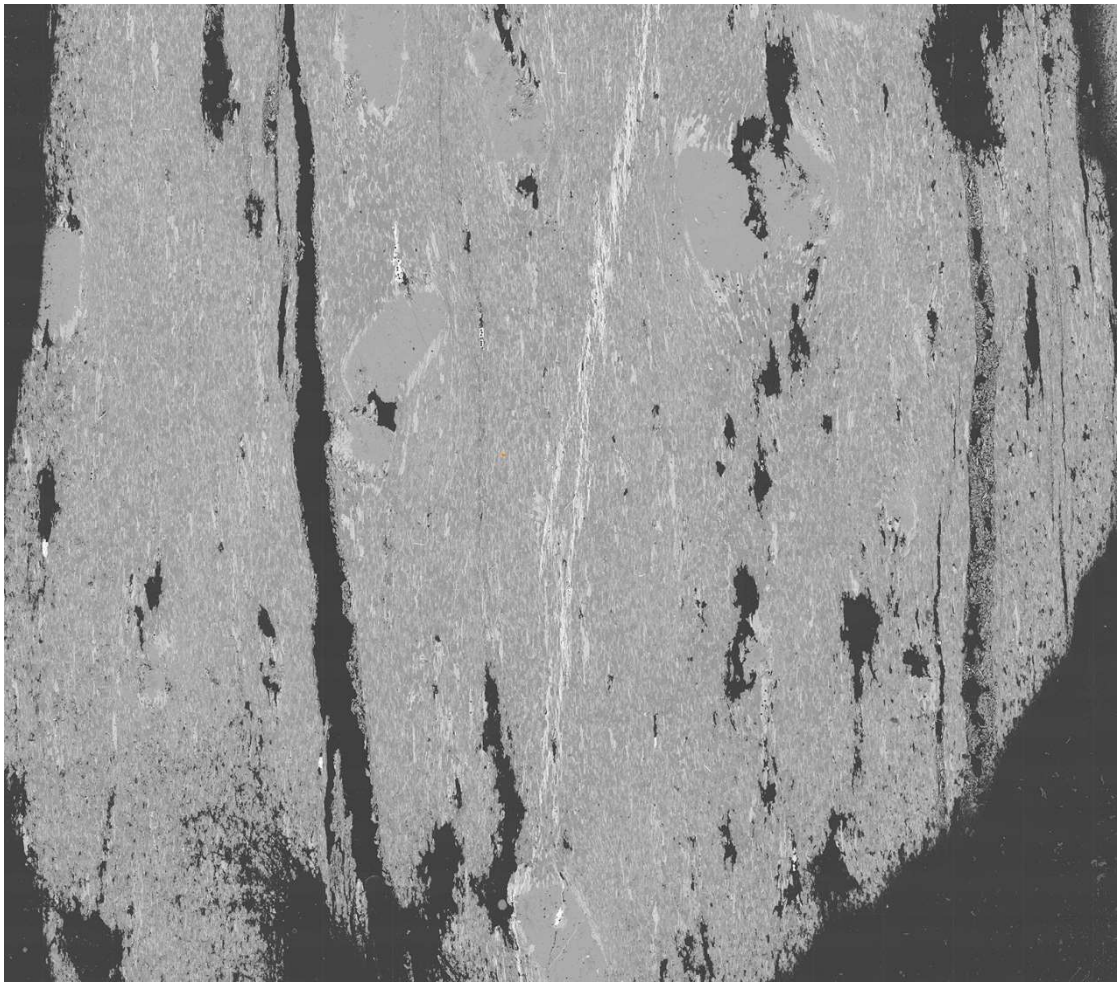

ST16-31J

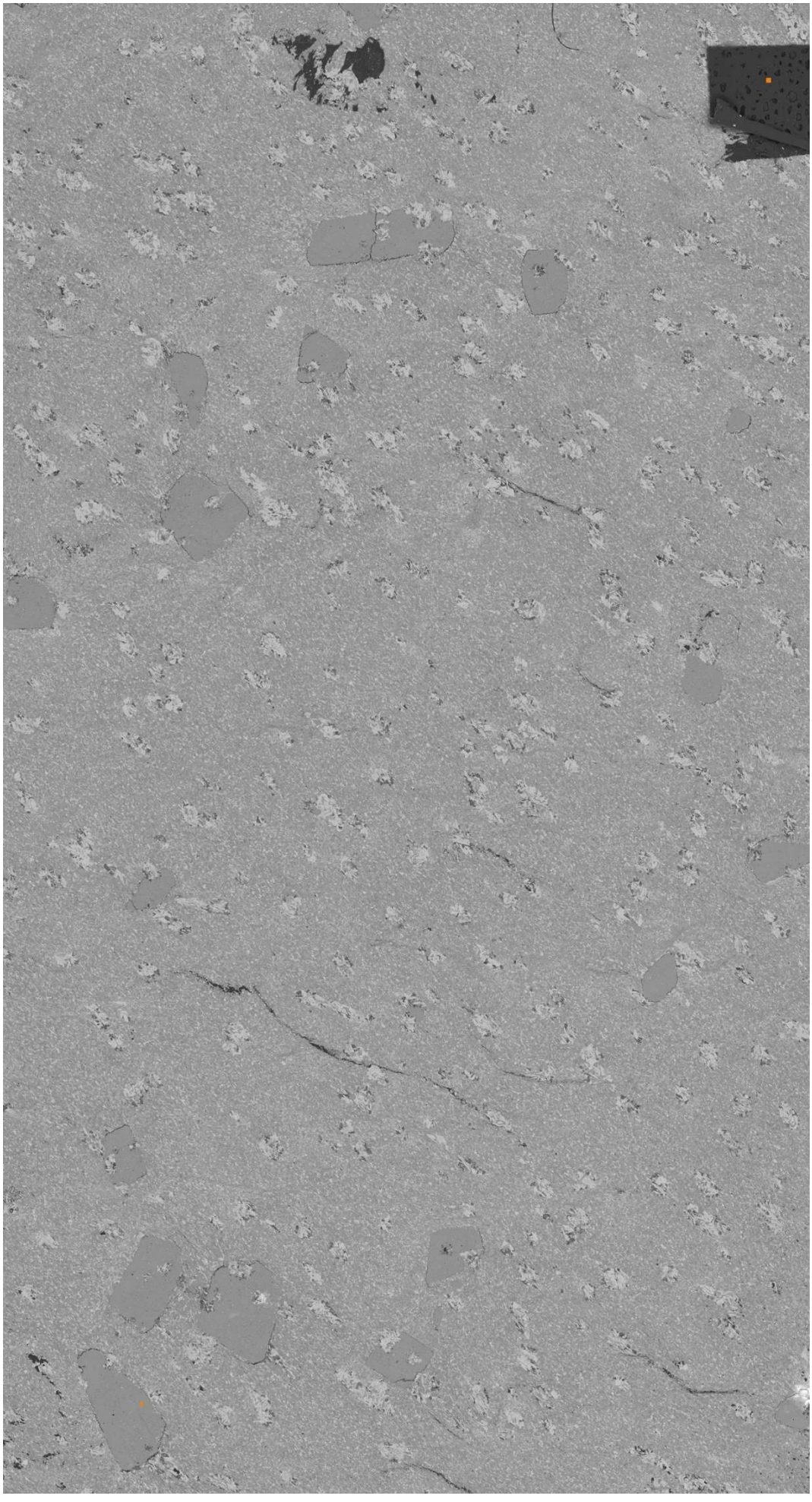

STF-02B

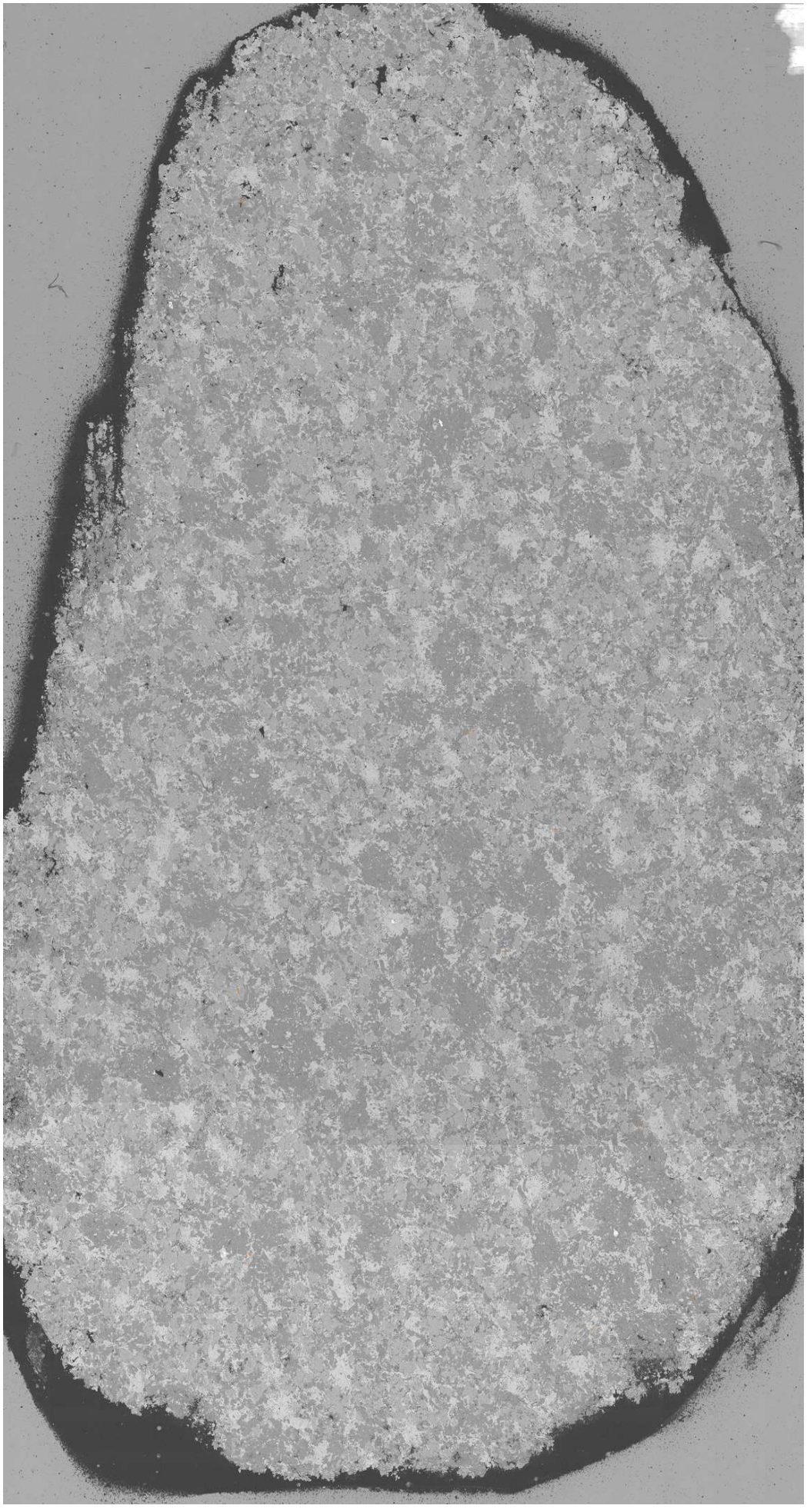

STF-16A

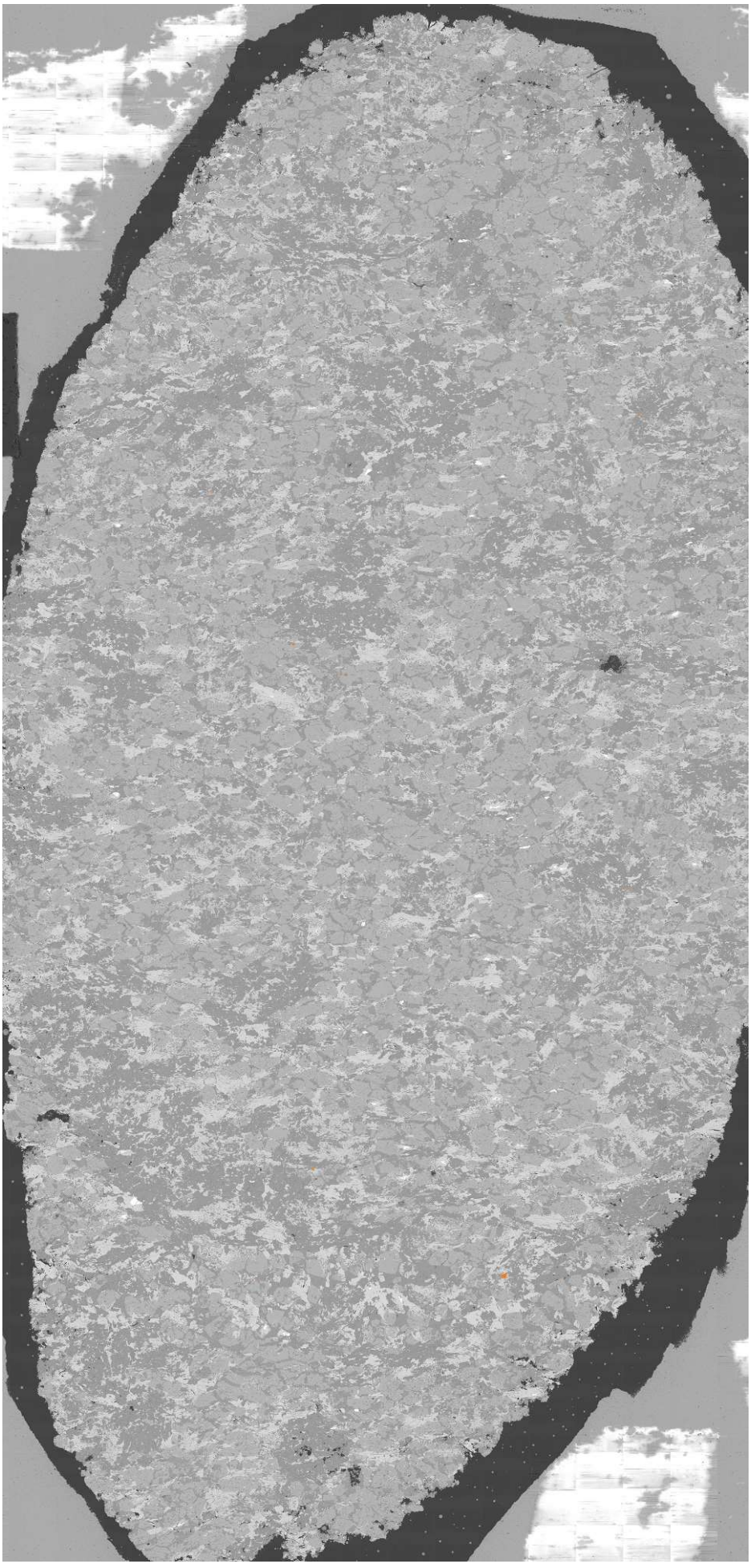

ST16-09

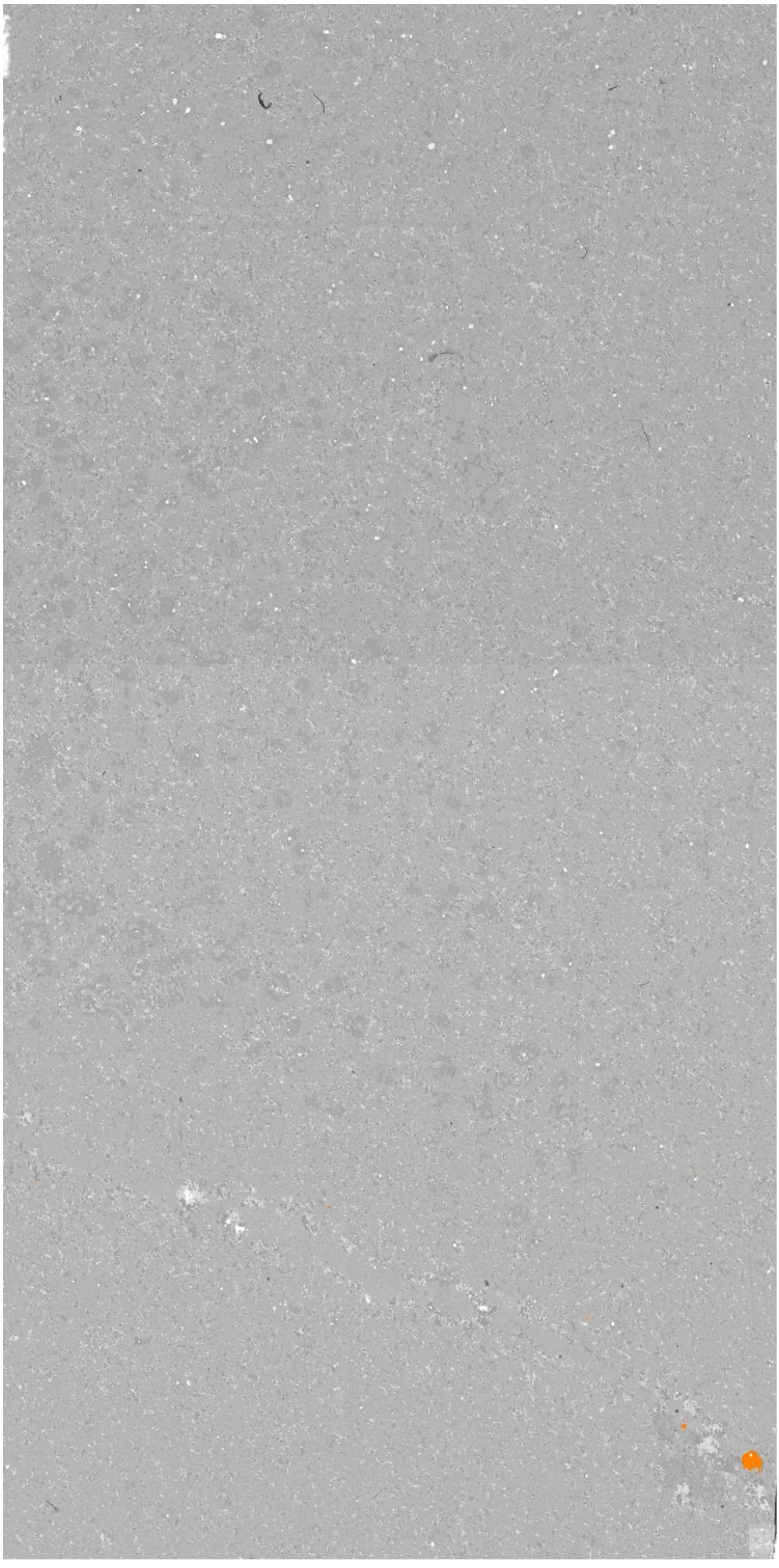

ST16-19A

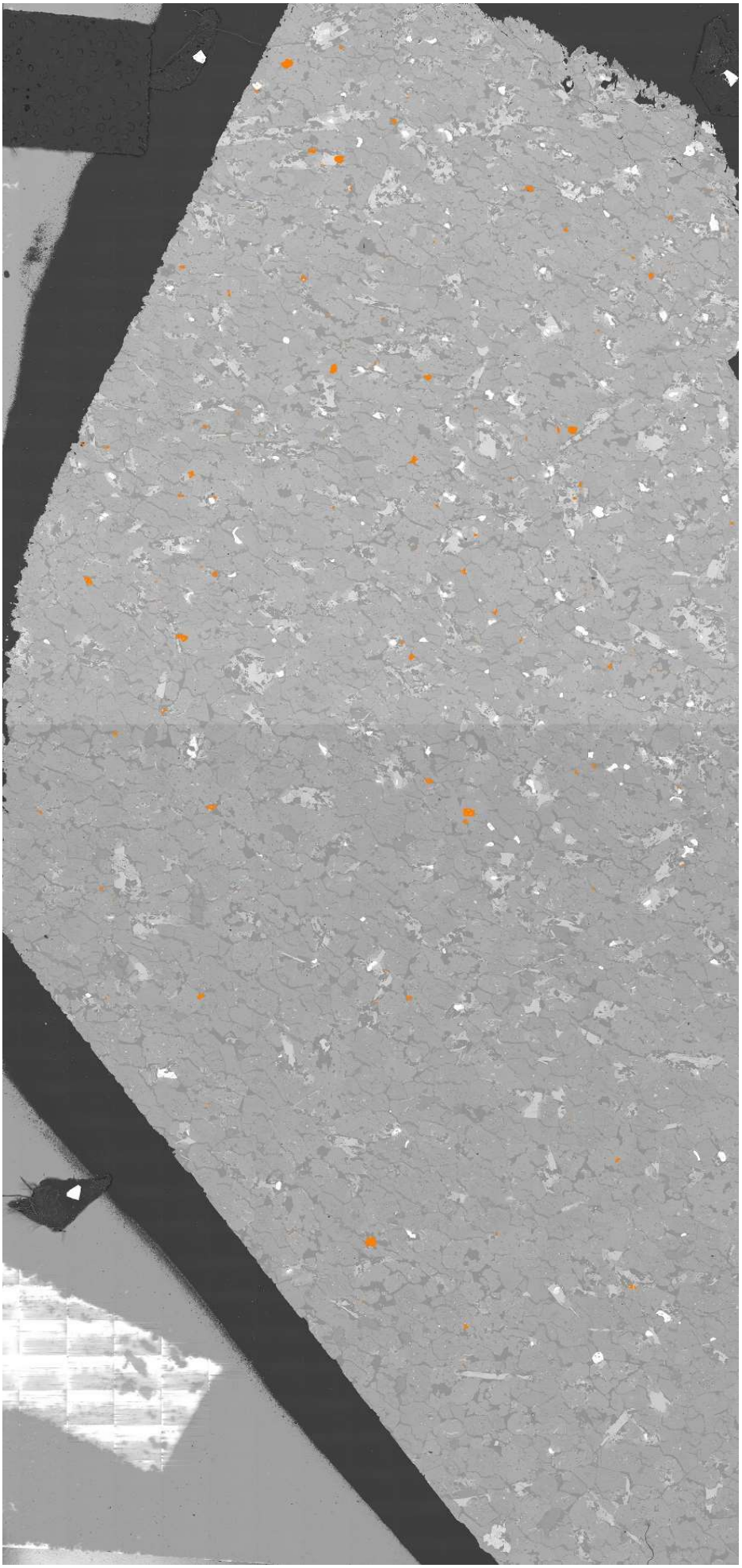

ST16-31A

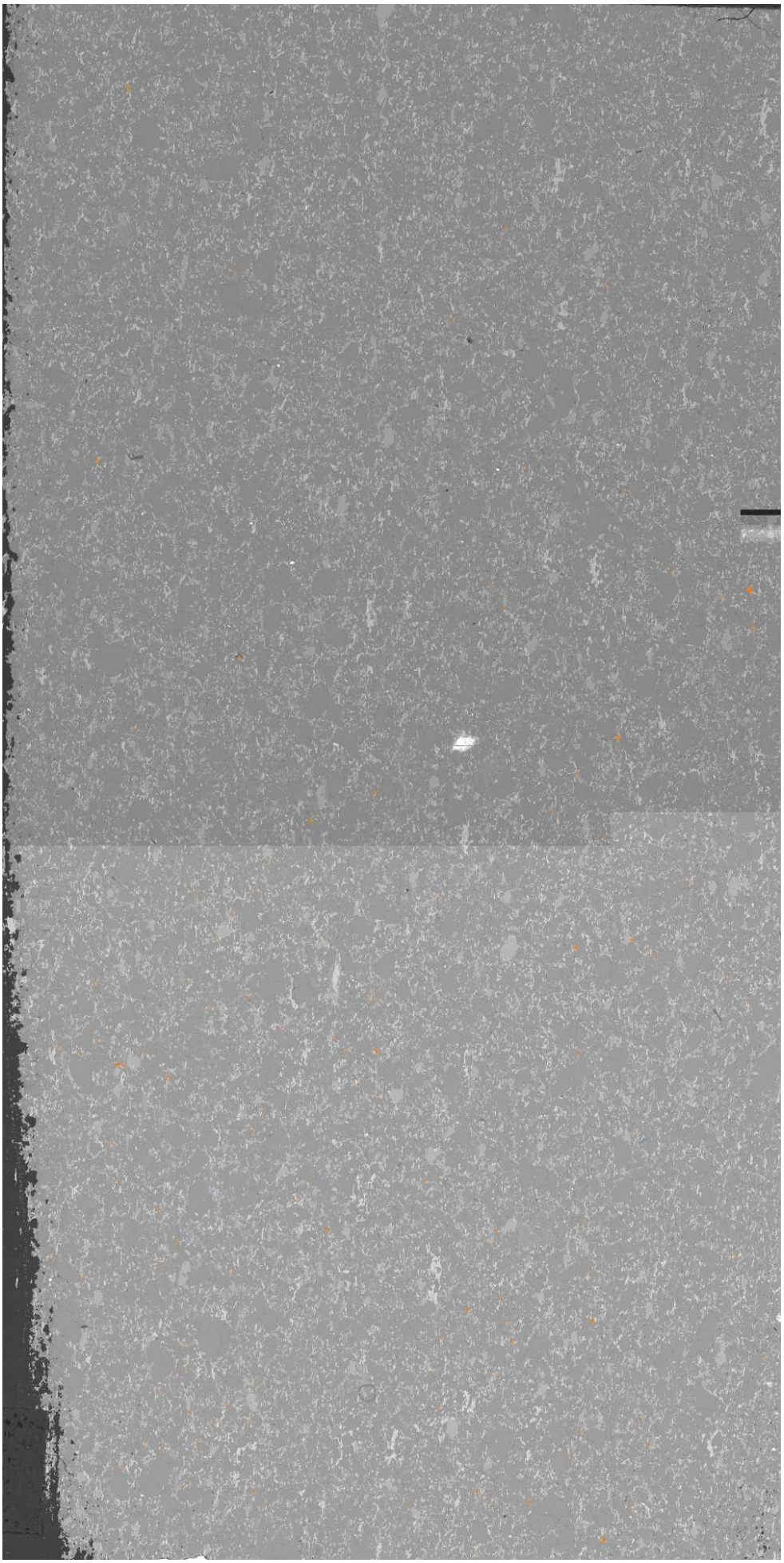

STF-33

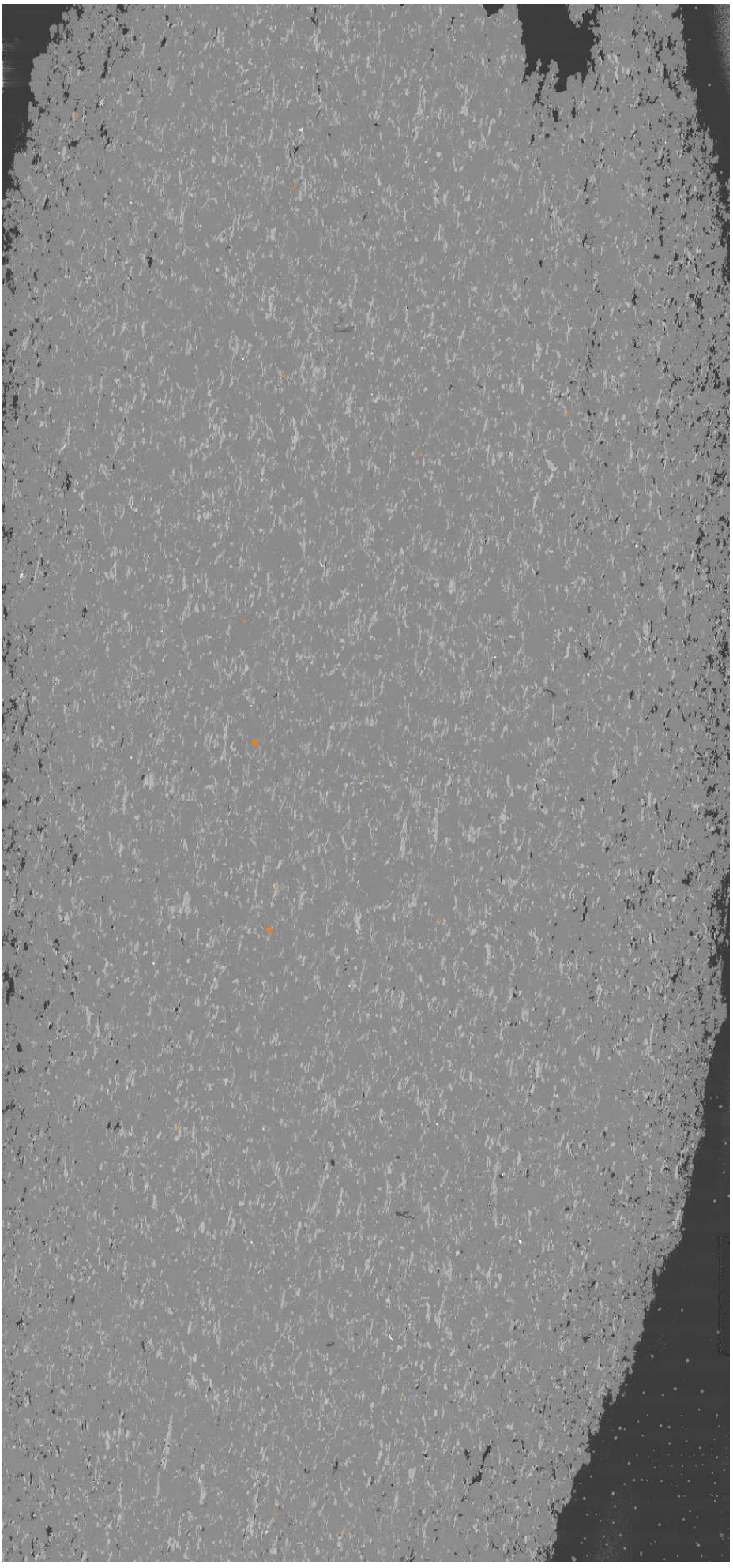

STF-04A

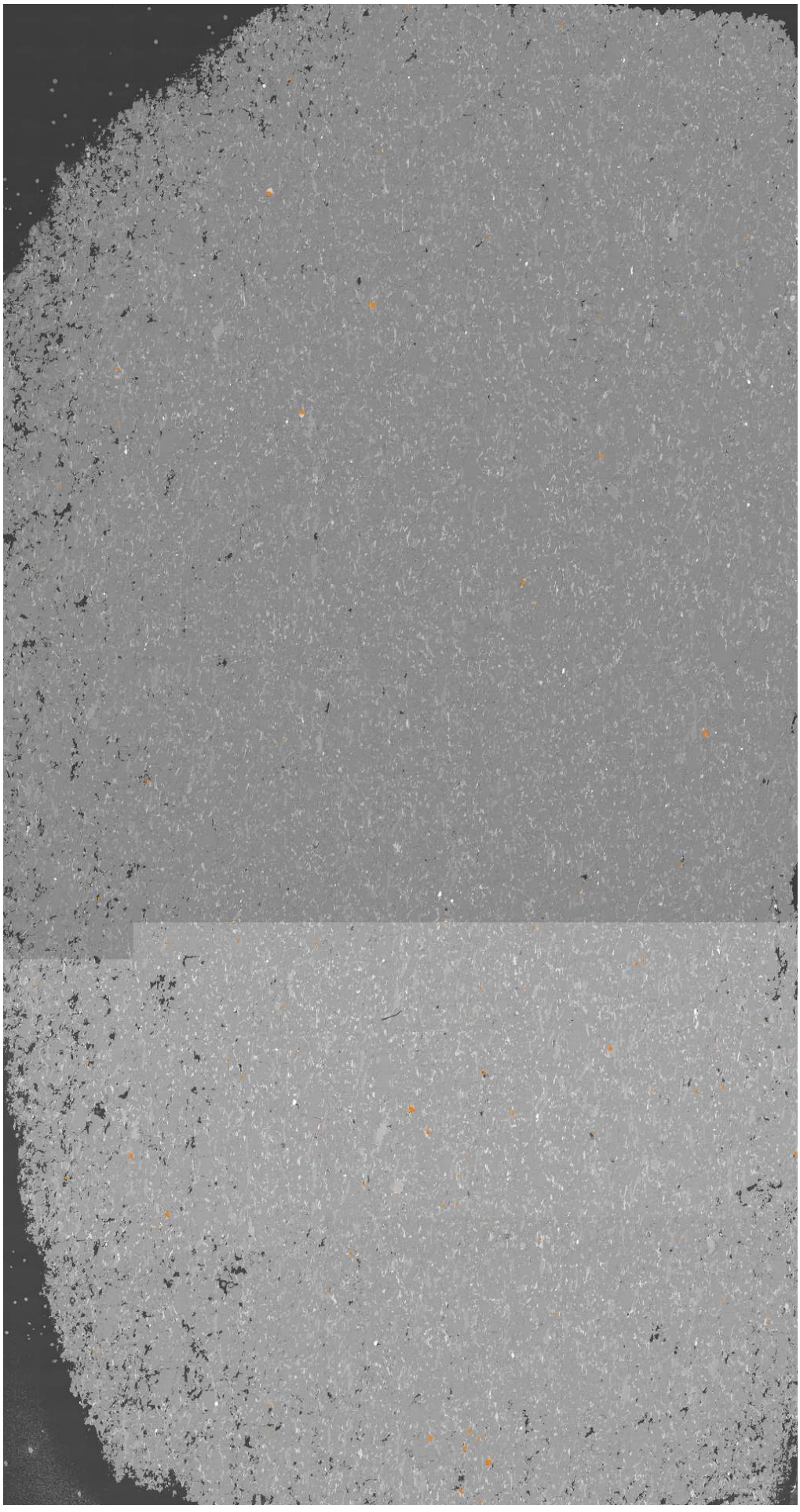

STF-10B

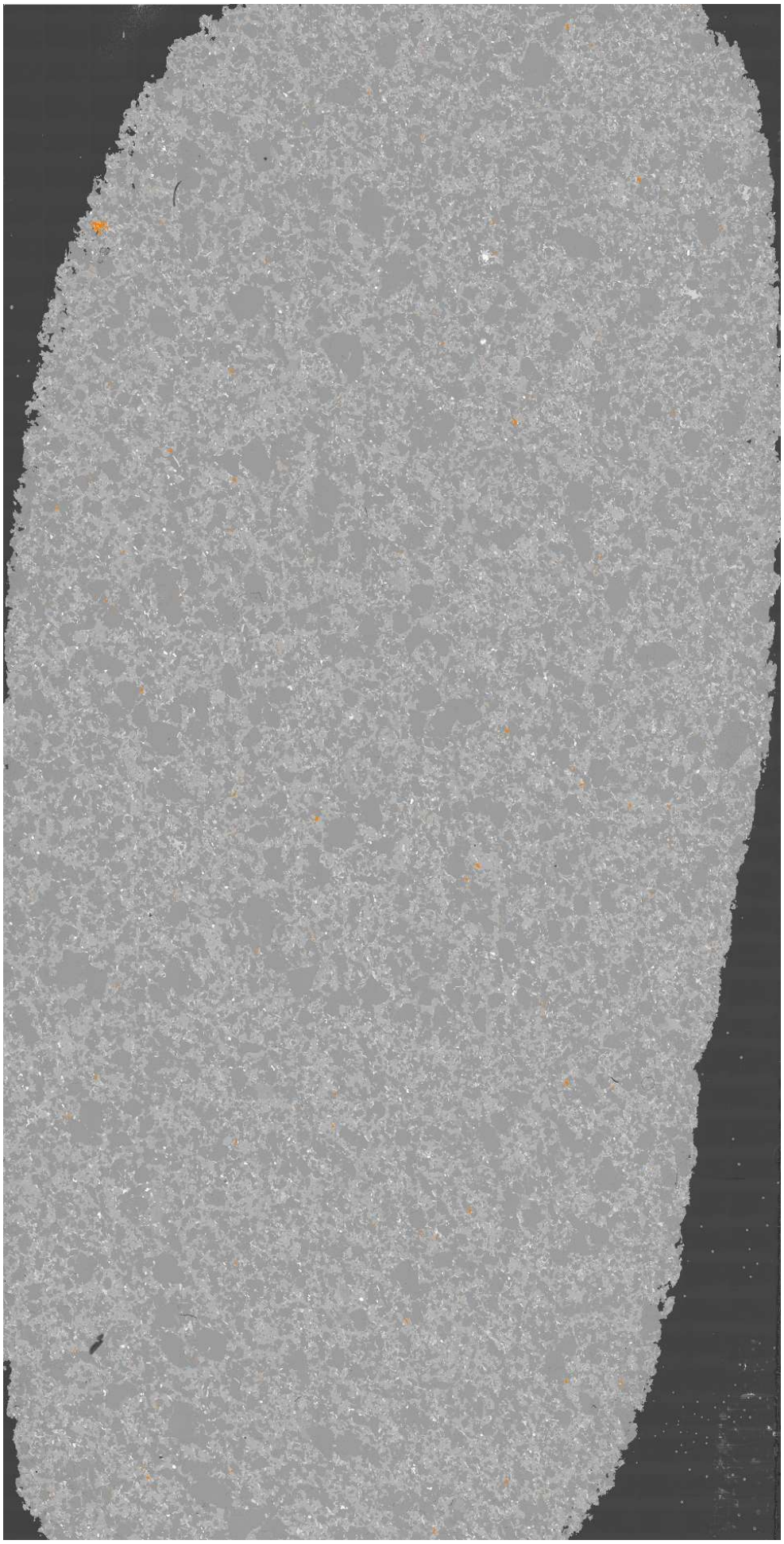

ST16-03C

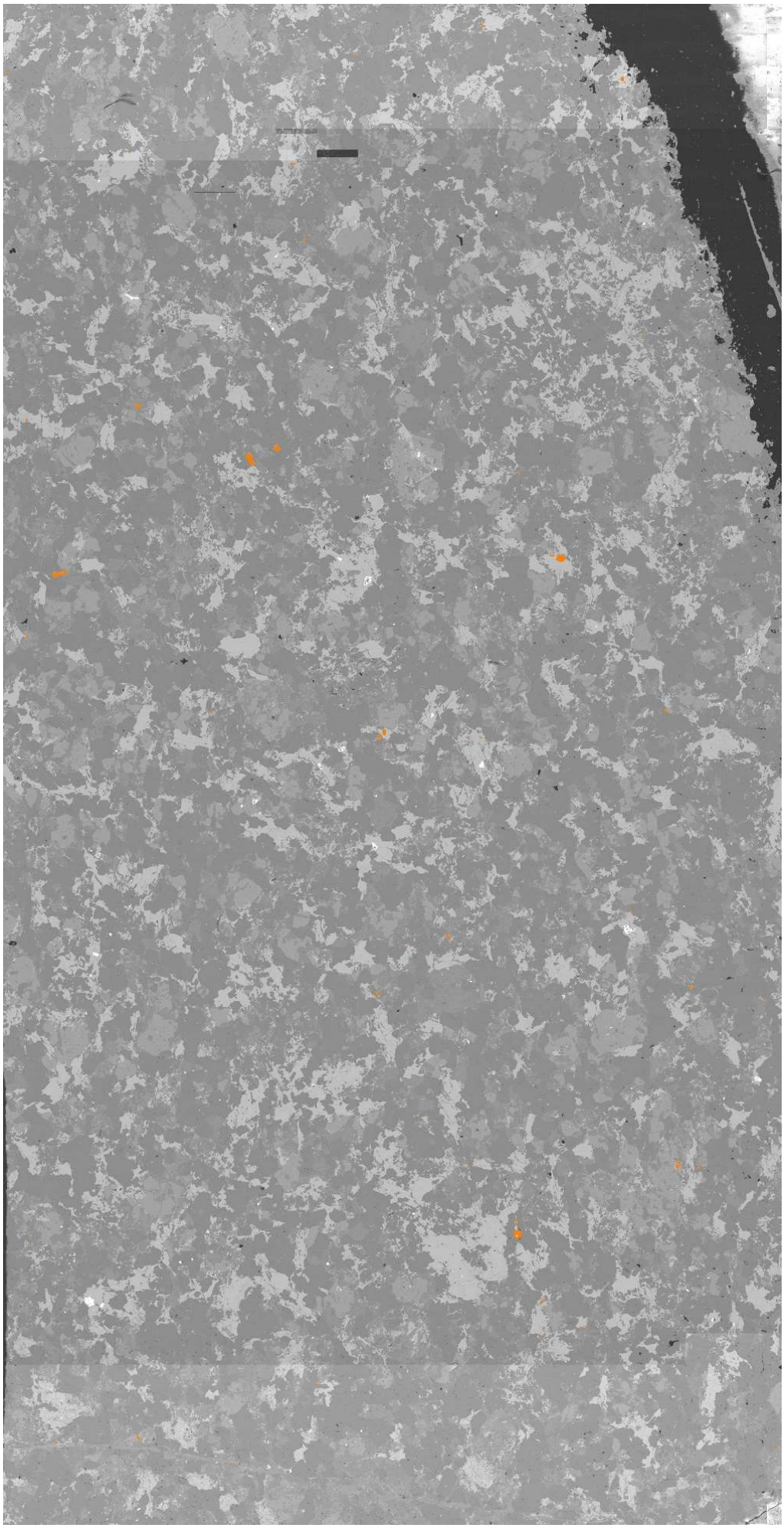

STF-26A

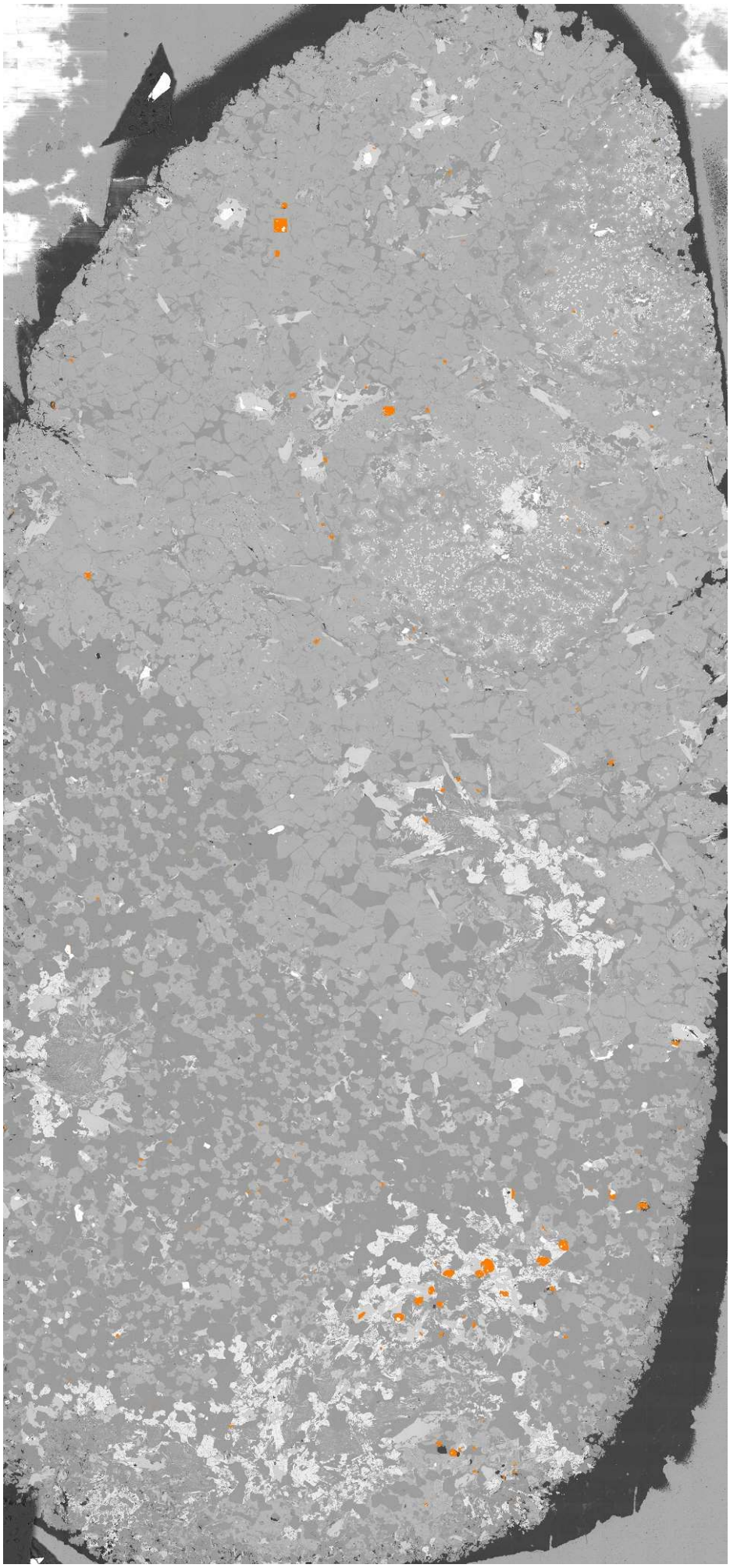

APPENDIX E: EPMA DATA

LA-ICP-MS is not included in tables here as data size is too high. Contact the author for the raw data in tabular format.

Section 1: Apatite Probe Data

Section 2: Monazite Probe Data

Section 3: Silicate Mineral Probe Data

SAMPLE	CaO	MgO	TiO2	SiO2	Al2O3	FeO	MnO	Cl	F	La2O3	Ce2O3	Nd2O3	K2O	P2O5	Na2O	Y2O3	O	TOTAL
STF26A Ap	52.80	0.09	0.03	0.45	0.33	1.78	0.12	0.03	3.85	0.00	0.10	0.14	0.01	35.18	0.06	0.13	-1.63	93.48
STF26A Ap	53.30	0.08	0.01	0.28	0.11	0.97	0.20	0.00	3.63	0.00	0.04	0.17	0.01	35.62	0.10	0.13	-1.53	93.13
STF26A Ap	53.09	0.08	0.00	0.35	0.68	0.95	0.13	0.02	3.78	0.00	0.05	0.12	0.01	35.20	0.15	0.12	-1.60	93.18
STF26A Ap	53.65	0.09	0.00	0.14	0.04	0.63	0.07	0.01	3.64	0.02	0.09	0.14	0.03	35.90	0.16	0.16	-1.54	93.23
STF26A Ap	54.63	0.06	0.01	0.09	0.01	0.71	0.13	0.00	3.85	0.00	0.05	0.16	0.00	35.01	0.10	0.21	-1.62	93.42
STF26A Ap	53.74	0.03	0.00	0.42	0.00	0.72	0.20	0.01	3.45	0.00	0.04	0.17	0.00	35.57	0.08	0.16	-1.45	93.16
STF26A Ap	53.92	0.01	0.00	0.12	0.00	0.72	0.09	0.00	3.54	0.00	0.10	0.14	0.00	35.64	0.10	0.18	-1.49	93.12
STF26A Ap	54.27	0.03	0.00	0.21	0.00	0.99	0.16	0.02	3.77	0.00	0.05	0.18	0.00	35.23	0.07	0.17	-1.59	93.60
STF26A Ap	48.94	0.29	0.00	0.14	0.02	0.67	0.10	0.33	3.38	0.00	0.05	0.14	0.05	34.59	4.60	0.17	-1.50	92.37
STF26A Ap	53.41	0.07	0.00	0.09	0.00	0.81	0.21	0.00	3.72	0.00	0.09	0.22	0.01	35.87	0.07	0.18	-1.57	93.21
STF26A Ap	44.29	1.71	0.01	4.10	2.85	6.75	0.14	0.01	3.10	0.00	0.08	0.16	0.01	31.72	0.09	0.14	-1.31	93.88
STF26A Ap	54.10	0.04	0.00	0.87	0.03	0.78	0.21	0.00	3.63	0.00	0.14	0.18	0.00	35.38	0.10	0.15	-1.53	94.10
STF26A Ap	54.17	0.07	0.00	0.29	0.00	0.78	0.04	0.02	3.55	0.00	0.09	0.15	0.01	36.16	0.10	0.21	-1.50	94.16
STF26A Ap	54.11	0.05	0.00	0.12	0.02	0.65	0.18	0.00	3.74	0.00	0.07	0.12	0.01	36.34	0.16	0.15	-1.57	94.19
STF26A Ap	54.47	0.07	0.00	0.13	0.00	0.95	0.13	0.00	4.25	0.01	0.07	0.17	0.00	35.42	0.06	0.17	-1.79	94.10
STF26A Ap	54.18	0.09	0.00	0.13	0.03	0.78	0.09	0.01	3.76	0.00	0.08	0.15	0.03	36.00	0.09	0.17	-1.58	94.05
STF26A Ap	54.90	0.10	0.00	0.11	0.00	0.86	0.21	0.01	3.42	0.00	0.02	0.17	0.02	36.62	0.19	0.18	-1.44	95.36
STF26A Ap	55.12	0.14	0.00	0.14	0.02	0.71	0.18	0.00	3.34	0.00	0.10	0.17	0.00	36.65	0.15	0.17	-1.41	95.47
STF26A Ap	54.17	0.50	0.02	0.22	0.00	1.05	0.14	0.00	3.05	0.00	0.05	0.13	0.01	36.94	0.10	0.11	-1.28	95.23
STF26A Ap	1.84	2.71	0.00	7.08	9.61	4.20	0.00	0.02	0.61	12.98	29.39	13.20	0.13	24.03	0.16	2.39	-0.26	108.09
STF26A Ap	53.96	0.11	0.04	0.20	0.03	0.62	0.09	0.02	3.82	0.04	0.12	0.16	0.03	35.52	0.09	0.15	-1.61	93.46
STF26A Ap	53.57	0.07	0.00	0.09	0.00	0.75	0.13	0.03	3.64	0.00	0.11	0.19	0.02	35.88	0.08	0.18	-1.54	93.23
STF26A Ap	53.38	0.09	0.00	0.12	0.12	0.92	0.05	0.00	3.59	0.04	0.19	0.16	0.02	35.85	0.06	0.16	-1.51	93.39
STF26A Ap	54.29	0.08	0.00	0.12	0.00	0.84	0.20	0.00	3.37	0.00	0.05	0.13	0.00	35.81	0.09	0.22	-1.42	93.81
STF26A Ap	53.36	0.08	0.01	0.09	0.00	1.04	0.22	0.00	3.62	0.01	0.12	0.15	0.00	35.88	0.06	0.16	-1.52	93.35
STF26A Ap	54.11	0.06	0.00	0.11	0.00	1.04	0.08	0.00	3.68	0.00	0.09	0.15	0.01	36.64	0.09	0.18	-1.55	94.69

STF26A Ap	53.44	0.02	0.00	0.18	0.00	0.90	0.21	0.00	3.84	0.00	0.04	0.16	0.02	36.41	0.08	0.19	-1.62	93.88
STF26A Ap	55.08	0.09	0.00	0.11	0.00	0.69	0.25	0.00	3.45	0.00	0.06	0.18	0.00	36.99	0.13	0.16	-1.45	95.73
STF26A Ap	53.37	0.07	0.00	0.12	0.01	0.78	0.20	0.00	3.77	0.00	0.05	0.17	0.01	36.83	0.11	0.17	-1.59	94.11
STF26A Ap	54.21	0.07	0.00	0.18	0.02	0.95	0.09	0.00	3.79	0.00	0.06	0.14	0.00	36.88	0.06	0.16	-1.60	95.06
STF26A Ap	49.29	7.35	0.00	0.06	0.00	1.48	0.08	0.00	4.62	0.02	0.09	0.17	0.00	36.88	0.07	0.15	-1.95	98.36
STF26A Ap	54.47	0.05	0.01	0.10	0.02	0.47	0.15	0.02	4.08	0.00	0.04	0.16	0.00	36.93	0.09	0.19	-1.72	95.12
STF26A Ap	52.84	0.10	0.00	0.12	0.00	0.81	0.16	0.01	3.75	0.00	0.06	0.14	0.02	36.51	0.12	0.14	-1.58	93.24
STF26A Ap	53.07	0.10	0.00	0.10	0.08	0.73	0.11	0.00	3.75	0.04	0.10	0.14	0.00	36.15	0.10	0.13	-1.58	93.04
STF26A Ap	53.09	0.10	0.00	0.06	0.00	0.63	0.19	0.00	3.99	0.00	0.07	0.18	0.00	36.45	0.13	0.20	-1.68	93.44
STF26A Ap	53.56	0.12	0.01	0.12	0.00	0.75	0.12	0.00	3.91	0.00	0.10	0.14	0.01	35.88	0.08	0.21	-1.65	93.36
STF26A Ap	53.29	0.13	0.00	0.20	0.01	0.93	0.17	0.02	3.83	0.00	0.04	0.18	0.01	36.84	0.08	0.19	-1.62	94.35
STF26A Ap	53.79	0.08	0.01	0.26	0.01	0.86	0.13	0.00	4.18	0.00	0.02	0.18	0.00	36.78	0.08	0.16	-1.76	94.81
STF26A Ap	54.64	0.05	0.00	0.22	0.04	0.25	0.00	0.00	3.88	0.00	0.04	0.16	0.06	36.39	0.06	0.20	-1.64	94.36
STF26A Ap	55.14	0.07	0.00	0.17	0.01	0.36	0.04	0.00	3.80	0.00	0.07	0.18	0.00	37.52	0.14	0.17	-1.60	96.08
STF26A Ap	54.72	0.08	0.00	0.36	0.37	0.27	0.00	0.00	3.83	0.00	0.03	0.16	0.04	34.80	0.04	0.19	-1.61	93.29
STF26A Ap	54.02	0.04	0.01	0.19	0.00	0.29	0.00	0.01	3.56	0.00	0.09	0.18	0.00	37.19	0.07	0.12	-1.50	94.27
STF26A Ap	27.11	0.12	0.00	34.68	9.22	0.32	0.00	0.04	0.93	0.03	0.11	0.14	0.11	20.19	0.18	0.18	-0.40	93.16
STF26A Ap	54.96	0.00	0.01	0.09	0.01	0.13	0.19	0.04	3.45	0.00	0.03	0.13	0.01	36.79	0.04	0.09	-1.46	94.52
STF26A Ap	55.35	0.00	0.00	0.08	0.02	0.12	0.10	0.02	3.55	0.01	0.05	0.14	0.00	37.49	0.06	0.10	-1.50	95.59
STF26A Ap	54.12	0.00	0.01	0.07	0.01	0.10	0.24	0.03	3.82	0.00	0.00	0.13	0.01	37.50	0.11	0.10	-1.62	94.65
STF26A Ap	55.35	0.00	0.00	0.15	0.01	0.22	0.32	0.04	3.65	0.00	0.04	0.13	0.00	37.18	0.04	0.06	-1.55	95.63
STF26A Ap	53.17	0.02	0.00	1.43	0.26	0.27	0.29	0.05	3.60	0.02	0.06	0.16	0.03	36.60	0.08	0.12	-1.53	94.63
STF26A Ap	55.37	0.00	0.00	0.05	0.01	0.23	0.11	0.04	3.65	0.00	0.00	0.15	0.00	37.24	0.00	0.11	-1.55	95.41
STF26A Ap	55.28	0.02	0.00	0.08	0.02	0.24	0.17	0.03	3.59	0.00	0.02	0.11	0.01	37.18	0.05	0.10	-1.52	95.39
STF26A Ap	54.97	0.01	0.00	0.12	0.34	0.39	0.27	0.01	3.17	0.00	0.02	0.08	0.01	37.32	0.03	0.14	-1.34	95.56
STF26A Ap	55.42	0.00	0.00	0.04	0.01	0.28	0.23	0.01	3.63	0.00	0.08	0.15	0.00	37.44	0.06	0.11	-1.53	95.94
STF26A Ap	18.96	0.09	0.00	1.73	26.57	0.13	0.04	0.03	2.21	0.00	0.00	0.14	0.10	19.27	0.22	0.08	-0.94	68.66
STF26A Ap	55.40	0.02	0.00	0.10	0.23	0.08	0.11	0.00	3.62	0.00	0.00	0.08	0.00	36.56	0.04	0.13	-1.52	94.87

STF26A Ap	55.23	0.00	0.00	0.11	0.02	0.49	0.16	0.03	3.76	0.00	0.08	0.13	0.00	37.02	0.06	0.13	-1.59	95.64
STF26A Ap	56.34	0.04	0.00	0.10	0.00	0.38	0.21	0.03	3.38	0.00	0.00	0.10	0.01	36.98	0.08	0.17	-1.43	96.40
STF26A Ap	55.19	0.01	0.00	0.17	0.02	0.39	0.15	0.05	3.52	0.00	0.04	0.13	0.05	37.55	0.03	0.09	-1.49	95.88
STF26A Ap	0.03	0.00	0.00	61.56	17.91	0.19	0.00	0.02	0.00	0.00	0.04	0.04	14.88	0.09	1.67	0.00	0.00	96.60
STF26A Ap	52.68	0.03	0.01	0.38	1.60	0.47	0.12	0.02	3.61	0.00	0.08	0.15	0.06	37.10	0.03	0.13	-1.53	95.00
STF26A Ap	55.11	0.02	0.00	0.09	0.07	0.36	0.11	0.01	4.04	0.00	0.04	0.10	0.00	37.62	0.06	0.11	-1.70	96.06
STF26A Ap	55.33	0.05	0.00	0.06	0.01	0.34	0.23	0.00	3.76	0.00	0.01	0.12	0.03	37.71	0.11	0.10	-1.58	96.27
STF26A Ap	54.46	0.05	0.01	0.05	0.02	0.56	0.24	0.00	4.13	0.00	0.07	0.12	0.04	38.24	0.08	0.09	-1.74	96.57
STF26A Ap	0.21	5.89	2.33	49.27	19.40	13.91	0.03	0.01	0.38	0.00	0.00	0.07	5.06	0.01	0.16	0.00	-0.16	96.76
ST16-19A Ap	53.54	0.07	0.01	0.24	0.03	0.63	0.15	0.00	3.32	0.00	0.06	0.18	0.18	37.37	0.03	0.06	-1.40	94.47
ST16-19A Ap	51.84	0.13	0.00	0.83	0.54	0.81	0.17	0.00	3.38	0.00	0.06	0.12	0.05	36.69	0.06	0.18	-1.42	93.46
ST16-19A Ap	53.62	0.05	0.00	0.12	0.01	0.88	0.10	0.01	3.30	0.00	0.11	0.17	0.00	36.77	0.06	0.15	-1.39	93.98
ST16-19A Ap	53.96	0.04	0.00	0.16	0.01	0.62	0.25	0.00	3.14	0.00	0.03	0.15	0.00	37.16	0.08	0.17	-1.32	94.46
ST16-19A Ap	53.21	0.05	0.00	0.23	0.23	0.75	0.19	0.01	3.39	0.00	0.07	0.09	0.01	36.95	0.04	0.13	-1.43	93.94
ST16-19A Ap	51.53	0.15	0.00	0.75	0.60	1.25	0.35	0.00	3.31	0.00	0.00	0.17	0.00	35.49	0.14	0.20	-1.39	92.61
ST16-19A Ap	53.42	0.06	0.00	0.14	0.01	0.61	0.42	0.02	3.15	0.00	0.05	0.12	0.00	36.16	0.09	0.13	-1.33	93.04
ST16-19A Ap	53.14	0.07	0.01	0.15	0.00	0.61	0.21	0.00	3.26	0.00	0.02	0.13	0.02	37.73	0.08	0.14	-1.37	94.21
ST16-19A Ap	52.83	0.10	0.00	0.30	1.01	0.53	0.27	0.03	3.10	0.00	0.04	0.12	0.00	36.11	0.07	0.13	-1.31	93.36
ST16-19A Ap	52.65	0.09	0.00	0.12	0.00	0.53	0.24	0.00	3.28	0.00	0.05	0.14	0.01	36.83	0.09	0.17	-1.38	92.86
ST16-19A Ap	53.49	0.06	0.00	0.04	0.00	0.65	0.23	0.01	3.34	0.00	0.05	0.16	0.00	37.69	0.12	0.13	-1.41	94.61
ST16-19A Ap	53.74	0.00	0.01	0.09	0.00	0.54	0.16	0.00	3.31	0.00	0.10	0.12	0.00	38.01	0.08	0.13	-1.39	94.95
ST16-19A Ap	54.29	0.05	0.01	0.08	0.00	0.74	0.31	0.02	3.37	0.00	0.07	0.15	0.03	37.23	0.03	0.20	-1.42	95.16
ST16-19A Ap	53.93	0.08	0.01	0.14	0.05	0.76	0.10	0.01	3.52	0.00	0.05	0.13	0.01	37.37	0.10	0.17	-1.48	94.97
ST16-19A Ap	53.75	0.02	0.00	0.22	0.12	0.42	0.28	0.01	3.52	0.00	0.07	0.18	0.01	37.05	0.09	0.16	-1.48	94.42
ST16-19A Ap	0.06	0.00	0.02	61.16	17.58	0.00	0.00	0.00	0.00	0.00	0.02	0.02	13.90	0.08	2.19	0.05	0.00	95.24
ST16-19A Ap	54.05	0.06	0.00	0.10	0.01	0.42	0.21	0.00	3.23	0.00	0.05	0.16	0.00	37.26	0.07	0.17	-1.36	94.45
ST16-19A Ap	53.87	0.07	0.00	0.10	0.01	0.79	0.24	0.01	3.36	0.00	0.03	0.13	0.00	37.13	0.07	0.18	-1.42	94.67
ST16-19A Ap	53.36	0.13	0.01	0.50	0.36	0.46	0.09	0.00	3.49	0.00	0.04	0.09	0.04	37.36	0.06	0.15	-1.47	94.69

ST16-19A Ap	53.93	0.09	0.01	0.06	0.04	0.66	0.44	0.01	3.38	0.00	0.04	0.13	0.00	36.95	0.04	0.14	-1.43	94.48
ST16-19A Ap	53.50	0.07	0.00	0.09	0.00	0.44	0.25	0.00	3.25	0.00	0.03	0.12	0.00	36.26	0.07	0.15	-1.37	92.88
ST16-19A Ap	54.35	0.09	0.00	0.06	0.00	0.33	0.14	0.00	3.54	0.00	0.02	0.09	0.01	37.50	0.11	0.14	-1.49	94.88
ST16-19A Ap	53.69	0.05	0.00	0.10	0.00	0.80	0.31	0.00	3.39	0.00	0.05	0.13	0.00	37.05	0.08	0.18	-1.43	94.41
ST16-19A Ap	53.01	0.07	0.01	0.47	0.29	0.49	0.37	0.01	3.35	0.00	0.01	0.12	0.02	36.59	0.07	0.14	-1.41	93.61
ST16-19A Ap	53.96	0.07	0.00	0.16	0.00	0.58	0.35	0.00	3.41	0.00	0.04	0.13	0.00	37.04	0.07	0.13	-1.43	94.51
ST16-19A Ap	54.16	0.04	0.00	0.11	0.02	0.76	0.25	0.01	3.44	0.00	0.03	0.19	0.00	36.79	0.07	0.15	-1.45	94.59
ST16-19A Ap	52.39	0.09	0.00	0.09	0.04	0.76	0.33	0.00	3.70	0.02	0.04	0.14	0.02	38.45	0.05	0.17	-1.56	94.77
ST16-19A Ap	53.50	0.06	0.00	0.10	0.00	0.56	0.28	0.00	3.66	0.00	0.05	0.11	0.01	37.39	0.08	0.17	-1.54	94.41
ST16-19A Ap	45.66	0.16	0.00	3.31	2.82	1.47	0.05	0.05	3.67	0.01	0.09	0.14	0.11	28.19	0.06	0.14	-1.56	84.45
ST16-19A Ap	53.30	0.08	0.00	0.16	0.00	0.68	0.24	0.00	3.53	0.01	0.05	0.15	0.01	37.17	0.08	0.14	-1.49	94.12
ST16-19A Ap	53.18	0.08	0.01	0.13	0.00	0.31	0.29	0.01	3.50	0.00	0.05	0.12	0.00	35.82	0.10	0.19	-1.47	92.35
ST16-19A Ap	53.10	0.04	0.00	0.07	0.00	0.56	0.42	0.00	3.60	0.00	0.05	0.13	0.01	37.98	0.03	0.16	-1.51	94.64
ST16-19A Ap	54.34	0.05	0.00	0.09	0.00	0.51	0.28	0.01	3.54	0.01	0.07	0.18	0.00	36.69	0.05	0.13	-1.50	94.49
ST16-19A Ap	53.15	0.06	0.00	0.09	0.00	0.43	0.35	0.00	3.61	0.00	0.07	0.15	0.01	36.84	0.08	0.23	-1.52	93.60
ST16-19A Ap	53.24	0.02	0.00	0.09	0.02	0.20	0.26	0.02	3.68	0.00	0.07	0.14	0.00	36.64	0.11	0.16	-1.55	93.13
ST16-19A Ap	51.98	0.03	0.01	0.08	0.00	1.15	0.19	0.02	3.63	0.00	0.02	0.16	0.01	35.88	0.02	0.18	-1.53	91.90
ST16-19A Ap	52.51	0.06	0.00	0.33	0.26	0.51	0.27	0.02	4.12	0.02	0.04	0.17	0.00	35.71	0.07	0.13	-1.74	92.52
ST16-19A Ap	51.56	0.03	0.00	0.17	0.01	0.70	0.31	0.01	3.62	0.02	0.06	0.18	0.02	36.70	0.05	0.15	-1.52	92.08
ST16-19A Ap	49.91	0.18	0.01	0.84	4.05	1.22	0.25	0.01	4.03	0.00	0.04	0.11	0.08	31.72	0.08	0.14	-1.70	91.14
ST16-19A Ap	0.21	7.29	2.43	33.90	18.43	22.67	0.00	0.04	0.54	0.00	0.00	0.09	8.81	0.04	0.15	0.00	-0.24	94.60
STF04A Ap	55.02	0.02	0.00	0.22	0.01	0.22	0.07	0.03	3.52	0.00	0.04	0.08	0.01	36.60	0.04	0.17	-1.49	94.64
STF04A Ap	55.26	0.00	0.00	0.23	0.01	0.17	0.15	0.00	3.41	0.00	0.02	0.12	0.01	37.12	0.03	0.16	-1.44	95.62
STF04A Ap	55.51	0.02	0.00	0.28	0.06	0.06	0.07	0.00	2.96	0.00	0.01	0.13	0.01	37.08	0.06	0.11	-1.25	95.30
STF04A Ap	55.06	0.00	0.01	0.24	0.04	0.24	0.04	0.00	3.27	0.00	0.02	0.10	0.01	37.15	0.04	0.13	-1.38	95.09
STF04A Ap	53.39	0.00	0.00	0.31	0.26	0.20	0.00	0.02	2.64	0.00	0.05	0.13	0.00	37.26	0.06	0.14	-1.12	93.75
STF04A Ap	55.13	0.00	0.00	0.18	0.02	0.14	0.00	0.01	3.29	0.00	0.04	0.09	0.02	36.19	0.00	0.15	-1.39	94.09
STF04A Ap	55.58	0.00	0.01	0.18	0.04	0.05	0.00	0.00	3.44	0.00	0.04	0.13	0.02	36.73	0.04	0.11	-1.45	95.12

STF04A Ap	55.15	0.00	0.00	0.12	0.02	0.19	0.03	0.00	3.19	0.00	0.01	0.07	0.00	36.93	0.00	0.08	-1.34	94.62
STF04A Ap	55.69	0.00	0.00	0.18	0.02	0.09	0.06	0.03	3.29	0.00	0.06	0.11	0.00	36.84	0.02	0.12	-1.39	95.11
STF04A Ap	4.94	0.00	0.00	59.82	23.88	0.22	0.03	0.02	0.00	0.00	0.02	0.05	0.07	0.05	8.87	0.00	0.00	98.12
STF04A Ap	54.12	0.00	0.01	0.36	0.02	0.14	0.10	0.01	3.17	0.00	0.08	0.16	0.04	36.32	0.02	0.32	-1.34	93.58
STF04A Ap	54.13	0.00	0.00	0.32	0.06	0.08	0.04	0.03	3.12	0.00	0.01	0.14	0.00	37.18	0.02	0.30	-1.32	94.27
STF04A Ap	54.63	0.00	0.00	0.32	0.00	0.12	0.14	0.03	3.31	0.00	0.15	0.18	0.01	38.09	0.00	0.28	-1.40	95.86
STF04A Ap	55.04	0.00	0.00	0.38	0.05	0.11	0.07	0.01	3.12	0.00	0.15	0.15	0.01	36.22	0.00	0.30	-1.32	94.30
STF04A Ap	54.71	0.00	0.00	0.33	0.01	0.08	0.17	0.03	3.19	0.00	0.06	0.18	0.00	37.09	0.07	0.38	-1.35	94.96
STF04A Ap	54.90	0.00	0.00	0.26	0.00	0.00	0.01	0.00	3.08	0.00	0.10	0.14	0.02	37.39	0.02	0.25	-1.30	94.86
STF04A Ap	55.10	0.00	0.00	0.25	0.04	0.07	0.11	0.04	3.16	0.01	0.10	0.15	0.00	36.60	0.09	0.29	-1.34	94.68
STF04A Ap	55.62	0.01	0.00	0.35	0.05	0.06	0.00	0.01	3.22	0.00	0.12	0.13	0.00	37.24	0.01	0.25	-1.36	95.70
STF04A Ap	54.87	0.00	0.00	0.41	0.21	0.00	0.00	0.04	3.01	0.01	0.09	0.14	0.01	35.49	0.05	0.33	-1.28	93.38
STF04A Ap	3.70	0.60	0.19	42.32	26.01	1.38	1.53	0.14	0.42	0.00	0.06	0.07	3.21	3.56	3.87	0.00	-0.21	87.23
STF04A Ap	54.35	0.00	0.00	0.73	0.58	0.05	0.06	0.03	3.84	0.00	0.09	0.12	0.09	35.38	0.10	0.38	-1.62	94.19
STF04A Ap	54.55	0.06	0.00	0.19	0.03	0.18	0.22	0.02	3.31	0.00	0.09	0.15	0.02	37.83	0.04	0.20	-1.40	95.51
STF04A Ap	55.39	0.03	0.00	0.31	0.47	0.05	0.00	0.01	2.84	0.00	0.08	0.06	0.03	36.10	0.03	0.16	-1.20	94.43
STF04A Ap	54.56	0.00	0.00	0.11	0.00	0.09	0.01	0.05	3.17	0.00	0.05	0.10	0.00	36.63	0.03	0.20	-1.35	93.69
STF04A Ap	54.24	0.00	0.00	0.17	0.00	0.02	0.13	0.03	3.24	0.00	0.06	0.12	0.00	37.58	0.07	0.21	-1.37	94.54
STF04A Ap	55.33	0.01	0.00	0.10	0.03	0.10	0.20	0.05	3.29	0.00	0.08	0.10	0.01	37.27	0.08	0.17	-1.40	95.43
STF04A Ap	54.98	0.00	0.00	0.16	0.00	0.13	0.05	0.04	3.15	0.00	0.07	0.12	0.00	37.42	0.03	0.19	-1.34	95.02
STF04A Ap	56.07	0.00	0.00	0.19	0.03	0.02	0.06	0.03	3.22	0.00	0.00	0.14	0.02	36.02	0.03	0.16	-1.36	94.65
STF04A Ap	49.71	0.01	0.01	0.41	6.16	0.09	0.16	0.01	3.89	0.00	0.04	0.11	0.12	33.33	0.04	0.10	-1.64	92.58
STF04A Ap	0.19	0.97	1.23	53.20	27.08	1.63	0.00	0.06	0.00	0.00	0.05	0.03	7.61	0.04	0.31	0.02	-0.01	92.60
STF04A Ap	54.47	0.01	0.01	0.21	0.42	0.04	0.11	0.03	4.01	0.00	0.02	0.07	0.00	37.01	0.04	0.07	-1.69	94.87
STF04A Ap	52.76	0.02	0.01	0.16	0.51	0.18	0.00	0.00	3.48	0.00	0.00	0.07	0.01	36.34	0.08	0.04	-1.47	92.21
STF04A Ap	54.86	0.00	0.00	0.02	0.00	0.00	0.00	0.00	3.69	0.01	0.06	0.04	0.03	37.56	0.03	0.06	-1.55	94.91
STF04A Ap	55.17	0.00	0.00	0.02	0.00	0.00	0.05	0.00	3.98	0.00	0.05	0.06	0.00	37.48	0.00	0.04	-1.68	95.20
STF04A Ap	54.81	0.04	0.00	0.11	0.08	0.20	0.07	0.02	3.62	0.00	0.04	0.06	0.04	35.80	0.07	0.08	-1.53	93.53

STF04A Ap	54.77	0.00	0.00	0.02	0.00	0.00	0.00	0.00	3.48	0.00	0.03	0.07	0.01	36.01	0.04	0.06	-1.47	93.10
STF04A Ap	55.40	0.00	0.00	0.06	0.03	0.07	0.05	0.01	3.64	0.00	0.01	0.06	0.00	36.33	0.04	0.06	-1.53	94.22
STF04A Ap	55.40	0.00	0.00	0.06	0.00	0.00	0.15	0.00	3.76	0.00	0.03	0.08	0.03	36.53	0.02	0.06	-1.58	94.57
STF04A Ap	53.33	0.00	0.00	0.11	0.08	0.00	0.00	0.02	3.69	0.00	0.04	0.10	0.01	37.29	0.12	0.06	-1.56	93.30
STF04A Ap	7.38	0.18	0.00	57.75	6.41	2.15	0.00	0.20	0.43	0.00	0.02	0.07	0.20	7.44	0.66	0.00	-0.23	83.62
STF16A Ap	53.40	0.01	0.01	0.10	0.02	0.32	0.21	0.02	3.55	0.00	0.00	0.08	0.07	34.72	0.04	0.11	-1.50	91.17
STF16A Ap	53.01	0.01	0.00	0.16	0.03	0.25	0.42	0.04	3.89	0.00	0.03	0.12	0.09	35.10	0.09	0.13	-1.65	91.78
STF16A Ap	52.37	0.04	0.00	0.20	0.61	0.28	0.51	0.00	4.09	0.00	0.07	0.05	0.03	33.73	0.06	0.07	-1.72	90.50
STF16A Ap	53.84	0.02	0.02	0.07	0.03	0.26	0.31	0.01	3.35	0.00	0.01	0.15	0.02	34.95	0.06	0.08	-1.41	91.81
STF16A Ap	52.11	0.27	0.00	0.09	0.05	0.36	0.34	0.00	3.67	0.00	0.07	0.11	0.01	34.80	0.13	0.09	-1.55	90.61
STF16A Ap	52.85	0.05	0.00	0.08	0.06	0.32	0.39	0.00	3.62	0.03	0.06	0.11	0.02	34.63	0.16	0.10	-1.52	90.95
STF16A Ap	51.50	0.04	0.00	0.03	0.05	0.41	0.28	0.03	4.09	0.00	0.00	0.11	0.04	41.35	0.09	0.10	-1.73	96.40
STF16A Ap	53.22	0.04	0.00	0.06	0.04	0.30	0.36	0.02	3.71	0.03	0.05	0.11	0.03	42.55	0.09	0.11	-1.57	99.15
STF16A Ap	53.11	0.02	0.00	0.12	0.00	0.33	0.41	0.00	3.68	0.00	0.00	0.13	0.00	43.22	0.04	0.12	-1.55	99.63
STF16A Ap	53.23	0.04	0.00	0.04	0.01	0.33	0.35	0.02	3.64	0.00	0.06	0.17	0.01	42.47	0.14	0.11	-1.54	99.13
STF16A Ap	52.17	0.04	0.00	0.04	0.02	0.25	0.38	0.01	3.75	0.00	0.02	0.11	0.00	43.12	0.10	0.07	-1.58	98.51
STF16A Ap	52.67	0.06	0.00	0.05	0.02	0.23	0.43	0.01	3.73	0.00	0.00	0.08	0.00	43.21	0.09	0.09	-1.58	99.11
STF16A Ap	52.68	0.03	0.00	0.11	0.10	0.33	0.48	0.00	3.88	0.00	0.02	0.15	0.01	42.28	0.19	0.10	-1.63	98.71
STF16A Ap	51.42	0.02	0.01	0.10	0.09	0.38	0.37	0.02	3.07	0.00	0.06	0.08	0.03	42.44	0.05	0.13	-1.30	97.02
STF16A Ap	13.55	0.14	0.00	1.11	60.90	0.19	0.09	0.08	0.60	0.00	0.02	0.14	0.11	12.60	0.32	0.08	-0.27	89.66
STF16A Ap	51.56	0.02	0.00	0.31	0.85	0.09	0.20	0.01	4.78	0.01	0.06	0.09	0.10	39.39	0.03	0.08	-2.01	95.57
STF16A Ap	0.50	0.01	0.00	68.75	13.09	0.08	0.00	0.05	0.16	0.00	0.03	0.07	4.63	0.23	2.16	0.02	-0.08	89.78
STF16A Ap	53.04	0.02	0.00	0.18	0.03	0.33	0.28	0.01	4.15	0.00	0.08	0.12	0.05	42.86	0.06	0.15	-1.75	99.61
STF16A Ap	22.62	0.66	0.00	1.77	40.01	0.89	0.00	0.09	2.09	0.00	0.06	0.10	0.19	15.48	0.21	0.12	-0.90	83.42
STF16A Ap	52.85	0.08	0.00	0.34	1.36	0.30	0.26	0.02	4.45	0.00	0.04	0.12	0.06	39.71	0.17	0.13	-1.88	98.11
STF16A Ap	11.30	0.19	0.00	1.62	68.58	0.35	0.02	0.09	0.96	0.00	0.01	0.10	0.09	4.59	0.18	0.10	-0.42	87.91
STF16A Ap	51.74	0.04	0.01	0.20	2.33	0.46	0.28	0.02	4.02	0.00	0.06	0.11	0.01	40.86	0.12	0.12	-1.70	98.67
STF16A Ap	52.23	0.04	0.00	0.30	0.41	0.50	0.26	0.00	4.07	0.00	0.05	0.08	0.08	42.62	0.03	0.13	-1.72	99.13

STF16A Ap	53.08	0.00	0.00	0.04	0.02	0.14	0.35	0.04	3.46	0.00	0.08	0.10	0.02	43.05	0.03	0.14	-1.46	99.14
STF16A Ap	52.91	0.00	0.01	0.12	0.06	0.70	0.48	0.00	3.82	0.00	0.04	0.12	0.10	43.58	0.03	0.11	-1.61	100.51
STF16A Ap	51.90	0.03	0.00	0.23	0.12	0.26	0.28	0.00	4.33	0.02	0.03	0.11	0.18	43.21	0.07	0.08	-1.82	99.05
STF16A Ap	53.70	0.02	0.00	0.15	0.06	0.20	0.31	0.02	4.08	0.00	0.08	0.13	0.08	43.55	0.13	0.09	-1.72	100.87
STF16A Ap	53.28	0.03	0.01	0.17	0.06	0.40	0.22	0.00	3.48	0.00	0.05	0.10	0.03	43.06	0.03	0.11	-1.47	99.59
STF16A Ap	52.17	0.02	0.00	0.15	0.45	0.17	0.16	0.05	3.00	0.00	0.03	0.08	0.09	42.27	0.08	0.08	-1.28	97.55
STF16A Ap	51.67	0.06	0.01	0.16	0.10	0.44	0.33	0.05	3.67	0.00	0.09	0.14	0.06	41.80	0.27	0.11	-1.56	97.44
STF16A Ap	26.64	0.09	0.00	50.16	6.14	1.08	0.05	0.08	1.12	0.00	0.03	0.10	0.06	15.60	0.20	0.08	-0.49	101.03
STF16A Ap	51.07	0.03	0.01	0.59	1.03	0.07	0.27	0.02	4.54	0.00	0.08	0.14	0.00	40.73	0.14	0.06	-1.92	96.92
STF16A Ap	52.92	0.01	0.00	0.04	0.01	0.22	0.17	0.00	3.33	0.00	0.03	0.17	0.04	43.38	0.03	0.08	-1.40	99.08
STF16A Ap	50.31	0.07	0.01	0.29	3.29	0.27	0.32	0.04	3.10	0.00	0.00	0.10	0.07	41.01	0.09	0.12	-1.31	97.76
STF16A Ap	52.69	0.03	0.00	0.11	0.06	0.14	0.18	0.03	3.45	0.00	0.02	0.12	0.02	42.65	0.04	0.07	-1.46	98.20
STF16A Ap	49.64	0.02	0.00	0.60	4.31	0.33	0.21	0.02	3.92	0.00	0.06	0.08	0.04	39.44	0.12	0.05	-1.65	97.28
STF16A Ap	51.34	0.13	0.20	0.79	4.98	0.72	0.63	0.10	4.09	0.24	0.30	0.32	0.12	39.15	0.23	0.08	-1.75	101.81
ST16-31J Ap	52.03	0.01	0.00	0.82	1.46	0.25	0.09	0.09	3.36	0.01	0.00	0.08	0.09	41.50	0.33	0.06	-1.44	98.81
ST16-31J Ap	49.88	0.03	0.00	1.70	2.16	0.09	0.23	0.04	3.18	0.01	0.05	0.06	0.02	40.25	0.16	0.01	-1.35	96.56
ST16-31J Ap	25.83	0.05	0.22	18.75	36.79	0.30	0.10	0.22	1.02	0.00	0.03	0.10	0.20	18.19	0.54	0.04	-0.48	102.14
ST16-31J Ap	0.32	0.04	0.01	27.61	43.97	0.55	0.00	0.46	0.00	0.00	0.03	0.17	1.20	0.13	5.43	0.03	-0.10	80.08
ST16-31J Ap	0.17	0.04	0.00	35.93	59.78	0.28	0.00	0.10	0.00	0.84	2.15	0.97	0.16	0.05	0.36	0.32	-0.02	101.23
ST16-31J Ap	6.66	0.06	0.02	33.65	56.25	0.29	0.00	0.13	0.20	0.00	0.06	0.12	0.13	2.29	0.54	0.08	-0.11	100.50
ST16-31J Ap	0.05	0.02	0.01	36.78	60.62	0.12	0.00	0.03	0.00	0.00	0.00	0.11	0.04	0.01	0.14	0.03	-0.01	98.01
ST16-31J Ap	0.35	0.02	0.00	36.83	59.06	0.25	0.00	0.00	0.00	0.00	0.03	0.12	0.02	0.10	0.04	0.05	0.00	96.88
ST16-31J Ap	54.53	0.00	0.01	0.13	0.10	0.19	0.20	0.01	2.68	0.00	0.04	0.11	0.01	43.50	0.00	0.05	-1.13	100.44
ST16-31J Ap	53.65	0.00	0.00	0.23	0.15	0.19	0.27	0.00	2.98	0.00	0.04	0.10	0.00	44.26	0.01	0.02	-1.26	100.68
ST16-31J Ap	51.88	0.01	0.00	2.13	0.13	0.06	0.04	0.02	2.19	0.00	0.03	0.08	0.01	43.14	0.02	0.02	-0.92	98.83
ST16-31J Ap	52.30	0.02	0.00	0.44	0.12	0.29	0.22	0.03	2.85	0.00	0.14	0.18	0.00	42.84	0.05	0.07	-1.21	98.36
ST16-31J Ap	35.44	0.10	0.00	14.71	26.65	0.78	0.11	0.04	2.73	0.00	0.07	0.15	0.17	25.86	0.22	0.05	-1.16	106.10
ST16-31J Ap	0.15	0.00	0.00	36.80	59.67	0.28	0.00	0.03	0.00	0.00	0.02	0.06	0.02	0.00	0.00	0.00	-0.01	97.23

ST16-31J Ap	0.06	0.02	0.01	37.15	60.36	0.26	0.00	0.01	0.00	0.00	0.08	0.13	0.02	0.04	0.00	0.00	0.00	98.18
ST16-31J Ap	13.56	0.03	0.02	28.55	52.08	0.18	0.00	0.00	0.33	0.00	0.01	0.08	0.00	8.87	0.03	0.03	-0.14	103.74
ST16-31J Ap	0.19	0.01	0.01	35.85	58.59	0.27	0.00	0.00	0.00	0.00	0.00	0.08	0.02	0.00	0.02	0.06	0.00	95.10
ST16-31J Ap	12.09	0.01	0.00	30.73	52.65	0.35	0.00	0.01	0.21	0.00	0.05	0.13	0.00	8.12	0.03	0.07	-0.09	104.44
ST16-31J Ap	5.53	0.93	0.00	30.29	13.38	3.85	0.03	0.10	1.24	0.00	0.01	0.11	1.88	9.30	0.95	0.07	-0.54	67.29
ST16-31J Ap	0.76	0.00	0.00	86.90	8.22	0.22	0.05	0.02	0.00	0.00	0.00	0.17	0.02	0.89	0.06	0.12	-0.01	97.43
ST16-31J Ap	0.12	0.03	0.00	35.90	59.21	0.28	0.00	0.02	0.00	0.00	0.04	0.14	0.01	0.08	0.03	0.14	0.00	96.01
ST16-31J Ap	45.23	0.00	0.00	7.11	17.35	0.24	0.05	0.01	2.39	0.03	0.05	0.12	0.00	30.86	0.00	0.04	-1.01	102.52
ST16-31J Ap	0.22	0.01	0.00	43.52	54.03	0.79	0.19	0.06	0.00	0.27	0.29	0.30	0.12	0.21	0.06	0.05	-0.01	100.30
ST16-31J Ap	0.22	0.02	0.00	35.35	59.53	0.57	0.00	0.00	0.00	0.00	0.03	0.12	0.01	0.04	0.03	0.05	0.00	96.00
ST16-31J Ap	0.19	0.01	0.00	36.38	59.60	0.24	0.00	0.02	0.00	0.00	0.01	0.15	0.03	0.04	0.02	0.08	0.00	96.77
STf-10B Ap	51.53	0.10	0.00	0.37	0.40	0.36	0.23	0.02	4.25	0.00	0.07	0.20	0.00	39.99	0.03	0.31	-1.79	96.15
STf-10B Ap	53.53	0.02	0.00	0.23	0.00	0.48	0.11	0.00	3.66	0.00	0.07	0.17	0.01	42.35	0.07	0.23	-1.54	99.38
STf-10B Ap	47.90	0.08	0.01	0.61	2.63	0.25	0.12	0.05	4.40	0.00	0.09	0.17	0.06	37.69	0.16	0.21	-1.87	92.59
STf-10B Ap	46.11	0.02	0.00	0.36	3.67	0.18	0.07	0.01	2.36	0.00	0.07	0.18	0.03	40.88	0.08	0.18	-1.00	93.24
STf-10B Ap	48.90	0.02	0.00	0.29	0.48	0.33	0.05	0.01	2.64	0.00	0.02	0.14	0.00	42.60	0.05	0.16	-1.11	94.67
STf-10B Ap	52.98	0.02	0.00	0.24	0.04	0.27	0.16	0.01	3.64	0.00	0.07	0.21	0.00	42.16	0.09	0.28	-1.53	98.67
STf-10B Ap	49.35	0.03	0.00	0.46	1.10	0.41	0.16	0.03	3.10	0.00	0.06	0.13	0.00	42.40	0.09	0.09	-1.31	96.13
STf-10B Ap	51.77	0.00	0.00	0.34	0.02	0.33	0.04	0.01	3.39	0.00	0.06	0.18	0.01	41.94	0.03	0.33	-1.43	97.06
STf-10B Ap	51.93	0.01	0.00	0.32	0.07	0.40	0.07	0.01	3.84	0.00	0.05	0.16	0.02	42.87	0.00	0.17	-1.62	98.46
STf-10B Ap	1.25	3.74	0.00	38.08	40.08	3.83	0.09	0.08	0.11	0.00	0.02	0.13	0.22	0.69	0.24	0.20	-0.06	88.77
STf-10B Ap	52.55	0.00	0.00	0.07	0.06	0.25	0.08	0.00	4.40	0.00	0.00	0.09	0.05	42.73	0.05	0.09	-1.85	98.60
STf-10B Ap	51.90	0.00	0.00	0.08	0.01	0.40	0.13	0.00	4.01	0.00	0.03	0.10	0.03	42.94	0.01	0.12	-1.69	98.08
STf-10B Ap	50.09	0.04	0.01	0.25	2.53	0.50	0.06	0.02	5.31	0.00	0.01	0.11	0.06	40.20	0.06	0.06	-2.24	97.11
STf-10B Ap	49.84	0.06	0.00	0.36	2.42	0.32	0.05	0.01	4.61	0.00	0.00	0.12	0.05	39.89	0.05	0.06	-1.94	95.90
STf-10B Ap	52.23	0.01	0.00	0.10	0.04	0.24	0.00	0.00	3.97	0.00	0.02	0.10	0.01	41.38	0.05	0.09	-1.67	96.69
STf-10B Ap	52.01	0.01	0.00	0.32	0.03	0.31	0.04	0.02	3.95	0.03	0.14	0.21	0.02	42.11	0.16	0.31	-1.67	98.05
STf-10B Ap	50.50	0.03	0.00	0.28	0.08	0.36	0.07	0.00	3.57	0.00	0.04	0.19	0.02	42.15	0.05	0.20	-1.51	96.10

STf-10B Ap	52.02	0.03	0.00	0.28	0.05	0.19	0.01	0.03	4.29	0.00	0.03	0.11	0.02	40.92	0.06	0.17	-1.81	96.42
STf-10B Ap	52.28	0.02	0.00	0.08	0.04	0.19	0.09	0.01	3.85	0.02	0.04	0.08	0.01	42.15	0.00	0.08	-1.62	97.34
STf-10B Ap	52.64	0.00	0.01	0.10	0.04	0.25	0.08	0.02	3.84	0.00	0.05	0.14	0.05	42.65	0.03	0.03	-1.62	98.31
STf-10B Ap	51.79	0.00	0.00	0.09	0.02	0.16	0.00	0.02	3.69	0.00	0.01	0.11	0.00	42.24	0.00	0.10	-1.56	96.66
STf-10B Ap	51.94	0.04	0.00	0.27	0.21	0.20	0.03	0.04	4.34	0.00	0.00	0.08	0.01	42.86	0.03	0.01	-1.84	98.24
STf-10B Ap	31.79	0.06	0.00	0.59	20.28	0.19	0.00	0.05	2.55	0.00	0.01	0.13	0.07	29.80	0.12	0.09	-1.08	84.68
STf-10B Ap	52.68	0.00	0.03	0.15	0.54	0.22	0.16	0.01	4.64	0.00	0.04	0.13	0.00	41.97	0.00	0.07	-1.96	98.82
STf-10B Ap	49.72	0.07	0.03	0.37	3.35	0.32	0.06	0.03	4.61	0.00	0.03	0.10	0.03	39.14	0.14	0.05	-1.95	96.08
STf-10B Ap	51.74	0.16	0.00	1.88	2.34	0.20	0.03	0.02	4.29	0.00	0.01	0.06	0.00	40.67	0.00	0.06	-1.81	99.66
STf-10B Ap	53.11	0.01	0.00	0.09	0.00	0.18	0.08	0.02	3.68	0.03	0.09	0.12	0.01	42.79	0.04	0.11	-1.55	98.82
STf-10B Ap	52.96	0.02	0.02	0.10	0.03	0.07	0.02	0.00	3.49	0.03	0.05	0.10	0.02	42.00	0.00	0.05	-1.47	97.50
STf-10B Ap	52.29	0.03	0.00	0.11	0.09	0.20	0.09	0.02	3.93	0.00	0.00	0.08	0.00	42.83	0.03	0.07	-1.66	98.10
STf-10B Ap	51.79	0.02	0.00	0.06	0.04	0.20	0.11	0.00	3.78	0.00	0.00	0.12	0.07	42.36	0.06	0.08	-1.59	97.11
STf-10B Ap	52.40	0.00	0.00	0.12	0.17	0.16	0.00	0.00	4.06	0.00	0.08	0.09	0.03	42.19	0.00	0.09	-1.71	97.67
STf-10B Ap	52.01	0.01	0.00	0.07	0.00	0.14	0.03	0.02	4.22	0.00	0.04	0.07	0.00	42.08	0.05	0.07	-1.78	97.02
STf-10B Ap	52.20	0.01	0.00	0.13	0.27	0.27	0.06	0.01	3.98	0.00	0.02	0.13	0.00	41.80	0.03	0.09	-1.68	97.38
STf-10B Ap	51.95	0.04	0.00	0.25	0.01	0.11	0.09	0.02	3.32	0.00	0.10	0.18	0.02	42.96	0.08	0.19	-1.40	97.98
STf-10B Ap	52.51	0.04	0.00	0.33	0.00	0.21	0.06	0.00	3.29	0.00	0.09	0.20	0.05	41.89	0.04	0.23	-1.38	97.57
STf-10B Ap	52.53	0.01	0.01	0.20	0.00	0.28	0.03	0.01	3.51	0.00	0.04	0.14	0.00	42.10	0.05	0.13	-1.48	97.64
STf-10B Ap	53.17	0.00	0.00	0.20	0.01	0.11	0.10	0.01	3.40	0.02	0.06	0.16	0.06	42.13	0.08	0.09	-1.43	98.24
STf-10B Ap	52.55	0.02	0.03	0.22	0.06	0.69	0.13	0.00	3.82	0.04	0.02	0.16	0.05	42.41	0.02	0.10	-1.61	98.73
STf-10B Ap	51.50	0.00	0.00	0.27	0.61	0.35	0.06	0.00	4.63	0.00	0.04	0.08	0.04	42.63	0.03	0.12	-1.95	98.52
STf-10B Ap	51.12	0.03	0.01	0.26	2.50	0.27	0.11	0.04	3.60	0.00	0.06	0.11	0.04	41.39	0.02	0.10	-1.53	98.15
STf-10B Ap	33.18	0.08	0.00	9.42	24.42	0.44	0.00	0.01	3.41	0.05	0.14	0.11	0.10	20.17	0.04	0.08	-1.44	90.22
ST16-09 Ap	53.63	0.04	0.00	0.08	0.00	0.35	0.22	0.14	3.07	0.00	0.05	0.13	0.00	44.31	0.02	0.07	-1.32	100.79
ST16-09 Ap	54.17	0.05	0.00	0.06	0.01	0.57	0.19	0.13	3.04	0.00	0.02	0.12	0.00	43.62	0.01	0.09	-1.31	100.77
ST16-09 Ap	53.45	0.07	0.00	0.09	0.02	0.58	0.23	0.13	2.86	0.06	0.01	0.08	0.00	43.77	0.05	0.12	-1.23	100.33
ST16-09 Ap	52.81	0.05	0.01	0.13	0.04	0.65	0.23	0.14	3.08	0.00	0.03	0.09	0.02	43.43	0.08	0.07	-1.33	99.54

ST16-09 Ap	53.07	0.01	0.00	0.09	0.00	0.49	0.37	0.18	2.80	0.00	0.00	0.13	0.02	43.86	0.04	0.11	-1.22	99.95
ST16-09 Ap	53.84	0.02	0.01	0.08	0.00	0.61	0.32	0.15	3.04	0.00	0.00	0.13	0.01	43.09	0.03	0.12	-1.31	100.22
ST16-09 Ap	47.53	0.07	0.00	0.02	0.00	0.66	0.06	0.13	2.68	0.00	0.01	0.11	0.00	41.79	0.10	0.13	-1.16	92.15
ST16-09 Ap	52.99	0.04	0.00	0.03	0.00	0.52	0.31	0.15	3.12	0.00	0.01	0.11	0.00	43.74	0.07	0.08	-1.35	99.84
ST16-09 Ap	52.16	0.07	0.01	0.08	0.03	0.68	0.12	0.15	3.02	0.00	0.00	0.05	0.02	42.89	0.14	0.14	-1.31	98.28
ST16-09 Ap	52.81	0.03	0.00	0.08	0.00	0.34	0.25	0.15	3.11	0.00	0.03	0.10	0.01	43.48	0.05	0.10	-1.34	99.21
ST16-09 Ap	53.20	0.04	0.00	0.07	0.00	0.64	0.15	0.20	2.98	0.00	0.01	0.10	0.02	43.80	0.04	0.11	-1.30	100.06
ST16-09 Ap	53.99	0.05	0.00	0.03	0.00	0.65	0.25	0.14	2.60	0.00	0.00	0.11	0.00	43.42	0.10	0.16	-1.13	100.41
ST16-09 Ap	53.55	0.06	0.01	0.07	0.02	0.41	0.27	0.12	3.05	0.00	0.03	0.11	0.00	43.48	0.06	0.13	-1.31	100.11
ST16-09 Ap	53.07	0.04	0.00	0.08	0.00	0.36	0.13	0.14	3.07	0.46	2.02	1.87	0.01	44.09	0.05	0.26	-1.32	104.37
ST16-09 Ap	52.66	0.10	0.01	0.19	0.08	0.71	0.15	0.14	3.05	0.01	0.04	0.07	0.02	44.37	0.12	0.09	-1.32	100.50
ST16-09 Ap	53.68	0.02	0.00	0.07	0.01	0.63	0.19	0.15	2.83	0.00	0.05	0.08	0.00	43.55	0.05	0.06	-1.22	100.26
ST16-09 Ap	54.11	0.04	0.00	0.08	0.02	0.50	0.26	0.15	3.00	0.00	0.00	0.15	0.00	43.49	0.04	0.12	-1.30	100.68
ST16-09 Ap	52.76	0.02	0.00	0.09	0.52	0.29	0.18	0.12	2.80	0.00	0.05	0.08	0.00	43.28	0.05	0.06	-1.21	99.12
ST16-09 Ap	54.06	0.03	0.01	0.04	0.00	0.34	0.22	0.15	3.07	0.06	0.04	0.12	0.00	43.09	0.00	0.08	-1.33	100.00
ST16-09 Ap	53.61	0.02	0.00	0.10	0.02	0.56	0.11	0.13	2.94	0.00	0.06	0.10	0.04	44.43	0.01	0.07	-1.27	101.05
ST16-09 Ap	53.17	0.05	0.01	0.07	0.00	0.45	0.16	0.12	3.27	0.00	0.03	0.13	0.04	43.89	0.03	0.07	-1.40	100.07
ST16-09 Ap	52.66	0.02	0.00	0.11	0.00	0.73	0.30	0.15	3.23	0.00	0.06	0.13	0.07	43.39	0.05	0.10	-1.39	99.73
ST16-09 Ap	53.94	0.04	0.00	0.06	0.00	0.38	0.18	0.16	3.05	0.00	0.01	0.12	0.00	43.78	0.13	0.07	-1.32	100.62
ST16-09 Ap	53.27	0.01	0.00	0.07	0.01	0.34	0.13	0.14	3.29	0.00	0.03	0.12	0.02	43.51	0.13	0.09	-1.42	99.77
ST16-09 Ap	53.36	0.03	0.00	0.11	0.00	0.59	0.29	0.15	2.93	0.00	0.08	0.09	0.00	43.87	0.04	0.11	-1.27	100.42
ST16-09 Ap	52.62	0.04	0.00	0.07	0.01	0.46	0.26	0.08	2.90	0.00	0.04	0.08	0.00	43.36	0.05	0.09	-1.24	98.85
ST16-09 Ap	39.84	0.03	0.01	0.08	0.00	0.28	0.10	0.13	2.41	0.00	0.04	0.08	0.03	38.57	0.04	0.09	-1.04	80.70
ST16-09 Ap	52.76	0.04	0.01	0.13	0.02	0.66	0.14	0.13	3.35	0.02	0.08	0.12	0.00	43.34	0.14	0.12	-1.44	99.67
ST16-09 Ap	53.00	0.08	0.00	0.08	0.00	0.47	0.17	0.14	3.12	0.00	0.00	0.05	0.00	44.13	0.12	0.10	-1.34	100.12
ST16-09 Ap	52.89	0.02	0.00	0.07	0.02	0.57	0.29	0.22	3.01	0.01	0.05	0.13	0.04	43.97	0.09	0.11	-1.32	100.25
ST16-09 Ap	52.86	0.04	0.00	0.07	0.03	0.66	0.27	0.14	3.11	0.00	0.03	0.10	0.00	43.32	0.05	0.13	-1.34	99.56
ST16-09 Ap	53.80	0.03	0.00	0.07	0.00	0.51	0.17	0.15	2.70	0.00	0.03	0.14	0.02	43.53	0.09	0.11	-1.17	100.22

ST16-09 Ap	50.88	0.03	0.00	0.10	0.85	0.52	0.18	0.17	2.89	0.03	0.01	0.08	0.02	41.94	0.07	0.10	-1.26	96.68
ST16-09 Ap	51.37	0.39	0.01	0.83	0.28	1.49	0.33	0.16	2.78	0.00	0.00	0.08	0.00	43.68	0.03	0.07	-1.21	100.34
ST16-09 Ap	53.63	0.04	0.12	0.06	0.00	0.38	0.31	0.12	3.20	0.00	0.03	0.08	0.02	43.49	0.10	0.12	-1.37	100.35
ST16-09 Ap	53.10	0.12	0.01	0.72	0.73	0.52	0.16	0.14	3.38	0.00	0.01	0.10	0.01	42.71	0.05	0.16	-1.46	100.49
ST16-09 Ap	53.52	0.06	0.01	0.11	0.02	0.60	0.26	0.16	3.14	0.00	0.00	0.10	0.01	43.52	0.04	0.10	-1.36	100.37
ST16-09 Ap	53.03	0.00	0.00	0.11	0.04	0.43	0.11	0.14	3.25	0.01	0.00	0.10	0.03	43.68	0.00	0.07	-1.40	99.61
ST16-09 Ap	54.96	0.02	0.00	0.04	0.02	0.35	0.19	0.03	3.48	0.02	0.02	0.11	0.02	44.12	0.03	0.12	-1.47	102.09
ST16-09 Ap	53.31	0.01	0.00	0.11	0.00	0.28	0.29	0.04	3.31	0.00	0.01	0.10	0.00	44.65	0.01	0.08	-1.40	100.87
ST16-09 Ap	54.30	0.02	0.00	0.06	0.00	0.33	0.24	0.04	3.38	0.00	0.06	0.12	0.00	43.32	0.01	0.08	-1.43	100.54
ST16-09 Ap	52.57	0.04	0.00	0.27	0.06	0.93	0.15	0.03	3.86	0.00	0.02	0.14	0.01	44.53	0.06	0.07	-1.63	101.10
ST16-09 Ap	53.34	0.01	0.01	0.06	0.00	0.62	0.11	0.02	4.10	0.00	0.02	0.08	0.05	43.61	0.04	0.06	-1.73	100.46
ST16-09 Ap	52.52	0.01	0.00	0.09	0.00	0.32	0.07	0.00	4.10	0.02	0.06	0.07	0.05	43.93	0.04	0.07	-1.73	99.64
ST16-09 Ap	54.07	0.02	0.00	0.12	0.01	0.42	0.07	0.03	3.11	0.00	0.02	0.09	0.07	43.19	0.01	0.12	-1.32	100.10
ST16-09 Ap	12.91	0.21	0.00	53.67	17.94	0.15	0.06	0.03	0.57	0.00	0.01	0.16	9.19	5.07	0.77	0.16	-0.24	100.74
ST16-09 Ap	54.26	0.02	0.00	0.18	0.03	0.64	0.00	0.03	3.72	0.03	0.06	0.09	0.01	43.83	0.07	0.13	-1.57	101.56
ST16-09 Ap	52.59	0.03	0.01	0.11	0.00	0.71	0.22	0.02	3.66	0.00	0.00	0.11	0.00	43.61	0.12	0.09	-1.55	99.76
ST16-09 Ap	53.70	0.03	0.00	0.14	0.01	0.32	0.03	0.05	3.63	0.00	0.00	0.10	0.06	43.81	0.05	0.12	-1.54	100.52
ST16-09 Ap	53.76	0.05	0.02	0.27	0.02	0.18	0.11	0.01	3.45	0.02	0.04	0.14	0.24	42.85	0.03	0.10	-1.46	99.90
ST16-09 Ap	53.12	0.01	0.01	0.16	0.03	0.70	0.16	0.01	3.36	0.00	0.04	0.14	0.06	44.20	0.00	0.08	-1.42	100.77
ST16-09 Ap	54.12	0.01	0.00	0.16	0.06	1.06	0.05	0.01	3.29	0.00	0.00	0.11	0.06	43.32	0.12	0.07	-1.39	101.13
ST16-09 Ap	15.02	5.17	0.00	42.11	30.97	5.70	0.23	0.04	0.97	0.00	0.04	0.11	0.03	3.35	0.07	0.05	-0.42	103.44
ST16-09 Ap	28.16	2.64	0.00	22.52	11.98	4.13	0.00	0.03	2.19	0.01	0.01	0.09	0.04	19.87	0.04	0.14	-0.93	90.97
ST16-09 Ap	51.43	0.01	0.00	0.15	0.02	0.55	0.01	0.04	3.59	0.00	0.01	0.10	0.01	42.37	0.09	0.08	-1.52	97.00
ST16-09 Ap	52.70	0.02	0.00	0.14	0.02	0.42	0.07	0.01	3.55	0.00	0.01	0.08	0.00	44.34	0.02	0.09	-1.50	100.00
ST16-31A Ap	52.07	0.00	0.00	0.54	0.07	0.00	0.04	0.00	4.50	0.05	0.13	0.17	0.06	40.61	0.02	0.34	-1.89	96.71
ST16-31A Ap	51.72	0.00	0.00	0.25	0.00	0.00	0.08	0.02	3.79	0.43	0.80	0.53	0.01	44.22	0.02	0.33	-1.60	100.60
ST16-31A Ap	50.10	0.01	0.00	0.32	0.08	0.00	0.10	0.01	3.94	0.03	0.10	0.12	0.00	41.04	0.06	0.24	-1.66	94.49
ST16-31A Ap	51.25	0.01	0.00	0.28	0.03	0.05	0.14	0.02	3.73	0.71	1.23	0.55	0.00	42.65	0.04	0.29	-1.58	99.48

ST16-31A Ap	49.93	0.07	0.00	0.60	3.55	0.35	0.12	0.01	4.40	0.09	0.47	0.37	0.01	37.36	0.02	0.27	-1.85	95.81
ST16-31A Ap	50.82	0.02	0.00	0.32	0.01	0.06	0.00	0.01	3.11	4.25	7.57	2.68	0.01	42.50	0.01	0.41	-1.31	110.59
ST16-31A Ap	50.24	0.00	0.00	0.34	0.00	0.11	0.03	0.01	3.15	0.67	4.35	2.70	0.02	42.72	0.00	0.34	-1.33	103.37
ST16-31A Ap	46.64	0.07	0.00	0.85	1.36	0.12	0.01	0.02	0.68	0.20	0.16	0.17	0.03	40.46	0.06	0.18	-0.29	90.73
ST16-31A Ap	52.81	0.00	0.00	0.29	0.00	0.00	0.01	0.00	3.57	0.00	0.04	0.13	0.02	41.28	0.06	0.28	-1.50	97.01
ST16-31A Ap	52.55	0.01	0.00	0.24	0.01	0.00	0.03	0.00	3.88	0.00	0.06	0.13	0.02	42.35	0.07	0.14	-1.63	97.84
ST16-31A Ap	51.90	0.00	0.00	0.17	0.00	0.09	0.08	0.00	4.01	0.07	0.30	0.25	0.04	43.28	0.00	0.18	-1.69	98.71
ST16-31A Ap	52.91	0.02	0.00	0.15	0.04	0.08	0.02	0.00	4.10	0.00	0.04	0.13	0.06	42.20	0.03	0.11	-1.73	98.19
ST16-31A Ap	34.75	0.90	0.00	13.57	19.51	0.94	0.00	0.05	1.16	0.00	0.01	0.10	0.86	24.84	0.09	0.11	-0.50	96.47
ST16-31A Ap	51.85	0.01	0.00	0.27	0.05	0.13	0.07	0.01	4.43	0.35	0.38	0.22	0.00	42.17	0.05	0.24	-1.87	98.41
ST16-31A Ap	52.10	0.00	0.00	0.17	0.03	0.27	0.14	0.00	3.66	0.02	0.09	0.15	0.06	41.68	0.05	0.20	-1.54	97.15
ST16-31A Ap	52.29	0.00	0.00	0.23	0.01	0.02	0.11	0.02	3.85	0.00	0.08	0.14	0.03	42.60	0.01	0.22	-1.63	98.00
ST16-31A Ap	48.92	0.01	0.00	0.61	0.38	0.24	0.08	0.06	4.66	0.00	0.03	0.14	0.19	38.48	0.00	0.07	-1.98	91.96
ST16-31A Ap	51.41	0.00	0.00	0.29	0.02	0.21	0.13	0.00	3.83	0.00	0.05	0.16	0.01	42.13	0.00	0.20	-1.61	96.88
ST16-31A Ap	52.06	0.01	0.00	0.44	0.01	0.13	0.01	0.02	3.51	0.00	0.00	0.09	0.03	43.08	0.04	0.12	-1.48	98.12
ST16-31A Ap	52.35	0.00	0.00	0.21	0.00	0.00	0.10	0.02	3.30	0.00	0.05	0.17	0.02	42.13	0.00	0.25	-1.39	97.23
ST16-31A Ap	44.06	0.05	0.00	0.54	2.83	0.04	0.04	0.00	4.26	0.00	0.05	0.14	0.06	25.46	0.05	0.26	-1.79	76.11
ST16-31A Ap	52.07	0.00	0.00	0.49	0.02	0.14	0.12	0.00	3.09	0.05	0.01	0.09	0.01	41.13	0.04	0.07	-1.30	96.02
ST16-31A Ap	51.78	0.03	0.00	0.72	0.15	0.38	0.08	0.01	3.24	0.22	0.28	0.29	0.02	42.16	0.15	0.54	-1.37	98.77
ST16-31A Ap	51.22	0.00	0.00	0.61	0.05	0.06	0.07	0.04	3.35	0.00	0.08	0.24	0.01	41.47	0.01	0.70	-1.42	96.50
ST16-31A Ap	51.91	0.03	0.00	0.21	0.04	0.43	0.03	0.01	3.74	0.04	0.17	0.29	0.09	42.39	0.00	0.79	-1.58	98.68
ST16-31A Ap	52.61	0.00	0.01	0.08	0.01	0.10	0.02	0.02	3.25	0.00	0.03	0.07	0.00	42.63	0.04	0.07	-1.37	97.60
ST16-31A Ap	52.96	0.00	0.00	0.08	0.00	0.13	0.12	0.03	3.57	0.00	0.02	0.06	0.01	42.04	0.04	0.03	-1.51	97.69
ST16-31A Ap	52.13	0.00	0.00	0.07	0.00	0.05	0.10	0.00	3.71	0.00	0.01	0.07	0.00	43.03	0.01	0.08	-1.56	97.77
ST16-31A Ap	52.11	0.01	0.00	0.11	0.04	0.07	0.00	0.00	3.79	0.00	0.05	0.13	0.02	42.01	0.00	0.09	-1.60	96.85
ST16-31A Ap	53.08	0.00	0.00	0.05	0.03	0.30	0.11	0.01	3.57	0.00	0.00	0.13	0.06	42.18	0.02	0.05	-1.51	98.10
ST16-31A Ap	53.49	0.00	0.00	0.05	0.00	0.16	0.11	0.02	4.09	0.00	0.02	0.11	0.04	42.34	0.06	0.05	-1.73	98.83
ST16-31A Ap	35.63	0.01	0.00	0.43	0.28	0.22	0.03	0.03	3.66	0.00	0.06	0.10	0.03	34.36	0.05	0.15	-1.55	73.56

ST16-31A Ap	52.39	0.02	0.00	0.29	0.04	0.01	0.12	0.02	3.81	0.00	0.06	0.16	0.02	42.01	0.06	0.05	-1.61	97.50
ST16-31A Ap	53.12	0.00	0.02	0.15	0.00	0.00	0.00	0.00	3.20	0.00	0.00	0.09	0.01	42.56	0.00	0.11	-1.35	97.90
ST16-31A Ap	52.78	0.01	0.00	0.06	0.03	0.33	0.15	0.01	3.36	0.02	0.00	0.12	0.01	42.21	0.01	0.10	-1.42	97.82
STF-02B Ap	52.92	0.01	0.00	0.14	0.03	0.39	0.11	0.00	3.77	0.00	0.04	0.08	0.12	43.17	0.04	0.07	-1.59	99.35
STF-02B Ap	52.02	0.04	0.00	0.08	0.03	0.31	0.14	0.00	3.86	0.01	0.03	0.14	0.03	42.96	0.12	0.11	-1.63	98.27
STF-02B Ap	53.08	0.00	0.02	0.16	0.04	0.35	0.30	0.00	4.06	0.00	0.07	0.10	0.04	43.57	0.03	0.07	-1.71	100.22
STF-02B Ap	50.81	0.05	0.00	0.59	0.14	0.46	0.10	0.02	4.11	0.00	0.02	0.11	0.01	41.90	0.17	0.10	-1.73	96.90
STF-02B Ap	53.10	0.00	0.00	0.20	0.02	0.07	0.13	0.00	4.30	0.00	0.00	0.09	0.04	42.29	0.05	0.11	-1.81	98.68
STF-02B Ap	49.56	0.07	0.01	0.47	1.34	0.46	0.36	0.02	4.54	0.00	0.03	0.12	0.04	39.89	0.16	0.08	-1.91	95.25
STF-02B Ap	53.44	0.02	0.01	0.18	0.06	0.59	0.19	0.02	3.83	0.01	0.03	0.10	0.07	43.34	0.04	0.07	-1.62	100.38
STF-02B Ap	51.68	0.00	0.00	0.15	0.04	0.43	0.10	0.04	4.17	0.00	0.08	0.08	0.05	43.73	0.03	0.07	-1.76	98.89
STF-02B Ap	53.91	0.02	0.01	0.43	0.19	0.07	0.17	0.01	4.87	0.00	0.02	0.10	0.27	42.67	0.02	0.06	-2.05	100.79
STF-02B Ap	48.17	0.10	0.01	2.53	1.80	1.23	0.13	0.02	4.25	0.00	0.01	0.11	0.22	37.55	0.12	0.12	-1.80	94.70
STF-02B Ap	47.06	0.02	0.00	1.83	0.32	0.32	0.05	0.01	5.95	0.00	0.06	0.08	0.46	41.07	0.24	0.07	-2.51	95.09
STF-02B Ap	52.45	0.00	0.00	0.20	0.03	0.01	0.21	0.01	3.70	0.00	0.02	0.10	0.02	43.66	0.03	0.08	-1.56	98.97
STF-02B Ap	53.92	0.01	0.00	0.21	0.02	0.32	0.15	0.00	3.66	0.00	0.03	0.09	0.13	43.14	0.06	0.06	-1.54	100.26
STF-02B Ap	52.84	0.04	0.01	0.13	0.01	0.41	0.32	0.00	3.74	0.04	0.07	0.12	0.20	41.31	0.11	0.09	-1.57	97.88
STF-02B Ap	48.36	0.02	0.00	1.53	0.67	0.34	0.11	0.04	4.06	0.01	0.08	0.10	2.07	34.42	0.12	0.11	-1.72	90.34
STF-02B Ap	41.76	0.21	0.00	1.95	4.73	1.29	0.21	0.14	3.47	0.00	0.05	0.14	0.17	30.88	0.71	0.13	-1.49	84.64
STF-02B Ap	47.58	0.01	0.01	3.29	1.46	0.17	0.00	0.06	4.92	0.00	0.00	0.10	0.07	33.25	0.20	0.08	-2.09	90.15
STF-02B Ap	54.54	0.01	0.00	0.09	0.03	0.16	0.22	0.01	3.27	0.00	0.01	0.07	0.00	43.06	0.07	0.11	-1.38	100.32
STF-02B Ap	50.90	0.02	0.00	0.48	1.26	0.36	0.14	0.07	3.42	0.00	0.04	0.12	0.03	40.41	0.14	0.08	-1.46	96.13
STF-02B Ap	52.38	0.01	0.02	0.09	0.04	0.35	0.17	0.01	2.92	0.02	0.07	0.13	0.01	42.77	0.07	0.11	-1.23	97.94
STF-02B Ap	53.86	0.02	0.00	0.28	0.09	0.11	0.04	0.00	4.45	0.00	0.00	0.05	0.04	41.23	0.09	0.09	-1.87	98.48
STF-02B Ap	43.12	0.33	0.01	1.93	1.64	0.93	0.10	0.08	1.28	0.00	0.07	0.11	0.31	38.55	0.30	0.14	-0.56	88.80
STF-02B Ap	52.35	0.00	0.00	0.12	0.06	0.38	0.12	0.03	3.50	0.00	0.05	0.08	0.01	43.41	0.02	0.13	-1.48	98.80
STF-02B Ap	50.87	0.05	0.00	0.58	2.33	0.19	0.00	0.02	3.63	0.00	0.04	0.10	0.09	39.74	0.15	0.09	-1.53	96.42
STF-02B Ap	49.94	0.12	0.00	2.67	4.23	0.44	0.11	0.19	3.72	0.00	0.01	0.12	0.14	35.01	0.20	0.11	-1.61	95.57

STF-02B Ap	53.23	0.00	0.02	0.15	0.05	0.50	0.22	0.01	3.69	0.00	0.06	0.15	0.11	42.11	0.06	0.12	-1.56	98.98
STF-02B Ap	52.00	0.12	0.00	1.26	2.14	0.38	0.19	0.04	3.90	0.00	0.04	0.04	0.10	41.25	0.20	0.07	-1.65	100.17
STF-02B Ap	52.85	0.02	0.01	0.31	0.05	0.17	0.18	0.00	4.06	0.00	0.02	0.07	0.01	42.61	0.05	0.07	-1.71	98.78
STF-02B Ap	52.33	0.01	0.00	0.29	0.24	0.14	0.13	0.03	3.57	0.00	0.01	0.07	0.04	42.80	0.04	0.09	-1.51	98.31
STF-02B Ap	54.01	0.03	0.01	0.12	0.10	0.29	0.24	0.02	3.90	0.00	0.05	0.10	0.05	43.06	0.04	0.12	-1.65	100.56
STF-02B Ap	22.66	0.25	0.01	23.27	32.29	4.35	0.03	0.11	1.69	0.00	0.04	0.14	0.31	14.33	0.35	0.07	-0.74	99.82
STF-02B Ap	49.18	0.01	0.00	1.01	0.95	0.33	0.17	0.04	2.97	0.00	0.08	0.16	0.25	40.09	0.26	0.18	-1.26	94.53
STF-02B Ap	50.85	0.03	0.01	0.63	0.22	0.46	0.25	0.00	3.38	0.00	0.03	0.15	0.15	38.71	0.23	0.12	-1.42	93.79
STF-02B Ap	53.29	0.02	0.00	0.32	0.13	0.38	0.25	0.03	3.37	0.00	0.01	0.11	0.07	42.44	0.10	0.06	-1.43	99.19
STF33 Ap	51.36	0.03	0.01	0.25	0.19	0.27	0.14	0.27	2.91	0.00	0.07	0.12	0.18	41.14	0.50	0.17	-1.29	96.47
STF33 Ap	45.77	0.04	0.00	0.73	7.40	0.32	0.00	0.15	3.02	0.00	0.04	0.12	0.16	36.57	0.25	0.27	-1.31	93.55
STF33 Ap	52.24	0.02	0.00	0.40	0.28	0.11	0.07	0.02	2.92	0.02	0.16	0.25	0.03	42.36	0.04	0.48	-1.24	98.24
STF33 Ap	50.69	0.00	0.00	0.28	0.00	0.01	0.08	0.02	3.05	0.00	0.07	0.12	0.01	40.94	0.00	0.31	-1.29	94.32
STF33 Ap	53.24	0.00	0.01	0.14	0.05	0.12	0.05	0.04	3.32	0.00	0.00	0.09	0.03	41.93	0.09	0.05	-1.41	97.83
STF33 Ap	52.00	0.00	0.00	0.24	0.21	0.20	0.09	0.04	3.76	0.00	0.00	0.11	0.14	41.53	0.07	0.06	-1.59	96.86
STF33 Ap	52.29	0.00	0.00	0.10	0.02	0.27	0.02	0.04	3.73	0.00	0.01	0.10	0.09	41.86	0.00	0.07	-1.58	97.03
STF33 Ap	52.62	0.00	0.00	0.07	0.00	0.12	0.00	0.05	3.67	0.00	0.04	0.07	0.02	41.63	0.01	0.00	-1.56	96.81
STF33 Ap	53.85	0.00	0.00	0.11	0.03	0.11	0.02	0.05	3.43	0.00	0.01	0.08	0.04	41.72	0.08	0.02	-1.46	98.10
STF33 Ap	52.25	0.00	0.00	0.12	0.13	0.23	0.19	0.03	3.42	0.00	0.00	0.16	0.07	42.33	0.03	0.08	-1.45	97.70
STF33 Ap	53.13	0.00	0.00	0.14	0.01	0.03	0.00	0.00	3.40	0.00	0.05	0.13	0.06	42.84	0.06	0.07	-1.43	98.48
STF33 Ap	53.02	0.00	0.01	0.15	0.03	0.01	0.11	0.02	3.64	0.03	0.02	0.10	0.01	42.16	0.02	0.10	-1.53	97.93
STF33 Ap	53.41	0.00	0.00	0.18	0.05	0.09	0.21	0.03	3.57	0.00	0.06	0.12	0.01	42.53	0.10	0.10	-1.51	98.98
STF33 Ap	52.26	0.01	0.00	0.13	0.01	0.29	0.09	0.01	3.80	0.00	0.03	0.15	0.02	42.02	0.07	0.12	-1.60	97.45
STF33 Ap	53.13	0.00	0.00	0.08	0.01	0.14	0.13	0.01	3.38	0.00	0.01	0.10	0.02	43.43	0.06	0.13	-1.43	99.23
STF33 Ap	52.83	0.01	0.00	0.26	0.16	0.00	0.00	0.03	4.09	0.03	0.04	0.09	0.05	41.43	0.11	0.03	-1.73	97.51
STF33 Ap	31.99	0.23	0.00	16.74	15.48	0.35	0.00	0.56	1.45	0.00	0.06	0.11	0.54	23.51	0.86	0.09	-0.74	91.49
STF33 Ap	51.97	0.03	0.01	0.62	0.01	0.14	0.07	0.00	3.43	0.00	0.12	0.15	0.01	42.12	0.04	0.43	-1.44	97.73
STF33 Ap	50.95	0.01	0.00	0.25	0.11	0.14	0.11	0.03	3.23	0.01	0.02	0.14	0.01	41.62	0.04	0.15	-1.37	95.48

STF33 Ap	51.08	0.00	0.01	0.58	0.02	0.10	0.00	0.02	2.92	0.04	0.16	0.22	0.00	41.74	0.05	0.52	-1.24	96.23
STF33 Ap	50.17	0.05	0.00	0.56	5.46	0.19	0.20	0.02	3.90	0.00	0.04	0.12	0.08	38.19	0.12	0.12	-1.65	97.66
STF33 Ap	53.17	0.00	0.02	0.10	0.02	0.05	0.20	0.01	3.65	0.00	0.00	0.12	0.01	41.87	0.00	0.07	-1.54	97.84
STF33 Ap	52.45	0.00	0.04	0.09	0.02	0.00	0.00	0.01	3.59	0.00	0.02	0.11	0.00	42.83	0.04	0.10	-1.51	97.80
STF33 Ap	52.72	0.02	0.00	0.06	0.04	0.00	0.04	0.02	3.33	0.03	0.09	0.16	0.00	42.09	0.01	0.07	-1.41	97.28
STF33 Ap	52.04	0.02	0.00	0.03	0.00	0.06	0.14	0.00	3.44	0.00	0.08	0.11	0.01	42.75	0.08	0.12	-1.45	97.54
STF33 Ap	53.24	0.03	0.00	0.08	0.02	0.02	0.10	0.02	3.60	0.01	0.02	0.10	0.01	42.26	0.04	0.09	-1.52	98.15
STF33 Ap	51.26	0.02	0.00	0.15	0.38	0.00	0.05	0.02	3.50	0.00	0.05	0.11	0.01	41.54	0.06	0.06	-1.48	95.79
STF33 Ap	53.10	0.00	0.00	0.13	0.00	0.14	0.00	0.00	3.48	0.00	0.05	0.10	0.04	42.26	0.02	0.09	-1.47	97.97
STF33 Ap	53.09	0.00	0.01	0.29	0.02	0.10	0.02	0.00	3.13	0.02	0.04	0.15	0.01	42.12	0.05	0.18	-1.32	97.97
STF33 Ap	52.57	0.02	0.00	0.15	0.11	0.08	0.05	0.02	2.97	0.01	0.08	0.14	0.03	41.47	0.02	0.17	-1.26	96.93
STF33 Ap	52.62	0.00	0.00	0.19	0.00	0.01	0.14	0.00	3.00	0.00	0.00	0.11	0.00	43.12	0.06	0.15	-1.26	98.20
STF33 Ap	50.81	0.02	0.00	0.18	1.72	0.22	0.00	0.04	3.04	0.00	0.04	0.08	0.00	41.08	0.09	0.20	-1.29	96.30
STF33 Ap	53.19	0.01	0.00	0.10	0.00	0.06	0.08	0.00	2.97	0.00	0.09	0.12	0.00	42.61	0.02	0.14	-1.25	98.30
STF33 Ap	54.94	0.00	0.01	0.16	0.15	0.04	0.11	0.01	3.63	0.05	0.06	0.10	0.05	41.63	0.02	0.06	-1.53	99.51
STF33 Ap	52.37	0.00	0.00	0.18	0.04	0.06	0.00	0.00	3.34	0.00	0.00	0.09	0.02	41.30	0.04	0.25	-1.41	96.32
STF33 Ap	50.70	0.06	0.01	0.43	1.29	0.03	0.07	0.01	3.48	0.00	0.06	0.11	0.04	41.01	0.01	0.08	-1.47	95.98
STF33 Ap	53.74	0.00	0.00	0.14	0.03	0.13	0.00	0.02	3.69	0.00	0.05	0.13	0.03	41.76	0.04	0.03	-1.56	98.24
STF33 Ap	0.00	0.00	0.01	0.14	0.21	0.14	0.06	0.01	0.00	0.00	0.04	0.08	0.00	41.88	0.01	0.06	0.00	42.64
STF33 Ap	0.00	0.01	0.00	0.10	0.15	0.00	0.02	0.00	0.00	0.02	0.07	0.09	0.00	42.19	0.02	0.08	0.00	42.88
STF33 Ap	0.00	0.00	0.00	0.10	0.13	0.02	0.00	0.00	0.00	0.26	0.27	0.33	0.00	42.57	0.10	0.15	0.00	44.01
STF33P Ap	0.08	0.58	0.04	44.74	35.86	0.68	0.00	0.04	0.00	0.00	0.01	0.10	4.90	0.09	0.60	0.03	-0.01	87.79
STF33P Ap	0.19	0.52	0.00	43.17	35.86	1.15	0.00	0.01	0.00	0.00	0.00	0.09	4.87	0.05	0.44	0.09	0.00	86.44
STF33P Ap	53.57	0.01	0.00	0.52	1.74	0.13	0.00	0.01	2.94	0.00	0.00	0.07	0.45	41.76	0.05	0.08	-1.24	100.11
STF33P Ap	0.17	0.88	0.05	43.94	35.59	2.51	0.00	0.04	0.00	0.05	0.03	0.11	5.30	0.05	0.54	0.01	-0.01	89.29
STF33P Ap	0.39	0.48	0.20	43.49	37.07	0.77	0.00	0.04	0.00	0.22	1.04	0.29	5.18	0.05	0.63	0.07	-0.01	90.11
STF33P Ap	0.23	1.30	0.00	46.36	35.88	1.79	0.00	0.00	0.00	1.87	4.38	1.32	4.54	0.09	0.53	0.21	0.00	98.60
STF33P Ap	0.34	2.13	0.00	39.38	31.75	5.94	0.00	0.11	0.19	0.07	0.59	0.42	7.82	0.05	0.47	0.09	-0.11	89.34

STF33P Ap	0.36	1.83	0.13	39.73	35.93	3.02	0.01	0.10	0.08	0.00	0.01	0.14	4.81	0.09	0.38	0.03	-0.06	86.70
STF33P Ap	0.16	1.09	0.05	44.42	34.45	1.38	0.00	0.00	0.05	0.00	0.00	0.05	5.56	0.05	0.38	0.03	-0.02	87.72
STF33P Ap	0.09	1.13	0.02	44.81	33.31	1.19	0.00	0.00	0.00	0.00	0.04	0.06	4.90	0.02	0.46	0.03	0.00	86.11
STF33P Ap	0.14	0.38	0.12	43.29	36.83	0.73	0.00	0.02	0.00	0.00	0.07	0.04	6.83	0.03	0.56	0.02	0.00	89.06
STF33P Ap	0.10	1.13	0.00	45.68	34.13	1.64	0.02	0.05	0.03	0.00	0.04	0.13	5.17	0.05	0.51	0.07	-0.02	88.78
STF33P Ap	53.56	0.01	0.03	0.14	0.07	0.10	0.00	0.02	3.69	0.00	0.00	0.07	0.29	42.37	0.05	0.05	-1.56	98.91
STF33P Ap	0.15	0.07	0.01	43.49	37.18	0.47	0.08	0.02	0.00	0.24	0.39	0.21	8.40	0.07	0.67	0.12	-0.01	91.64
STF33P Ap	0.33	0.48	0.01	43.68	36.79	1.41	0.00	0.03	0.00	0.00	0.03	0.12	6.32	0.03	0.49	0.05	-0.01	89.81
STF33P Ap	0.08	0.00	0.04	83.13	0.04	0.02	0.00	0.01	0.00	0.00	0.02	0.12	0.01	0.02	0.05	0.00	0.00	83.64
ST16-03C Ap	54.47	0.00	0.00	0.15	0.04	0.04	0.17	0.26	2.83	0.00	0.03	0.06	0.01	44.26	0.05	0.08	-1.25	101.19
ST16-03C Ap	54.35	0.03	0.00	0.08	0.00	0.24	0.38	0.27	3.06	0.00	0.00	0.08	0.00	44.17	0.05	0.12	-1.35	101.49
ST16-03C Ap	53.71	0.00	0.00	0.12	0.00	0.51	0.56	0.26	2.82	0.00	0.08	0.16	0.00	44.60	0.05	0.12	-1.25	101.76
ST16-03C Ap	54.04	0.05	0.00	0.06	0.00	0.47	0.55	0.24	2.79	0.00	0.05	0.12	0.00	43.35	0.04	0.14	-1.23	100.69
ST16-03C Ap	54.45	0.03	0.00	0.11	0.00	0.15	0.43	0.26	3.08	0.02	0.09	0.11	0.00	43.92	0.02	0.08	-1.35	101.42
ST16-03C Ap	53.54	0.05	0.00	0.09	0.03	0.15	0.33	0.29	2.95	0.00	0.03	0.11	0.01	44.02	0.07	0.16	-1.31	100.58
ST16-03C Ap	53.91	0.00	0.00	0.09	0.00	0.30	0.21	0.30	3.19	0.00	0.05	0.08	0.01	43.24	0.03	0.14	-1.41	100.14
ST16-03C Ap	53.73	0.02	0.00	0.05	0.00	0.35	0.38	0.23	3.07	0.00	0.08	0.14	0.00	43.73	0.10	0.13	-1.35	100.71
ST16-03C Ap	54.90	0.02	0.00	0.12	0.02	0.12	0.39	0.25	3.19	0.00	0.01	0.11	0.00	43.32	0.07	0.11	-1.40	101.24
ST16-03C Ap	54.15	0.01	0.00	0.07	0.00	0.13	0.47	0.27	2.96	0.00	0.06	0.10	0.01	44.44	0.04	0.06	-1.31	101.48
ST16-03C Ap	54.15	0.04	0.00	0.07	0.00	0.18	0.39	0.19	3.81	0.02	0.03	0.15	0.02	43.99	0.03	0.06	-1.65	101.48
ST16-03C Ap	54.31	0.02	0.00	0.05	0.00	0.21	0.39	0.15	3.63	0.00	0.04	0.15	0.00	43.90	0.04	0.06	-1.56	101.42
ST16-03C Ap	53.40	0.06	0.00	0.05	0.03	0.25	0.32	0.23	3.50	0.00	0.03	0.12	0.02	44.28	0.06	0.07	-1.53	100.89
ST16-03C Ap	53.61	0.01	0.01	0.06	0.00	0.21	0.45	0.14	3.94	0.00	0.07	0.10	0.00	44.83	0.02	0.09	-1.69	101.84
ST16-03C Ap	52.87	0.01	0.01	0.07	0.02	0.32	0.50	0.17	4.27	0.00	0.00	0.11	0.01	44.09	0.02	0.07	-1.84	100.74
ST16-03C Ap	54.03	0.00	0.01	0.06	0.02	0.00	0.27	0.14	3.99	0.03	0.00	0.10	0.03	43.80	0.00	0.09	-1.71	100.86
ST16-03C Ap	54.30	0.00	0.01	0.07	0.02	0.01	0.12	0.14	4.33	0.00	0.00	0.17	0.00	44.19	0.00	0.08	-1.85	101.66
ST16-03C Ap	54.60	0.01	0.00	0.12	0.01	0.12	0.44	0.14	3.79	0.02	0.03	0.10	0.01	44.67	0.03	0.05	-1.63	102.54
ST16-03C Ap	55.51	0.00	0.01	0.05	0.01	0.06	0.17	0.12	3.79	0.04	0.05	0.05	0.00	44.58	0.01	0.07	-1.62	102.89

ST16-03C Ap	54.83	0.00	0.01	0.09	0.01	0.04	0.22	0.33	3.31	0.00	0.00	0.04	0.00	43.44	0.02	0.01	-1.47	100.94
ST16-03C Ap	54.45	0.00	0.00	0.06	0.00	0.28	0.50	0.39	3.20	0.00	0.05	0.11	0.00	44.09	0.02	0.07	-1.44	101.80
ST16-03C Ap	55.83	0.02	0.00	0.06	0.01	0.19	0.26	0.30	3.32	0.00	0.04	0.11	0.02	44.10	0.04	0.05	-1.47	102.88
ST16-03C Ap	54.55	0.00	0.00	0.03	0.01	0.18	0.31	0.29	3.01	0.00	0.02	0.10	0.02	44.25	0.00	0.13	-1.33	101.56
ST16-03C Ap	55.09	0.00	0.00	0.03	0.00	0.02	0.25	0.29	3.63	0.00	0.03	0.10	0.00	44.48	0.00	0.01	-1.59	102.35
ST16-03C Ap	54.35	0.01	0.00	0.05	0.00	0.14	0.40	0.27	3.17	0.00	0.08	0.10	0.02	43.72	0.00	0.04	-1.40	100.95
ST16-03C Ap	54.56	0.01	0.01	0.08	0.03	0.08	0.34	0.29	3.21	0.02	0.07	0.14	0.01	43.25	0.01	0.08	-1.41	100.79
ST16-03C Ap	54.22	0.03	0.00	0.03	0.00	0.41	0.44	0.14	3.75	0.00	0.03	0.10	0.03	44.94	0.06	0.09	-1.61	102.68
ST16-03C Ap	53.39	0.00	0.01	0.03	0.01	0.16	0.15	0.12	4.06	0.00	0.02	0.08	0.00	45.01	0.01	0.06	-1.74	101.41
ST16-03C Ap	55.07	0.01	0.00	0.05	0.02	0.11	0.10	0.14	3.65	0.00	0.00	0.10	0.01	44.45	0.07	0.06	-1.57	102.34
ST16-03C Ap	52.48	0.00	0.00	0.10	0.08	0.28	0.22	0.11	3.44	0.00	0.03	0.05	0.01	43.57	0.00	0.04	-1.47	98.97
ST16-03C Ap	54.76	0.00	0.00	0.11	0.00	0.04	0.14	0.09	3.48	0.00	0.00	0.10	0.00	43.96	0.02	0.07	-1.49	101.32
ST16-03C Ap	53.97	0.00	0.01	0.02	0.01	0.00	0.06	0.12	4.14	0.05	0.08	0.11	0.00	44.03	0.04	0.08	-1.77	100.94
ST16-03C Ap	53.26	0.00	0.01	0.06	0.01	0.16	0.16	0.11	4.28	0.00	0.05	0.10	0.05	44.05	0.05	0.05	-1.82	100.56
ST16-03C Ap	55.35	0.00	0.00	0.12	0.02	0.08	0.23	0.08	4.36	0.06	0.09	0.09	0.02	44.37	0.00	0.07	-1.85	103.16
ST16-03C Ap	53.84	0.00	0.00	0.08	0.00	0.13	0.07	0.06	3.82	0.00	0.00	0.06	0.00	43.71	0.02	0.02	-1.62	100.25
ST16-03C Ap	54.27	0.00	0.01	0.09	0.02	0.15	0.36	0.16	3.67	0.00	0.02	0.05	0.01	44.16	0.05	0.13	-1.58	101.60
ST16-03C Ap	54.15	0.02	0.00	0.07	0.02	0.15	0.31	0.13	3.77	0.00	0.00	0.12	0.00	43.57	0.06	0.10	-1.61	100.88
ST16-03C Ap	54.06	0.00	0.00	0.05	0.00	0.28	0.39	0.11	3.76	0.00	0.07	0.13	0.00	43.85	0.00	0.10	-1.61	101.21
ST16-03C Ap	54.17	0.03	0.00	0.07	0.00	0.08	0.28	0.21	3.20	0.00	0.02	0.04	0.00	44.18	0.04	0.09	-1.39	101.02
ST16-03C Ap	54.72	0.03	0.02	0.08	0.00	0.34	0.41	0.12	3.78	0.00	0.07	0.12	0.04	43.76	0.03	0.07	-1.62	102.02
ST16-03C Ap	53.88	0.01	0.01	0.03	0.00	0.17	0.39	0.09	3.90	0.05	0.06	0.10	0.00	43.58	0.00	0.09	-1.66	100.71
ST16-03C Ap	53.63	0.00	0.00	0.05	0.00	0.09	0.34	0.14	3.41	0.00	0.12	0.11	0.00	43.63	0.03	0.12	-1.47	100.26
ST16-03C Ap	53.43	0.01	0.00	0.05	0.00	0.27	0.67	0.12	3.42	0.00	0.05	0.06	0.00	44.16	0.04	0.11	-1.47	100.91
ST16-03C Ap	54.07	0.01	0.02	0.06	0.01	0.31	0.25	0.12	3.60	0.00	0.06	0.09	0.00	44.60	0.01	0.06	-1.54	101.73

Analysis No.	SiO2	CaO	Y2O3	Ce2O3	Pr2O3	Nd2O3	Sm2O3	Gd2O3	La2O3	ThO2	UO2	PbO	P2O5	Total
STF26Amnz	0.51	1.23	2.47	27.42	2.86	9.84	1.48	1.26	13.53	5.88	0.60	0.58	29.89	97.55
STF26Amnz	0.18	0.44	1.91	31.34	2.95	10.36	1.50	1.16	16.49	0.81	0.54	0.20	30.64	98.51
STF26Amnz	0.62	0.94	1.85	29.03	2.82	10.51	1.42	1.15	14.65	4.92	0.14	0.37	29.88	98.30
STF26Amnz	0.58	1.08	2.65	27.72	2.86	10.52	1.61	1.37	13.23	6.03	0.16	0.48	30.50	98.77
STF26Amnz	0.51	0.94	1.79	28.79	2.89	10.72	1.40	1.07	14.69	5.08	0.15	0.39	29.99	98.41
STF26Amnz	0.42	0.95	1.37	29.64	2.86	10.45	1.41	1.08	15.17	5.15	0.13	0.38	30.25	99.27
STF26Amnz	0.50	1.15	2.97	26.91	2.82	10.25	1.63	1.51	13.38	5.80	0.31	0.48	30.73	98.45
STF26Amnz	0.47	0.92	2.12	28.59	2.93	10.91	1.53	1.32	13.99	5.31	0.10	0.40	31.12	99.72
STF26Amnz	0.26	0.63	1.99	28.59	2.84	10.41	1.63	1.35	15.27	3.15	0.27	0.28	30.04	96.73
STF26Amnz	0.52	0.90	1.90	28.91	2.88	10.68	1.34	1.17	14.82	5.20	0.11	0.38	31.13	99.94
STF26Amnz	0.46	0.91	1.58	29.29	3.00	10.68	1.37	1.05	14.87	5.12	0.12	0.40	30.92	99.79
STF26Amnz	0.52	0.95	2.29	28.50	2.95	10.71	1.53	1.35	13.91	5.41	0.13	0.42	31.33	100.01
STF26Amnz	0.10	0.26	2.37	30.77	3.16	11.12	1.83	1.45	15.98	0.22	0.36	0.08	30.58	98.29
STF26Amnz	0.59	1.17	3.41	27.07	2.79	10.30	1.74	1.61	12.67	6.26	0.29	0.52	31.08	99.49
STF26Amnz	0.47	0.91	1.69	28.68	3.00	10.62	1.51	1.14	14.84	5.05	0.11	0.39	31.00	99.39
STF26Amnz	0.58	1.08	2.37	27.85	2.90	10.54	1.70	1.40	13.40	6.03	0.17	0.50	30.82	99.32
STF26Amnz	0.55	0.87	1.66	29.35	2.89	10.62	1.40	1.09	14.79	5.08	0.13	0.44	30.63	99.50
ST16-19Amnz	0.67	0.96	2.01	27.79	2.83	10.30	1.53	1.26	14.13	5.17	0.14	0.41	30.91	98.14
ST16-19Amnz	0.26	1.00	2.41	28.61	2.96	10.58	1.69	1.45	13.88	3.64	0.36	0.33	31.93	99.11
ST16-19Amnz	0.39	0.99	1.44	28.59	2.88	10.47	1.51	1.12	14.68	5.15	0.09	0.43	31.02	98.76
ST16-19Amnz	0.23	0.75	2.21	29.14	2.98	10.70	1.65	1.25	14.88	2.66	0.56	0.31	31.39	98.71
ST16-19Amnz	0.34	1.09	3.02	27.39	2.90	10.03	1.42	1.37	14.19	4.94	0.24	0.42	31.44	98.80
ST16-19Amnz	0.44	1.01	1.69	27.91	2.97	10.59	1.52	1.30	14.28	5.18	0.15	0.39	31.25	98.69
ST16-19Amnz	0.14	0.80	2.51	29.07	3.05	10.65	1.67	1.36	14.18	1.89	1.14	0.48	31.75	98.70
ST16-19Amnz	0.41	0.97	1.72	28.04	2.95	10.56	1.47	1.15	14.24	5.13	0.13	0.38	30.90	98.06
ST16-19Amnz	0.46	1.12	1.37	28.39	2.93	10.52	1.53	1.17	14.44	5.37	0.17	0.44	31.25	99.16

ST16-19Amnz	0.37	1.29	2.38	27.49	2.85	10.18	1.67	1.36	13.77	5.61	0.36	0.49	30.95	98.78
ST16-19Amnz	0.43	0.98	1.02	28.94	2.92	10.68	1.65	1.18	14.54	5.06	0.11	0.38	30.80	98.70
ST16-19Amnz	0.43	1.01	1.59	28.55	2.86	10.51	1.53	1.20	14.43	5.22	0.14	0.43	30.92	98.82
ST16-19Amnz	0.40	1.01	1.32	28.77	2.94	10.83	1.58	1.30	14.54	5.05	0.11	0.41	30.78	99.04
ST16-19Amnz	0.24	0.90	2.21	28.35	3.04	10.24	1.55	1.30	14.18	3.53	0.62	0.43	31.61	98.20
ST16-19Amnz	0.37	1.00	3.29	27.35	2.85	10.45	1.59	1.41	13.81	4.92	0.17	0.39	31.49	99.08
ST16-19Amnz	0.43	1.00	1.37	28.77	2.99	11.06	1.73	1.40	14.42	5.12	0.13	0.40	31.33	100.15
ST16-19Amnz	0.41	0.93	0.91	29.06	2.88	10.68	1.53	1.06	15.03	4.89	0.10	0.41	31.14	99.03
ST16-19Amnz	0.35	1.26	2.51	27.60	2.75	9.97	1.54	1.32	13.88	5.81	0.36	0.52	31.39	99.25
ST16-19Amnz	0.34	1.09	1.72	28.60	2.96	10.47	1.58	1.23	14.47	4.77	0.47	0.47	31.66	99.83
ST16-19Amnz	0.41	1.03	1.18	28.92	3.01	10.67	1.54	1.21	14.63	5.14	0.10	0.38	32.13	100.34
ST16-19Amnz	0.43	0.97	0.91	29.32	3.04	10.79	1.54	1.13	14.88	5.11	0.11	0.40	31.58	100.21
ST16-19Amnz	0.30	0.70	2.09	29.40	2.95	10.85	1.65	1.29	14.84	2.67	0.59	0.34	31.28	98.93
ST16-19Amnz	0.49	1.01	0.85	29.11	2.83	10.84	1.56	1.19	14.64	5.48	0.12	0.44	31.37	99.93
ST16-19Amnz	0.32	1.32	2.20	27.69	2.76	10.24	1.59	1.35	14.03	5.69	0.50	0.59	31.05	99.34
ST16-19Amnz	0.40	0.89	1.13	29.51	3.01	10.80	1.51	1.10	15.36	4.77	0.08	0.38	31.20	100.14
ST16-19Amnz	0.45	1.01	1.24	28.95	2.96	10.75	1.59	1.12	14.67	5.12	0.13	0.37	30.91	99.27
ST16-19Amnz	0.46	0.99	1.66	28.66	2.85	10.73	1.47	1.22	14.63	5.11	0.10	0.41	31.13	99.41
ST16-19Amnz	0.39	1.03	1.66	28.66	2.94	10.70	1.63	1.24	14.47	5.03	0.19	0.40	31.07	99.43
ST16-19Amnz	0.41	0.92	0.91	29.52	2.90	10.54	1.45	0.99	15.25	4.77	0.11	0.35	31.06	99.17
ST16-19Amnz	0.43	1.04	1.29	29.10	2.89	10.69	1.53	1.23	14.84	5.19	0.12	0.43	32.08	100.86
ST16-03cmnz	0.59	1.29	3.77	26.10	2.68	9.67	1.71	1.65	12.34	7.07	0.24	0.62	31.00	98.72
ST16-03cmnz	0.85	1.05	1.95	27.49	2.89	10.59	1.58	1.36	13.16	6.82	0.11	0.55	29.53	97.93
ST16-03cmnz	0.30	0.67	1.74	29.86	3.15	11.03	1.50	1.16	15.12	2.84	0.13	0.21	31.85	99.56
ST16-03cmnz	0.39	1.66	2.68	26.13	2.78	9.41	1.75	1.36	12.72	6.84	0.94	0.77	31.84	99.26
ST16-03cmnz	0.62	1.26	3.57	24.91	2.67	9.42	1.63	1.64	12.12	6.79	0.31	0.59	30.41	95.93
ST16-03cmnz	0.47	1.12	2.42	27.73	2.81	10.25	1.55	1.29	13.56	6.17	0.22	0.53	31.14	99.27
ST16-03cmnz	0.76	0.95	2.45	26.99	2.81	10.24	1.54	1.47	13.60	6.47	0.16	0.53	29.56	97.55

ST16-03cmnz	0.74	1.41	3.04	25.66	2.53	9.69	1.35	1.32	12.20	9.20	0.29	0.74	30.32	98.48
ST16-03cmnz	0.62	1.23	3.43	25.87	2.69	9.85	1.72	1.64	12.44	6.74	0.23	0.56	30.46	97.49
ST16-03cmnz	0.56	1.48	3.33	25.23	2.66	9.23	1.75	1.52	12.11	7.58	0.61	0.76	30.81	97.64
ST16-03cmnz	0.41	0.70	1.78	29.03	2.98	10.85	1.48	1.11	14.83	3.76	0.12	0.31	31.92	99.26
ST16-03cmnz	0.81	1.24	2.59	26.51	2.77	10.18	1.72	1.63	12.49	7.63	0.11	0.61	30.60	98.91
ST16-03cmnz	0.35	1.56	1.99	26.30	2.76	9.55	1.63	1.33	13.88	5.99	0.61	0.59	32.52	99.06
ST16-03cmnz	0.45	0.68	1.40	28.96	2.95	10.60	1.42	1.00	14.96	4.17	0.08	0.36	29.82	96.85
ST16-03cmnz	0.79	1.09	2.06	27.90	2.87	10.60	1.68	1.30	13.37	7.02	0.11	0.54	31.39	100.73
ST16-03cmnz	0.16	0.71	1.66	28.69	2.85	10.66	1.75	1.43	15.05	3.13	0.46	0.45	31.28	98.28
ST16-03cmnz	0.73	0.80	1.51	28.83	2.87	10.67	1.28	0.96	15.07	5.87	0.11	0.42	31.09	100.22
ST16-03cmnz	0.66	1.15	2.49	26.54	2.94	10.31	1.67	1.42	12.89	6.80	0.17	0.53	30.42	97.97
ST16-03cmnz	0.30	1.67	1.79	27.46	2.56	8.65	1.29	1.14	15.07	7.01	0.72	0.71	31.60	99.96
ST16-03cmnz	0.56	1.32	3.40	26.35	2.74	9.89	1.64	1.42	12.89	6.83	0.31	0.59	31.17	99.11
ST16-03cmnz	0.28	0.49	1.39	30.68	2.92	10.56	1.60	1.18	15.07	3.30	0.34	0.29	31.17	99.28
ST16-03cmnz	0.21	1.64	2.14	26.68	2.68	9.65	1.51	1.32	13.19	6.76	0.93	0.77	31.29	98.78
ST16-03cmnz	1.32	0.98	1.52	27.22	2.71	9.49	1.38	1.10	14.11	9.74	0.30	0.77	29.66	100.29
ST16-03cmnz	0.40	1.73	2.24	26.34	2.76	9.83	1.51	1.26	12.96	7.81	0.63	0.74	31.71	99.91
ST16-03cmnz	0.39	1.09	2.04	27.62	3.00	10.21	1.54	1.29	14.21	5.64	0.34	0.49	31.25	99.12
ST16-03cmnz	0.13	0.36	2.77	29.13	3.13	10.72	1.68	1.34	16.00	1.69	0.11	0.15	31.46	98.68
ST16-03cmnz	0.69	1.16	2.45	26.65	2.81	10.40	1.75	1.52	12.59	7.13	0.12	0.54	30.96	98.76
ST16-03cmnz	0.60	1.12	2.60	26.87	2.77	10.37	1.54	1.50	13.27	6.58	0.13	0.55	30.72	98.62
STF10Bmnz	0.29	0.23	1.56	31.70	2.91	10.34	1.67	1.27	16.66	0.54	0.22	0.11	31.31	98.79
STF10Bmnz	0.24	0.93	1.70	29.53	2.87	10.63	1.92	1.53	15.03	3.02	0.32	0.30	30.99	99.00
STF10Bmnz	0.28	0.49	2.13	30.26	2.85	10.59	1.87	1.43	15.83	1.77	0.30	0.26	32.03	100.10
STF10Bmnz	0.27	0.13	0.83	32.78	2.83	9.89	1.13	0.70	19.77	0.32	0.06	0.03	31.87	100.58
STF10Bmnz	0.21	0.41	2.54	30.15	2.98	10.44	1.90	1.47	15.52	0.61	0.42	0.13	31.69	98.47
STF10Bmnz	0.33	0.93	1.60	22.53	2.34	8.01	1.32	0.98	11.04	3.54	0.36	0.40	23.36	76.73
STF10Bmnz	0.20	0.42	1.19	15.10	1.81	5.39	0.81	0.64	8.00	3.23	0.22	0.25	10.76	48.04

STF10Bmnz	0.33	0.37	1.24	29.41	2.93	10.89	2.06	1.56	14.67	1.57	0.27	0.22	27.14	92.66
STF10Bmnz	3.02	3.55	1.64	16.73	1.77	6.72	1.32	1.17	7.82	25.20	0.28	1.93	26.59	97.74
STF10Bmnz	1.35	2.18	2.28	22.88	2.31	8.46	1.44	1.32	11.20	13.93	0.53	1.22	29.45	98.55
STF10Bmnz	2.23	2.48	1.98	20.76	2.08	7.84	1.29	1.20	9.93	16.54	0.48	1.42	26.72	94.95
STF10Bmnz	3.20	2.68	1.74	16.96	1.76	6.69	1.24	1.13	7.90	27.18	0.41	2.10	26.51	99.50
STF10Bmnz	2.66	2.65	1.48	19.61	2.02	7.82	1.33	1.03	8.49	19.49	0.33	1.51	26.47	94.88
STF10Bmnz	2.38	2.37	1.41	21.47	2.34	9.05	1.49	1.05	9.11	18.07	0.32	1.37	28.30	98.74
STF10Bmnz	2.12	2.81	2.00	19.98	2.08	7.89	1.36	1.04	8.85	20.51	0.34	1.64	28.43	99.05
STF10Bmnz	1.52	2.42	2.34	22.55	2.29	8.48	1.44	1.23	10.78	14.84	0.47	1.28	29.55	99.19
STF10Bmnz	1.24	2.59	2.05	22.52	2.32	8.61	1.49	1.15	10.43	14.82	0.43	1.28	29.64	98.56
STF10Bmnz	0.22	1.21	2.41	27.06	2.81	10.57	1.76	1.49	13.66	3.69	0.89	0.54	31.23	97.52
STF10Bmnz	0.72	1.47	2.80	25.82	2.61	9.61	1.46	1.37	12.47	7.92	0.57	0.78	30.77	98.38
STF10Bmnz	0.38	0.97	2.05	26.82	2.80	10.33	1.66	1.43	13.51	3.90	0.89	0.65	28.60	93.99
STF10Bmnz	0.17	1.52	2.98	26.80	2.74	10.64	1.71	1.59	13.30	3.84	0.67	0.51	31.59	98.07
STF10Bmnz	0.87	1.68	2.48	25.33	2.64	9.27	1.47	1.30	12.32	8.09	0.48	0.72	29.30	95.93
STF10Bmnz	0.15	1.25	2.48	26.61	2.78	10.70	1.81	1.46	13.58	3.70	0.80	0.53	31.42	97.27
STF10Bmnz	1.20	1.43	2.64	25.62	2.66	9.54	1.44	1.35	12.37	7.98	0.57	0.74	29.12	96.67
STF10Bmnz	0.52	0.57	2.35	29.08	2.96	10.69	2.19	1.72	13.72	1.42	0.29	0.22	29.94	95.65
STF10Bmnz	1.03	1.78	2.79	24.44	2.49	9.09	1.54	1.40	11.64	10.44	0.55	0.99	30.65	98.82
STF10Bmnz	2.34	3.39	1.71	18.05	1.92	7.05	1.42	1.21	8.26	23.47	0.34	1.68	28.05	98.90
STF10Bmnz	1.38	2.26	2.42	23.11	2.36	8.60	1.47	1.30	11.27	13.07	0.52	1.15	31.27	100.17
STF10Bmnz	1.14	2.00	1.26	23.19	2.36	8.81	1.53	1.18	11.31	13.90	0.29	1.16	29.39	97.53
STF10Bmnz	0.40	0.58	1.47	29.82	2.76	10.15	1.54	1.17	15.16	1.39	0.25	0.18	32.13	97.01
STF10Bmnz	0.13	0.26	2.84	30.77	2.97	10.35	1.50	1.31	16.04	0.40	0.19	0.08	31.45	98.30
STF10Bmnz	0.58	0.21	1.01	29.20	2.70	9.87	1.51	1.04	15.16	1.29	0.11	0.14	26.14	88.98
STF10Bmnz	0.80	1.33	1.98	26.24	2.56	9.43	1.48	1.25	13.14	6.32	0.41	0.60	28.61	94.16
STF10Bmnz	1.50	2.21	2.27	22.39	2.33	8.42	1.49	1.21	10.67	14.51	0.48	1.28	29.12	97.88
STF10Bmnz	2.35	2.51	2.30	19.87	2.06	7.54	1.30	1.23	9.65	18.92	1.19	1.73	27.89	98.55

STF10Bmnz	1.66	2.19	2.39	22.00	2.15	8.07	1.36	1.15	10.56	14.98	0.57	1.40	27.88	96.36
STF10Bmnz	0.36	0.83	2.07	28.73	2.80	9.95	1.65	1.25	14.68	3.09	0.28	0.39	30.52	96.60
STF10Bmnz	0.86	1.56	1.96	24.93	2.49	9.34	1.50	1.27	12.32	8.90	0.44	0.81	27.17	93.54
STF10Bmnz	0.92	1.10	1.12	18.27	1.39	5.67	0.87	0.72	8.59	6.70	0.38	0.59	14.39	60.71
STF10Bmnz	0.72	0.95	0.93	29.13	2.93	10.83	1.20	0.81	14.74	6.28	0.08	0.51	30.88	99.98
STF10Bmnz	1.79	2.58	1.84	21.30	2.31	8.76	1.38	1.16	9.32	17.69	0.30	1.41	28.74	98.57
STF10Bmnz	1.21	2.13	2.11	22.73	2.45	8.75	1.49	1.14	10.97	13.32	0.47	1.18	28.18	96.11
ST16-31Amnz	0.67	0.62	1.35	28.83	2.76	10.18	1.58	1.07	14.34	3.99	0.14	0.33	31.66	97.51
ST16-31Amnz	0.65	0.72	1.34	28.23	2.77	9.88	1.40	1.11	14.32	3.95	0.23	0.29	29.48	94.36
ST16-31Amnz	0.56	0.65	1.44	29.06	2.85	10.13	1.55	1.21	14.67	4.22	0.20	0.29	31.33	98.18
ST16-31Amnz	0.54	0.54	1.28	30.39	2.98	10.52	1.51	1.01	15.56	2.57	0.15	0.15	31.75	98.94
ST16-31Amnz	1.27	1.49	1.55	24.12	2.45	9.02	1.51	1.08	12.69	10.86	0.19	0.58	29.91	96.72
ST16-31Amnz	0.91	0.89	1.61	28.82	2.90	10.30	1.60	1.26	14.45	4.85	0.24	0.37	30.01	98.20
ST16-31Amnz	0.88	0.41	1.24	27.05	2.51	9.41	1.46	1.05	13.24	2.46	0.32	0.20	31.99	92.24
ST16-31Amnz	0.41	0.45	1.20	28.91	2.83	10.52	1.59	1.17	14.74	2.06	0.25	0.35	27.92	92.41
ST16-31Amnz	0.37	0.47	1.43	30.11	2.99	10.66	1.62	1.15	15.27	2.64	0.15	0.19	30.72	97.78
ST16-31Amnz	0.75	0.89	1.33	29.17	2.99	10.48	1.68	1.21	14.39	4.25	0.11	0.36	29.33	96.94
ST16-31Amnz	0.51	0.66	1.58	28.13	2.75	10.34	1.62	1.17	14.45	4.68	0.18	0.28	30.58	96.94
ST16-31Amnz	1.49	1.35	1.58	26.13	2.53	9.55	1.51	1.16	13.15	10.19	0.25	0.78	30.28	99.95
ST16-31Amnz	0.78	0.71	1.58	27.63	2.76	10.20	1.61	1.20	13.83	5.32	0.20	0.33	29.94	96.08
ST16-31Amnz	0.89	1.61	2.25	24.91	2.30	8.47	1.48	1.35	13.81	8.22	0.49	0.87	29.07	95.71
ST16-31Amnz	0.67	1.58	1.34	26.37	2.41	8.21	1.17	0.99	15.91	8.47	0.38	0.83	30.62	98.96
ST16-31Amnz	0.60	0.63	1.50	28.93	2.85	10.45	1.69	1.19	14.12	4.67	0.26	0.29	30.14	97.32
ST16-31Amnz	1.08	0.84	1.30	27.81	2.72	10.09	1.56	1.16	14.04	6.42	0.16	0.51	29.41	97.08
ST16-31Amnz	0.85	0.71	1.41	29.30	2.78	10.33	1.55	1.21	14.58	4.95	0.17	0.39	30.83	99.07
ST16-31Amnz	1.05	0.92	1.57	28.18	2.70	9.99	1.49	1.13	14.64	6.09	0.20	0.45	31.62	100.02
ST16-31Jmnz	0.35	1.07	0.93	28.45	2.88	10.47	1.83	1.37	14.82	4.74	0.17	0.40	30.99	98.47
ST16-31Jmnz	0.48	0.73	1.04	28.43	2.80	10.09	1.54	1.12	14.96	4.15	0.43	0.36	29.55	95.68

ST16-31Jmnz	0.60	1.14	1.10	26.23	2.75	10.11	1.68	1.27	13.72	5.23	0.33	0.41	26.64	91.20
ST16-31Jmnz	0.23	0.52	1.30	29.78	3.00	10.67	1.85	1.44	15.36	1.86	0.51	0.25	31.29	98.05
ST16-31Jmnz	0.37	0.45	8.86	22.40	2.43	8.03	1.39	2.19	12.48	3.29	0.45	0.35	27.12	89.79
ST16-31Jmnz	0.32	0.88	1.09	28.53	2.78	10.61	1.86	1.34	14.32	3.29	0.58	0.43	30.73	96.76
ST16-31Jmnz	0.25	0.67	1.09	29.17	2.96	10.49	1.66	1.22	15.33	3.35	0.46	0.37	30.69	97.72
ST16-31Jmnz	0.21	0.48	1.05	30.09	3.02	10.84	1.73	1.27	15.67	2.25	0.41	0.29	31.34	98.65
ST16-31Jmnz	0.32	0.54	1.45	29.54	2.94	11.06	2.20	1.88	14.73	1.46	0.65	0.29	30.27	97.32
ST16-31Jmnz	0.32	0.65	1.15	29.49	3.04	10.80	2.10	1.78	14.89	2.13	0.43	0.24	30.93	97.96
ST16-31Jmnz	0.22	0.45	0.99	31.20	3.00	10.60	1.72	1.23	16.28	0.84	0.14	0.09	30.13	96.89
ST16-31Jmnz	0.51	0.67	1.59	28.05	2.74	10.20	2.03	1.60	14.25	2.94	0.56	0.32	29.56	95.02
ST16-31Jmnz	0.28	1.45	1.28	27.12	2.66	9.65	1.61	1.28	14.04	4.76	1.12	0.66	29.36	95.27
ST16-31Jmnz	0.31	0.75	0.78	27.28	2.69	9.70	1.55	1.12	14.29	4.33	0.33	0.32	25.22	88.67
ST16-31Jmnz	0.49	0.42	1.47	29.06	2.93	10.65	1.85	1.36	15.48	0.62	0.81	0.29	27.17	92.59
ST16-31Jmnz	0.20	1.58	1.48	26.80	2.69	9.44	1.54	1.12	14.21	5.14	1.80	0.91	30.06	96.98
ST16-31Jmnz	0.51	0.90	1.10	27.98	2.77	10.20	1.69	1.14	14.77	4.10	0.38	0.38	28.16	94.07
ST16-31Jmnz	0.73	0.22	0.99	28.02	2.64	9.74	1.51	1.03	14.54	0.73	0.32	0.15	30.74	91.36
ST16-31Jmnz	0.76	0.53	0.94	29.95	2.75	10.15	1.58	1.18	15.81	1.85	0.33	0.24	30.54	96.60
ST16-31Jmnz	0.38	0.89	1.06	28.21	2.85	10.57	1.87	1.50	14.10	3.42	0.36	0.39	26.91	92.49
ST16-31Jmnz	0.42	1.32	1.19	25.16	2.56	8.94	1.39	1.07	13.35	5.22	0.82	0.72	26.76	88.92
ST16-31Jmnz	0.32	1.47	1.16	27.69	2.83	10.33	1.71	1.18	14.41	4.97	0.60	0.55	30.62	97.86
ST16-31Jmnz	0.32	0.82	1.16	29.10	3.13	10.66	1.85	1.47	14.83	2.64	0.42	0.35	31.23	97.99
ST16-31Jmnz	0.28	0.73	0.91	29.37	2.96	10.91	1.94	1.46	14.81	2.35	0.22	0.27	31.26	97.48
ST16-31Jmnz	0.16	1.40	1.32	27.52	2.78	9.80	1.58	1.25	14.41	4.81	1.14	0.59	31.35	98.11
ST16-31Jmnz	0.29	1.30	1.05	26.83	2.78	9.91	1.49	1.09	14.61	4.17	0.58	0.55	27.75	92.40
ST16-31Jmnz	0.48	0.85	1.15	28.81	2.86	11.09	2.35	1.83	13.41	4.86	0.22	0.45	31.31	99.67
ST16-31Jmnz	0.32	1.26	1.20	28.31	2.83	10.22	1.76	1.26	14.49	5.21	0.55	0.54	32.27	100.21
ST16-31Jmnz	0.21	0.32	0.93	30.67	2.95	10.65	1.68	1.09	16.66	1.11	0.34	0.17	30.53	97.33
ST16-31Jmnz	0.33	0.56	0.95	28.42	2.92	10.70	2.05	1.61	14.33	3.57	0.38	0.36	30.11	96.28

ST16-31Jmnz	0.39	0.68	1.06	29.47	2.97	10.85	1.72	1.26	15.80	1.61	0.36	0.27	31.03	97.46
ST16-31Jmnz	0.50	1.51	1.21	26.57	2.57	9.25	1.45	1.17	13.99	5.79	1.45	0.79	28.03	94.29
STF02Bmnz	0.51	0.51	1.08	29.29	2.82	9.93	1.64	1.36	17.01	2.23	0.24	0.28	30.83	97.71
STF02Bmnz	0.37	0.70	1.26	29.24	2.77	9.80	1.53	1.38	15.95	3.71	0.34	0.35	30.52	97.92
STF02Bmnz	0.47	0.77	1.58	29.62	2.76	10.32	1.75	1.31	14.99	3.90	0.31	0.35	31.90	100.04
STF02Bmnz	0.73	0.99	1.05	28.33	2.83	10.15	1.63	1.35	14.56	4.26	0.27	0.44	29.31	95.92
STF02Bmnz	0.53	0.53	1.11	29.93	2.88	10.25	1.62	1.20	15.53	2.05	0.29	0.26	29.56	95.74
STF02Bmnz	0.78	1.28	1.85	27.06	2.76	9.64	1.53	1.30	13.34	6.99	0.30	0.59	29.15	96.57
STF02Bmnz	0.78	0.96	1.44	28.83	2.68	9.67	1.51	1.20	14.52	5.22	0.30	0.43	29.62	97.17
STF02Bmnz	0.43	0.62	1.50	30.03	2.96	10.25	1.75	1.39	15.46	2.91	0.37	0.32	32.28	100.28
STF02Bmnz	0.97	0.46	0.78	27.59	2.77	9.47	1.42	1.02	14.25	2.13	0.26	0.23	20.93	82.29
STF02Bmnz	0.49	0.84	1.45	29.60	2.86	10.51	1.62	1.27	15.04	3.68	0.23	0.34	31.03	98.95
STF02Bmnz	0.55	0.68	1.41	28.40	2.76	9.89	1.60	1.18	14.73	4.45	0.29	0.32	30.14	96.39
STF02Bmnz	0.47	0.46	1.30	31.17	2.94	9.90	1.38	1.23	17.12	1.68	0.29	0.25	31.65	99.83
STF02Bmnz	0.64	1.04	1.85	28.41	2.79	10.12	1.60	1.37	14.40	5.07	0.30	0.48	31.36	99.44
STF02Bmnz	0.80	1.03	1.68	28.28	2.67	10.18	1.61	1.27	14.42	5.11	0.29	0.47	30.88	98.69
STF02Bmnz	0.87	0.86	1.40	28.74	2.76	9.80	1.53	1.30	14.80	3.72	0.39	0.35	31.47	97.99
STF02Bmnz	0.60	1.28	1.82	27.67	2.79	9.88	1.59	1.39	13.66	6.69	0.33	0.59	30.71	98.99
STF02Bmnz	0.50	0.55	1.77	30.34	2.95	9.78	1.15	0.99	16.39	0.59	0.73	0.26	29.27	95.26
STF02Bmnz	0.60	0.31	1.79	31.29	2.84	9.67	1.31	1.01	16.92	0.53	0.45	0.16	30.16	97.04
STF02Bmnz	0.43	1.06	1.80	29.04	2.76	9.67	1.46	1.23	15.24	4.89	0.56	0.48	32.09	100.71
STF02Bmnz	0.20	0.56	2.02	29.52	2.97	10.56	1.65	1.23	15.17	1.54	0.52	0.31	30.20	96.42
STF02Bmnz	0.62	0.70	1.28	28.40	2.76	10.39	1.60	1.27	14.47	2.59	0.23	0.29	26.60	91.20
STF02Bmnz	0.55	0.42	2.09	28.41	2.98	10.14	1.59	1.31	14.48	1.02	0.38	0.20	27.97	91.55
STF02Bmnz	0.20	0.51	1.29	30.14	2.86	9.98	1.43	1.17	16.59	1.56	0.30	0.22	30.73	96.99
STF02Bmnz	0.48	0.96	1.38	27.96	2.58	9.51	1.51	1.28	14.75	4.81	0.33	0.52	29.38	95.46
STF02Bmnz	0.99	1.07	1.37	26.20	2.65	9.39	1.48	1.09	13.47	5.81	0.37	0.57	25.51	89.96
STF02Bmnz	0.54	1.08	1.77	27.32	2.78	10.00	1.57	1.35	13.88	5.86	0.33	0.53	30.47	97.47

STF02Bmnz	0.57	1.10	1.90	27.38	2.66	9.72	1.53	1.27	13.68	5.83	0.36	0.55	29.18	95.72
STF02Bmnz	0.71	1.28	1.86	26.61	2.76	9.75	1.46	1.27	13.35	6.93	0.34	0.63	28.99	95.92
STF02Bmnz	0.60	1.22	1.91	26.85	2.66	9.72	1.48	1.30	13.58	6.86	0.35	0.63	29.98	97.16
STF02Bmnz	0.44	0.92	1.63	28.65	2.88	10.07	1.57	1.24	14.63	4.27	0.35	0.41	30.34	97.38
STF02Bmnz	0.58	0.90	1.51	29.13	2.80	9.90	1.52	1.29	15.48	3.16	0.30	0.33	31.32	98.21
STF02Bmnz	0.67	0.57	2.65	28.66	2.96	11.28	2.20	1.98	13.73	1.38	0.48	0.24	30.72	97.54
STF02Bmnz	0.31	0.53	1.10	29.12	2.76	10.25	1.77	1.45	16.07	2.88	0.25	0.24	30.97	97.69
STF02Bmnz	0.33	0.72	1.30	29.37	2.81	10.02	1.55	1.16	15.24	3.52	0.32	0.36	30.70	97.40
STF02Bmnz	0.43	0.81	1.57	29.44	2.80	9.97	1.49	1.30	15.65	3.12	0.37	0.39	30.17	97.52
ST16-09mnz	0.32	1.00	3.34	26.59	2.46	8.65	1.43	1.41	16.49	3.76	1.01	0.58	31.56	98.59
ST16-09mnz	0.78	1.05	4.45	25.16	2.82	10.82	1.85	1.83	11.23	5.80	0.72	0.66	31.05	98.21
ST16-09mnz	0.30	1.41	4.49	24.56	2.63	10.15	1.86	1.88	11.38	5.40	1.28	0.77	31.59	97.71
ST16-09mnz	0.36	0.98	2.53	27.42	2.86	10.41	1.81	1.53	13.88	4.57	0.45	0.49	31.10	98.39
ST16-09mnz	0.44	1.02	3.89	25.73	2.82	10.82	1.87	1.71	11.86	5.27	0.71	0.57	31.09	97.81
ST16-09mnz	0.43	1.04	2.81	26.87	2.83	10.65	1.81	1.61	13.26	4.88	0.57	0.54	31.56	98.84
ST16-09mnz	0.42	1.15	4.08	25.43	2.61	9.53	1.68	1.72	13.63	4.52	1.11	0.66	31.57	98.11
ST16-09mnz	0.27	1.18	4.32	25.54	2.78	10.47	1.99	1.82	11.77	3.40	1.57	0.67	30.27	96.05
ST16-09mnz	0.45	1.13	4.70	25.39	2.78	10.46	1.92	1.84	11.26	3.97	1.24	0.66	31.57	97.37
ST16-09mnz	0.22	1.15	4.54	25.93	2.95	10.30	1.91	1.80	11.75	3.45	1.66	0.70	31.58	97.95
ST16-09mnz	0.22	1.22	4.46	26.01	2.84	10.14	1.95	1.77	12.08	3.27	1.77	0.78	32.15	98.65
ST16-09mnz	0.28	1.29	4.57	25.47	2.78	10.35	1.84	1.80	11.67	4.02	1.68	0.75	31.39	97.89
ST16-09mnz	0.29	1.18	4.19	26.30	2.85	10.11	1.81	1.74	12.27	3.64	1.56	0.71	31.11	97.75
ST16-09mnz	0.37	1.32	4.61	25.43	2.73	10.27	1.90	1.77	11.58	4.85	1.23	0.76	31.47	98.29
ST16-09mnz	0.48	1.04	2.29	27.61	2.88	10.40	1.80	1.43	13.91	4.98	0.39	0.50	31.19	98.89
ST16-09mnz	0.35	1.19	4.48	25.79	2.85	10.21	1.89	1.73	12.09	4.30	1.14	0.65	31.49	98.16
ST16-09mnz	0.31	1.18	3.35	26.52	2.63	9.22	1.61	1.44	15.17	3.32	1.23	0.63	31.15	97.75
ST16-09mnz	0.23	1.23	5.03	25.71	2.83	10.18	2.02	1.92	11.69	3.27	1.71	0.78	32.53	99.14
ST16-09mnz	0.26	1.18	5.10	25.45	2.73	9.87	1.88	1.78	12.05	3.52	1.64	0.76	32.01	98.24

ST16-09mnz	0.21	1.13	4.73	25.72	2.76	10.05	1.91	1.82	12.09	3.61	1.57	0.71	31.92	98.23
ST16-09mnz	0.32	1.06	4.17	26.33	2.81	10.07	1.70	1.64	12.41	3.89	1.14	0.60	31.17	97.32
ST16-09mnz	0.33	1.28	4.60	25.39	2.79	10.36	1.89	1.82	11.55	4.62	1.30	0.77	30.94	97.66
ST16-09mnz	0.42	1.22	4.37	25.89	2.74	9.83	1.86	1.74	11.87	4.39	1.19	0.70	30.56	96.77
ST16-09mnz	0.27	1.24	4.65	25.50	2.77	10.30	1.91	1.87	11.73	4.06	1.49	0.76	31.50	98.04
ST16-09mnz	0.30	1.18	4.61	25.35	2.67	9.88	1.79	1.78	12.13	4.03	1.44	0.75	31.47	97.37
ST16-09mnz	0.28	1.19	4.62	25.45	2.77	10.23	1.96	1.84	12.00	3.94	1.45	0.71	31.31	97.76
ST16-09mnz	0.25	1.18	4.25	25.34	2.80	10.03	1.79	1.71	11.84	3.97	1.25	0.66	31.66	96.71
ST16-09mnz	0.28	1.07	4.57	25.78	2.75	9.98	1.86	1.77	12.50	3.47	1.52	0.71	31.73	97.99
ST16-09mnz	0.31	1.23	4.40	25.57	2.81	10.01	1.71	1.61	12.34	4.10	1.34	0.73	31.64	97.80
ST16-09mnz	0.32	1.30	4.59	24.92	2.73	10.14	1.81	1.83	12.00	5.34	0.92	0.69	31.56	98.14
ST16-09mnz	0.30	1.22	4.36	25.43	2.74	10.21	1.83	1.79	12.20	5.04	0.83	0.62	31.70	98.27
ST16-09mnz	0.37	1.07	3.91	26.41	2.75	10.29	1.77	1.61	12.48	4.99	0.61	0.56	31.10	97.91
ST16-09mnz	0.30	1.29	4.65	25.14	2.72	10.23	1.80	1.83	11.91	5.45	0.85	0.69	31.21	98.07
ST16-09mnz	0.31	1.08	4.12	26.41	2.70	9.89	1.67	1.63	13.39	4.15	0.89	0.59	31.17	98.02
ST16-09mnz	0.23	0.94	3.28	26.88	2.72	10.21	1.85	1.68	14.80	1.59	1.08	0.45	31.18	96.90
ST16-09mnz	0.38	1.06	4.73	25.79	2.81	10.23	1.81	1.87	12.25	4.45	0.79	0.55	31.48	98.20
ST16-09mnz	0.33	1.17	4.63	25.33	2.76	9.96	1.82	1.76	12.27	4.79	1.00	0.66	31.10	97.60
ST16-09mnz	0.41	1.11	4.36	26.02	2.63	9.95	1.75	1.70	13.08	4.31	1.00	0.63	31.01	97.97
ST16-09mnz	0.34	1.25	4.26	25.40	2.75	10.14	1.86	1.78	12.09	5.33	0.85	0.65	31.52	98.23
ST16-09mnz	0.32	1.07	4.04	26.40	2.69	9.72	1.73	1.67	14.08	4.08	1.00	0.61	31.78	99.19
ST16-09mnz	0.42	1.08	3.76	26.25	2.74	9.99	1.76	1.66	12.87	5.20	0.64	0.60	31.24	98.21
ST16-09mnz	0.37	1.09	4.27	25.29	2.68	9.75	1.83	1.75	12.44	4.35	0.94	0.60	30.65	96.03
ST16-09mnz	0.34	1.28	4.46	25.27	2.74	10.31	1.83	1.84	12.19	5.08	0.94	0.67	31.56	98.52
ST16-09mnz	0.35	0.89	2.70	27.54	2.90	10.53	1.75	1.47	13.57	4.55	0.46	0.45	31.25	98.41
ST16-09mnz	0.36	1.14	4.41	25.92	2.86	9.93	1.83	1.71	12.42	4.56	1.07	0.64	31.35	98.19
ST16-09mnz	0.42	1.13	2.04	26.83	2.79	10.17	1.73	1.41	13.47	5.67	0.38	0.54	30.73	97.30
ST16-09mnz	0.44	1.01	3.06	27.00	2.77	10.34	1.74	1.47	13.17	4.84	0.68	0.54	31.37	98.42

ST16-09mnz	0.54	1.09	4.34	25.40	2.83	10.35	1.70	1.81	11.69	5.34	0.88	0.68	31.20	97.85
STF33mnz	0.27	2.72	1.58	23.47	2.51	8.92	1.77	1.38	11.62	10.58	0.56	0.99	30.96	97.34
STF33mnz	0.18	0.10	1.03	31.28	2.96	10.84	1.76	1.21	16.65	0.00	0.00	0.00	29.91	95.94
STF33mnz	0.40	0.58	1.23	28.36	2.80	10.32	1.85	1.29	14.39	0.00	0.00	0.00	29.96	91.17
STF33mnz	0.27	0.54	1.31	30.52	3.02	10.94	1.91	1.38	15.97	0.00	0.00	0.00	31.81	97.67
STF33mnz	0.17	0.39	1.53	29.95	2.97	11.09	2.03	1.44	15.87	0.00	0.00	0.00	31.52	96.96
STF33mnz	0.38	0.67	1.31	28.48	2.82	10.41	1.78	1.34	14.68	0.00	0.00	0.00	30.90	92.78
STF33mnz	0.25	0.25	1.66	29.40	2.99	11.40	2.28	1.74	15.59	0.00	0.00	0.00	29.12	94.68
STF33mnz	0.44	0.35	1.18	26.72	2.73	9.84	1.79	1.28	14.50	0.00	0.00	0.00	30.08	88.91
STF33mnz	0.35	1.19	1.52	27.00	2.77	10.23	1.89	1.42	13.57	4.70	0.42	0.45	31.89	97.39
STF33mnz	0.45	1.16	1.30	28.05	2.86	10.41	1.97	1.37	14.12	4.80	0.40	0.43	30.26	97.59
STF33mnz	0.19	0.21	1.41	30.39	2.87	10.81	2.02	1.48	15.32	1.86	0.16	0.10	30.51	97.32
STF33mnz	0.43	0.45	1.73	30.23	2.83	10.67	2.04	1.64	15.25	1.85	0.14	0.15	32.72	100.13
STF33mnz	0.18	0.24	1.58	30.12	2.95	10.64	1.83	1.44	15.60	0.92	0.13	0.09	30.53	96.26
STF33mnz	0.45	0.73	1.35	27.70	2.75	10.94	2.30	1.87	13.77	3.31	0.18	0.29	30.39	96.04
STF33mnz	0.35	1.24	1.41	27.85	2.80	10.13	1.86	1.31	14.07	5.38	0.43	0.46	31.49	98.79
STF33mnz	0.22	0.22	1.53	30.10	2.98	10.75	2.27	1.85	15.08	0.85	0.16	0.09	30.78	96.86
STF33mnz	0.36	0.76	1.40	29.01	3.12	10.61	2.14	1.72	14.55	1.89	0.20	0.26	29.99	96.00
STF33mnz	0.44	1.39	1.74	26.46	2.75	9.71	1.72	1.40	13.22	5.34	0.61	0.52	30.63	95.93
STF33mnz	0.32	0.91	2.13	28.08	2.82	10.49	1.92	1.56	15.32	2.26	0.27	0.28	31.81	98.16
STF33mnz	0.54	0.78	1.00	28.50	2.85	10.51	1.93	1.41	14.68	2.58	0.30	0.30	26.44	91.81
STF33mnz	0.47	0.55	1.24	29.10	2.92	10.39	1.90	1.31	15.79	2.12	0.07	0.21	29.95	96.03
STF33mnz	0.20	0.19	1.61	31.31	3.00	10.77	1.88	1.27	17.23	0.09	0.06	0.00	31.58	99.20
STF33mnz	0.36	0.81	1.18	28.96	2.99	10.55	1.81	1.41	14.71	3.69	0.23	0.31	31.06	98.06
STF33mnz	0.22	0.28	1.14	30.06	2.88	10.52	1.79	1.22	15.91	2.05	0.22	0.12	31.09	97.50
STF33mnz	0.37	0.32	1.21	29.69	2.83	10.74	1.91	1.26	15.61	1.55	0.25	0.13	28.97	94.82
STF33mnz	0.88	3.80	1.59	17.53	1.78	6.99	1.47	1.20	7.91	22.62	0.72	1.71	28.51	96.71
STF33mnz	0.46	2.41	1.40	23.89	2.55	9.29	1.66	1.38	11.95	10.32	0.51	1.06	30.21	97.10

STF33mnz	0.60	2.28	1.65	24.19	2.44	9.22	1.75	1.37	11.71	10.39	0.53	0.82	29.41	96.37
STF33mnz	0.51	1.77	1.28	25.88	2.52	9.30	1.71	1.29	13.14	8.70	0.28	0.67	30.23	97.28
STF33mnz	0.39	1.42	1.74	26.57	2.65	9.74	1.76	1.38	13.29	5.09	0.45	0.59	30.58	95.64
STF33mnz	0.15	0.29	1.38	29.82	2.93	11.02	2.01	1.47	15.32	0.80	0.22	0.11	31.00	96.52
STF33mnz	0.39	1.22	1.21	27.39	2.80	10.12	1.84	1.29	13.68	5.76	0.41	0.53	31.54	98.19
STF33mnz	0.31	0.43	1.07	29.98	2.99	10.69	1.90	1.36	15.24	3.13	0.18	0.22	32.12	99.61
STF16Amnz	0.64	0.77	1.25	27.87	2.93	10.57	1.85	1.50	13.41	3.20	0.38	0.00	30.29	94.66
STF16Amnz	0.37	1.32	2.05	27.29	3.09	10.46	1.64	1.36	14.10	5.43	0.71	0.00	29.73	97.55
STF16Amnz	0.49	1.26	2.51	26.19	2.97	10.64	1.76	1.42	13.26	5.60	0.58	0.00	28.36	95.03
STF16Amnz	0.36	1.22	2.71	26.15	3.01	10.62	1.68	1.37	13.06	5.16	0.59	0.00	30.03	95.96
STF16Amnz	0.67	1.32	2.13	26.89	2.81	10.00	1.58	1.31	13.82	5.19	0.75	0.00	31.04	97.51
STF16Amnz	0.40	1.28	1.91	26.74	2.99	10.64	1.74	1.43	13.64	5.54	0.60	0.00	30.33	97.24
STF16Amnz	0.25	1.58	1.35	27.21	2.85	10.18	1.58	1.24	14.47	4.62	1.45	0.00	31.10	97.86
STF16Amnz	0.22	0.86	1.11	28.98	2.97	10.86	1.93	1.45	14.16	5.36	0.57	0.00	31.02	99.48
STF16Amnz	0.51	1.18	1.26	26.51	2.81	10.18	1.73	1.33	13.61	5.46	1.47	0.00	29.61	95.67
STF16Amnz	0.45	1.30	1.98	26.61	2.98	10.78	1.79	1.46	13.24	5.70	0.61	0.00	30.35	97.25
STF16Amnz	0.42	1.35	1.46	26.73	2.95	10.31	1.59	1.27	13.91	5.09	0.63	0.00	30.19	95.91
STF16Amnz	0.52	1.32	2.43	26.81	2.90	10.27	1.57	1.42	13.82	4.70	0.60	0.00	30.46	96.83
STF16Amnz	0.65	1.16	2.31	25.95	2.96	10.24	1.67	1.25	13.14	4.94	0.45	0.00	31.11	95.85
STF16Amnz	0.40	0.74	1.41	27.81	3.09	10.42	1.58	1.10	15.09	3.86	0.43	0.00	28.46	94.37
STF16Amnz	0.46	1.27	2.93	25.76	2.89	10.47	1.78	1.46	12.85	5.17	0.47	0.00	30.09	95.60
STF16Amnz	0.34	0.73	1.08	29.64	3.27	11.13	1.74	1.23	16.11	1.84	0.52	0.00	30.16	97.79
STF16Amnz	0.40	1.30	2.05	26.73	3.01	10.55	1.59	1.37	13.79	5.25	0.59	0.00	30.42	97.06
STF16Amnz	1.02	1.31	2.35	25.61	2.74	9.71	1.44	1.27	13.40	4.95	0.74	0.00	31.33	95.85
STF16Amnz	0.45	1.37	1.44	26.95	2.91	10.15	1.52	1.22	14.50	4.61	0.70	0.00	29.08	94.88
STF16Amnz	0.39	1.31	1.61	27.63	3.09	10.53	1.62	1.25	14.82	4.98	0.50	0.00	29.55	97.27
STF16Amnz	0.47	1.20	1.96	26.68	2.95	10.31	1.64	1.22	13.73	5.70	0.62	0.00	29.83	96.31
STF16Amnz	0.30	1.04	0.96	28.48	3.25	11.19	1.70	1.08	14.86	1.72	0.40	0.00	29.62	94.61

STF16Amnz	0.78	1.22	1.43	27.44	3.02	10.11	1.54	1.13	14.45	5.13	1.04	0.00	30.04	97.34
STF33Pmnz	0.28	0.82	0.88	28.36	3.05	10.78	1.79	1.29	15.54	4.85	0.18	0.00	30.25	98.07
STF33Pmnz	0.33	0.63	0.87	30.26	3.29	10.97	1.65	1.22	16.66	1.32	0.29	0.00	29.82	97.31
STF33Pmnz	0.33	0.87	1.11	28.44	2.98	11.14	2.01	1.70	14.60	4.20	0.32	0.00	29.74	97.43
STF33Pmnz	0.32	0.78	1.05	28.19	3.09	11.07	2.01	1.35	14.82	4.51	0.24	0.00	29.67	97.10
STF33Pmnz	0.35	1.18	1.06	22.88	2.05	8.31	1.38	1.03	11.64	2.20	0.26	0.00	29.78	82.12
STF33Pmnz	0.37	1.13	1.29	28.00	3.14	10.95	1.83	1.32	14.87	4.59	0.39	0.00	30.22	98.10
STF33Pmnz	0.35	1.11	1.04	27.58	3.08	10.69	1.81	1.40	14.52	4.73	0.37	0.00	29.88	96.56
STF33Pmnz	0.31	0.92	1.00	27.96	3.01	10.66	1.95	1.24	14.90	4.77	0.24	0.00	29.75	96.72
STF33Pmnz	0.37	0.33	0.75	30.22	3.41	11.54	2.14	1.60	15.92	0.98	0.20	0.00	31.93	99.40
STF33Pmnz	0.32	0.38	0.35	13.22	1.23	4.74	0.80	0.54	7.25	1.76	0.27	0.00	29.73	60.60
STF33Pmnz	0.43	0.56	0.76	29.49	3.32	11.61	1.99	1.42	15.38	1.86	0.17	0.00	29.48	96.49
STF33Pmnz	0.51	0.51	0.82	29.66	3.23	11.63	2.24	1.66	15.32	1.17	0.18	0.00	28.45	95.37
STF33Pmnz	0.57	0.17	29.05	2.98	0.87	1.79	0.04	2.01	1.74	0.79	0.89	0.00	29.33	70.24
STF33Pmnz	6.92	1.78	1.31	25.72	2.84	9.66	1.41	0.99	14.28	1.47	0.16	0.00	21.96	88.51
STF33Pmnz	4.27	1.32	1.03	25.48	2.63	10.00	1.72	1.26	12.90	4.12	0.52	0.00	29.16	94.41
STF33Pmnz	0.46	1.06	1.22	27.06	2.99	10.67	1.73	1.17	14.20	5.32	0.60	0.00	30.62	97.12
STF33Pmnz	2.59	1.06	1.01	26.63	3.03	10.79	1.82	1.23	14.15	4.64	0.44	0.00	27.52	94.92
STF33Pmnz	0.58	1.16	1.16	27.43	3.01	10.69	1.73	1.26	14.37	5.34	0.59	0.00	30.33	97.67
STF33Pmnz	0.40	0.94	0.96	28.12	3.00	10.72	1.92	1.30	14.71	4.64	0.44	0.00	30.59	97.75
STF33Pmnz	0.90	1.67	0.87	27.01	2.92	11.10	2.07	1.61	13.78	5.54	0.21	0.00	27.62	95.30
STF33Pmnz	87.28	0.24	0.54	7.23	1.70	3.93	0.62	0.26	4.42	2.46	0.16	0.00	3.22	112.06
STF33Pmnz	84.74	0.40	0.84	10.81	2.49	5.87	0.87	0.52	6.58	3.93	0.21	0.00	6.68	123.93
STF33Pmnz	44.33	0.86	1.20	26.77	2.69	10.08	1.72	1.19	14.28	4.61	0.40	0.00	18.86	127.01
STF33Pmnz	97.69	0.05	0.00	0.08	0.05	0.05	0.02	0.00	0.05	0.06	0.02	0.00	0.11	98.17
STF04Amnz	0.42	0.50	1.41	30.42	3.19	11.49	1.93	1.43	15.34	2.11	0.15	0.00	32.60	100.99
STF04Amnz	0.48	0.47	1.53	30.17	3.15	11.55	1.85	1.35	15.09	2.45	0.14	0.00	31.83	100.06
STF04Amnz	0.46	0.48	1.37	31.37	3.41	11.50	1.86	1.31	15.87	2.38	0.15	0.00	31.05	101.21

STF04Amnz	0.48	0.67	1.39	30.68	3.28	11.73	1.87	1.23	15.29	1.97	0.19	0.00	31.08	99.87
STF04Amnz	0.51	0.91	2.00	26.51	2.95	10.73	1.80	1.30	13.05	5.51	0.46	0.00	29.58	95.30
STF04Amnz	0.71	0.71	2.26	28.28	3.12	10.99	1.77	1.45	14.12	3.59	0.35	0.00	30.61	97.96
STF04Amnz	0.37	0.50	1.28	30.04	3.27	11.14	1.69	1.17	15.06	3.24	0.12	0.00	30.43	98.32
STF04Amnz	0.38	0.52	1.38	29.52	3.16	11.04	1.75	1.21	15.16	3.40	0.19	0.00	29.73	97.45
STF04Amnz	0.40	0.59	1.28	30.75	3.18	11.62	1.74	1.17	15.75	2.78	0.14	0.00	31.52	100.93
STF04Amnz	0.45	0.62	1.27	30.68	3.20	11.21	1.89	1.16	15.32	2.53	0.15	0.00	29.39	97.88
STF04Amnz	0.85	0.70	1.16	27.71	3.16	10.93	1.69	1.17	13.87	3.59	0.14	0.00	29.35	94.32
STF04Amnz	0.71	0.85	1.37	28.84	3.05	10.81	1.70	1.14	14.35	4.21	0.23	0.00	29.43	96.69
STF04Amnz	1.24	0.24	0.65	30.91	3.02	10.90	1.42	0.89	16.83	2.83	0.04	0.00	27.48	96.45
STF04Amnz	0.50	0.48	1.34	28.48	3.17	10.69	1.76	1.18	14.35	1.94	0.18	0.00	31.20	95.26
STF04Amnz	0.51	0.59	1.33	28.88	3.21	11.23	1.71	1.24	14.44	2.60	0.21	0.00	29.69	95.64
STF04Amnz	0.63	0.56	1.43	29.39	3.05	11.15	1.74	1.30	14.57	3.28	0.34	0.00	28.34	95.78
STF04Amnz	0.60	0.81	1.25	29.56	3.22	10.84	1.69	1.21	15.14	3.89	0.18	0.00	30.97	99.38
STF04Amnz	0.70	0.80	1.24	29.71	3.07	10.54	1.62	1.15	15.22	4.16	0.15	0.00	31.77	100.12
STF04Amnz	0.64	0.77	1.26	29.74	3.16	10.91	1.70	1.28	15.00	4.42	0.16	0.00	30.85	99.88
STF04Amnz	0.45	0.70	1.53	29.15	3.17	10.90	1.82	1.33	14.55	3.59	0.26	0.00	32.15	99.59
STF04Amnz	1.70	1.19	1.28	24.66	2.79	9.68	1.52	1.11	11.96	11.76	0.25	0.00	26.75	94.65
STF04Amnz	0.43	0.54	1.20	30.34	3.23	11.33	1.75	1.20	15.30	2.45	0.13	0.00	29.48	97.38
STF04Amnz	0.56	0.69	1.28	28.32	3.18	11.04	1.76	1.23	14.10	3.75	0.21	0.00	28.11	94.24
STF04Amnz	0.53	0.55	1.15	28.98	3.14	10.78	1.72	1.16	14.45	4.04	0.15	0.00	27.75	94.41
STF04Amnz	0.51	0.65	1.28	27.12	3.20	11.02	1.71	1.15	13.46	3.61	0.26	0.00	28.05	92.02

SAMPLE	CaO	MgO	TiO2	SiO2	Al2O3	FeO	MnO	Cr2O3	Cl	F	K2O	P2O5	Na2O	ZnO	ZrO2	TOTAL
ST16-31J and1	0.05	0.04	0.02	36.52	61.92	0.13	0.00	0.00	0.02	0.01	0.00	0.00	0.05	0.00	0.02	98.77
ST16-31J and1	0.01	0.03	0.01	36.73	62.81	0.15	0.01	0.00	0.00	0.00	0.00	0.00	0.04	0.00	0.00	99.78
ST16-31J and1	0.02	0.03	0.01	36.25	62.51	0.19	0.00	0.00	0.00	0.00	0.00	0.00	0.09	0.00	0.00	99.11
ST16-31J and1	0.03	0.03	0.00	36.83	62.31	0.10	0.00	0.00	0.00	0.00	0.00	0.00	0.05	0.00	0.02	99.38
ST16-31J and1	0.03	0.02	0.02	36.67	62.42	0.15	0.00	0.00	0.00	0.00	0.00	0.00	0.03	0.00	0.00	99.37
ST16-31J bt1	0.16	6.93	1.73	35.23	19.59	19.94	0.14	0.00	0.03	0.51	8.30	0.00	0.33	0.00	0.01	92.76
ST16-31J bt1	0.12	6.99	1.72	34.12	18.98	20.65	0.16	0.00	0.07	0.43	8.23	0.00	0.61	0.04	0.00	91.97
ST16-31J bt1	0.09	7.10	1.76	34.02	19.13	21.43	0.18	0.00	0.07	0.32	8.63	0.00	0.49	0.03	0.00	93.19
ST16-31J bt1	0.17	7.24	1.62	34.16	18.90	21.20	0.16	0.02	0.04	0.41	8.26	0.00	0.46	0.08	0.00	92.65
ST16-31J bt1	0.15	6.93	2.17	34.01	18.10	17.96	0.17	0.03	0.11	0.40	8.07	0.04	0.21	0.00	0.00	88.24
ST16-31J mu1	0.06	0.39	0.28	47.03	37.08	0.82	0.01	0.00	0.12	0.12	8.33	0.00	1.40	0.00	0.01	95.76
ST16-31J mu1	0.06	0.40	0.35	46.62	37.17	0.82	0.01	0.00	0.12	0.12	7.69	0.00	1.26	0.00	0.01	94.78
ST16-31J mu1	0.06	0.42	0.31	49.06	38.75	0.76	0.00	0.00	0.05	0.17	5.10	0.00	0.56	0.00	0.00	95.34
ST16-31J mu1	0.05	0.39	0.23	47.31	37.51	0.66	0.00	0.00	0.03	0.45	7.45	0.00	1.21	0.00	0.00	95.29
ST16-31J mu1	0.04	0.33	0.24	46.00	36.08	0.68	0.00	0.00	0.05	0.17	6.70	0.00	1.00	0.00	0.00	91.34
ST16-31J bi2	0.14	7.09	1.56	34.94	19.46	20.93	0.14	0.02	0.01	0.44	8.65	0.00	0.21	0.02	0.00	93.52
ST16-31J bi2	0.04	7.86	1.52	36.21	20.34	21.75	0.15	0.00	0.01	0.20	8.64	0.00	0.25	0.05	0.00	97.03
ST16-31J bi2	0.08	7.00	1.56	34.97	19.27	20.35	0.13	0.02	0.01	0.31	8.14	0.00	0.23	0.01	0.00	92.06
ST16-31J bi2	0.04	7.28	1.56	34.11	18.60	20.68	0.20	0.00	0.01	0.35	8.81	0.00	0.27	0.00	0.00	91.84
ST16-31J bi2	0.07	6.77	1.55	35.45	20.33	19.19	0.16	0.02	0.03	0.25	8.27	0.00	0.23	0.06	0.06	92.37
ST16-31J mu2	0.12	0.39	0.31	47.02	37.50	0.73	0.00	0.00	0.01	0.38	7.65	0.00	1.10	0.00	0.00	95.21
ST16-31J mu2	0.03	0.50	0.30	51.39	40.11	0.72	0.00	0.00	0.00	0.02	8.02	0.01	1.44	0.00	0.00	102.69
ST16-31J mu2	0.01	0.41	0.28	46.85	37.15	0.80	0.00	0.00	0.00	0.02	7.74	0.00	1.19	0.00	0.00	94.60
ST16-31J mu2	0.06	0.57	0.29	47.70	37.49	0.94	0.00	0.00	0.00	0.31	8.02	0.00	1.10	0.00	0.02	96.51
ST16-31J mu2	0.05	0.44	0.30	47.90	37.73	0.82	0.00	0.00	0.00	0.18	8.63	0.00	1.32	0.00	0.00	97.48
STF-33P ksp	0.08	0.37	0.07	46.27	37.74	1.21	0.00	0.00	0.00	0.00	9.19	0.00	0.50	0.00	0.01	95.56

STF-33P ksp	0.04	0.80	0.13	47.70	37.01	1.11	0.00	0.00	0.00	0.05	8.62	0.00	0.36	0.00	0.00	95.84
STF-33P ksp	0.02	0.92	0.22	75.27	15.26	1.74	0.00	0.01	0.00	0.00	5.28	0.00	0.17	0.00	0.03	98.93
STF-33P ksp	0.01	0.00	0.00	100.07	0.09	0.00	0.02	0.00	0.00	0.00	0.00	0.00	0.00	0.00	0.00	100.20
STF-33P ksp	0.03	1.64	0.17	47.99	34.62	2.59	0.00	0.00	0.00	0.06	8.58	0.00	0.34	0.00	0.01	96.02
STF-33P ox	0.15	0.57	0.00	3.83	4.01	65.42	0.12	0.02	0.01	0.00	0.05	1.09	0.11	0.00	0.05	75.44
STF-33P ox	0.15	0.57	0.00	4.24	4.03	63.45	0.13	0.00	0.02	0.02	0.05	1.19	0.23	0.00	0.05	74.13
STF-33P ox	0.10	0.58	0.01	3.85	4.10	63.69	0.07	0.00	0.01	0.00	0.04	1.26	0.16	0.00	0.04	73.92
STF-33P ox	0.14	0.64	0.00	4.09	4.49	64.81	0.11	0.00	0.02	0.00	0.05	1.13	0.24	0.00	0.08	75.80
STF-33P ox	0.17	0.62	0.01	3.94	4.23	64.82	0.11	0.01	0.00	0.00	0.03	1.15	0.15	0.01	0.11	75.36
STF-33P mu2	0.03	0.47	0.30	47.95	37.92	0.65	0.00	0.00	0.00	0.13	7.99	0.00	0.90	0.00	0.00	96.41
STF-33P mu2	0.05	0.44	0.30	46.59	37.15	0.87	0.00	0.01	0.01	0.36	8.41	0.00	0.93	0.00	0.00	95.04
STF-33P mu2	0.02	0.44	0.31	46.99	37.47	0.66	0.00	0.00	0.01	0.27	8.77	0.00	1.01	0.00	0.00	95.93
STF-33P mu2	0.01	1.03	0.42	45.86	35.35	2.51	0.00	0.01	0.01	0.08	7.96	0.00	1.07	0.00	0.01	94.47
STF-33P mu2	0.02	0.45	0.28	46.98	36.77	0.77	0.00	0.00	0.01	0.10	8.36	0.05	1.19	0.00	0.02	95.13
STF-33P bi1	0.11	7.97	1.47	34.31	18.63	22.23	0.10	0.01	0.04	0.51	7.84	0.02	0.29	0.00	0.00	93.37
STF-33P bi1	0.13	7.61	1.25	33.56	18.70	21.49	0.14	0.00	0.05	0.40	6.90	0.04	0.25	0.00	0.00	90.33
STF-33P bi1	0.07	8.00	1.13	31.70	18.50	23.07	0.17	0.01	0.05	0.45	6.33	0.03	0.23	0.07	0.00	89.68
STF-33P bi1	0.10	7.99	1.41	33.57	18.69	22.43	0.11	0.02	0.05	0.51	7.86	0.01	0.28	0.00	0.00	92.85
STF-33P bi1	0.08	8.10	1.26	32.80	18.58	22.48	0.15	0.02	0.04	0.43	7.20	0.00	0.23	0.06	0.01	91.29
STF-33P bi2	0.11	7.90	1.21	33.49	18.41	21.99	0.12	0.01	0.06	0.40	6.96	0.04	0.15	0.04	0.00	90.73
STF-33P bi2	0.12	7.22	1.10	34.15	18.05	20.66	0.10	0.00	0.13	0.28	6.60	0.11	0.15	0.06	0.00	88.64
STF-33P bi2	0.05	7.66	1.54	34.37	18.48	21.59	0.11	0.00	0.05	0.32	8.60	0.00	0.20	0.00	0.01	92.95
STF-33P bi2	0.07	8.39	1.34	34.59	19.11	21.60	0.14	0.00	0.04	0.34	7.57	0.02	0.10	0.05	0.00	93.27
STF-33P bi2	0.12	8.21	1.35	35.05	19.20	21.34	0.16	0.01	0.04	0.35	7.78	0.00	0.13	0.02	0.02	93.69
STF-33 ox	0.35	0.14	55.27	1.09	0.47	26.08	4.01	0.00	0.04	0.76	0.07	0.03	0.27	0.06	0.04	89.53
STF-33 ox	0.20	0.09	56.35	1.07	0.37	28.01	2.36	0.00	0.02	0.08	0.06	0.09	0.29	0.04	0.00	90.19
STF-33 ox	0.25	0.10	60.91	1.34	0.94	22.55	1.61	0.00	0.04	0.36	0.13	0.12	0.33	0.09	0.10	90.05
STF-33 ox	0.16	0.15	56.32	0.88	0.42	28.45	2.73	0.00	0.03	0.47	0.07	0.06	0.28	0.08	0.00	91.09

STF-33 mu	0.06	0.79	0.92	45.79	35.09	1.54	0.00	0.00	0.09	0.34	8.73	0.00	1.14	0.00	0.00	94.42
STF-33 mu	0.07	0.58	0.80	46.17	35.83	0.76	0.00	0.00	0.07	0.36	7.90	0.00	1.37	0.00	0.00	93.77
STF-33 mu	0.07	0.63	0.79	46.26	35.47	1.01	0.00	0.00	0.07	0.35	8.11	0.00	1.41	0.00	0.00	94.10
STF-33 mu	0.07	0.64	0.82	47.48	36.81	1.06	0.00	0.00	0.02	0.04	8.00	0.00	0.94	0.00	0.00	95.97
STF-33 mu	0.07	0.95	0.50	47.97	36.66	1.65	0.00	0.00	0.00	0.00	8.82	0.00	0.62	0.00	0.00	97.40
STF-33 kspcore	0.21	1.75	0.40	34.64	30.92	12.98	0.04	0.00	0.03	0.39	0.04	0.00	1.93	0.00	0.04	83.20
STF-33 kspcore	0.16	1.52	0.41	34.79	31.95	14.60	0.08	0.00	0.00	0.07	0.02	0.00	1.98	0.00	0.00	85.56
STF-33 kspcore	0.16	1.14	0.46	34.47	29.56	14.84	0.10	0.00	0.03	0.46	0.07	0.00	2.43	0.00	0.01	83.53
STF-33 kspcore	0.17	1.20	0.47	34.43	30.58	15.34	0.12	0.00	0.01	0.16	0.04	0.00	2.35	0.00	0.00	84.80
STF-33 kspcore	0.21	2.62	0.63	35.12	31.75	12.74	0.05	0.00	0.02	0.31	0.03	0.00	2.03	0.00	0.00	85.38
STF-33 ksprim	0.46	5.60	0.65	36.00	33.20	6.78	0.01	0.02	0.00	0.18	0.00	0.00	1.87	0.00	0.04	84.74
STF-33 ksprim	0.19	1.05	0.52	33.59	30.06	15.99	0.13	0.00	0.00	0.49	0.04	0.00	2.25	0.00	0.00	84.10
STF-33 ksprim	0.19	1.63	0.45	34.27	30.72	13.96	0.13	0.00	0.01	0.36	0.03	0.00	2.11	0.00	0.01	83.71
STF-33 ksprim	0.46	5.78	0.83	36.16	32.69	7.08	0.02	0.00	0.00	0.12	0.00	0.00	2.00	0.00	0.00	85.11
STF-33 ksprim	0.43	5.98	0.81	35.70	32.35	7.20	0.00	0.00	0.00	0.13	0.00	0.00	1.95	0.00	0.00	84.53
STF-33 bi	0.04	7.37	1.66	33.16	16.88	21.61	0.16	0.01	0.04	0.39	9.33	0.00	0.09	0.02	0.00	90.66
STF-33 bi	0.03	8.40	1.63	35.59	18.64	21.57	0.16	0.02	0.03	0.28	9.04	0.01	0.14	0.03	0.03	95.55
STF-33 bi	0.04	8.22	1.55	34.46	18.03	21.19	0.17	0.01	0.02	0.29	8.82	0.00	0.15	0.01	0.06	93.00
STF-33 bi	0.01	7.74	1.63	33.75	18.01	21.06	0.23	0.00	0.00	0.27	8.96	0.00	0.12	0.03	0.00	91.80
STF-33 bi	0.00	8.02	1.66	34.12	18.07	21.66	0.20	0.00	0.02	0.36	8.82	0.00	0.08	0.02	0.00	92.98
ST16-31A mu	0.12	0.68	0.78	46.85	35.53	1.32	0.00	0.01	0.06	0.29	8.56	0.00	0.58	0.00	0.00	94.69
ST16-31A mu	0.12	0.90	0.88	47.34	34.20	1.33	0.00	0.00	0.06	1.11	8.73	0.00	0.66	0.00	0.02	94.92
ST16-31A mu	0.04	0.00	0.04	100.92	0.22	0.11	0.02	0.00	0.00	0.12	0.03	0.00	0.00	0.00	0.00	101.44
ST16-31A mu	0.16	0.95	0.69	46.84	35.13	1.94	0.03	0.00	0.01	0.21	8.55	0.00	0.32	0.00	0.03	94.91
ST16-31A mu	0.09	0.86	0.71	48.65	35.88	1.16	0.00	0.00	0.00	0.07	8.17	0.00	0.27	0.00	0.02	95.99
ST16-31A bi	0.08	7.14	3.07	35.98	18.07	21.46	0.34	0.01	0.01	0.33	9.26	0.00	0.07	0.03	0.00	95.86
ST16-31A bi	0.08	6.93	2.90	35.32	18.04	21.41	0.30	0.00	0.01	0.31	9.43	0.00	0.09	0.01	0.00	94.81
ST16-31A bi	0.08	7.11	2.87	36.05	17.98	21.76	0.36	0.02	0.01	0.33	9.26	0.00	0.08	0.00	0.00	95.89

ST16-31A bi	0.01	7.21	2.81	35.91	18.16	22.42	0.30	0.03	0.02	0.26	9.44	0.00	0.08	0.09	0.01	96.79
ST16-31A bi	0.02	7.03	2.81	35.63	18.17	21.99	0.37	0.04	0.01	0.28	9.47	0.00	0.06	0.00	0.00	95.87
ST16-31A fsp	0.06	0.00	0.02	64.89	19.64	0.00	0.00	0.00	0.00	0.01	15.30	0.04	0.74	0.00	0.00	101.27
ST16-31A fsp	0.07	0.01	0.07	64.88	19.72	0.00	0.00	0.00	0.00	0.00	15.43	0.08	0.77	0.00	0.00	101.61
ST16-31A fsp	0.03	0.01	0.01	64.43	19.66	0.00	0.01	0.00	0.00	0.00	15.23	0.02	0.80	0.00	0.00	100.81
ST16-31A fsp	0.07	0.00	0.03	64.77	19.46	0.00	0.00	0.00	0.00	0.00	14.86	0.00	0.94	0.00	0.00	100.59
ST16-31A fsp	0.06	0.00	0.04	64.97	19.84	0.00	0.00	0.00	0.00	0.00	15.21	0.00	0.94	0.00	0.00	101.68
ST16-19A ox	0.02	0.10	52.03	0.05	0.02	45.39	0.50	0.02	0.00	0.00	0.02	0.01	0.00	0.02	0.00	99.36
ST16-19A ox	0.02	0.09	51.76	0.06	0.00	45.82	0.45	0.02	0.01	0.00	0.03	0.01	0.00	0.04	0.00	99.54
ST16-19A ox	0.04	0.10	51.70	0.08	0.03	45.51	0.42	0.06	0.01	0.00	0.01	0.01	0.00	0.05	0.00	99.18
ST16-19A ox	0.03	0.10	51.98	0.07	0.04	45.90	0.44	0.03	0.01	0.00	0.02	0.00	0.00	0.00	0.00	99.82
ST16-19A ox	0.03	0.09	51.91	0.04	0.00	44.46	0.45	0.02	0.01	0.07	0.01	0.00	0.00	0.00	0.02	98.32
ST16-19A ksp	0.02	0.00	0.04	64.61	19.41	0.00	0.01	0.00	0.00	0.00	14.97	0.18	1.23	0.00	0.02	100.80
ST16-19A ksp	0.04	0.00	0.02	64.70	19.55	0.00	0.00	0.00	0.00	0.00	14.36	0.08	1.60	0.00	0.00	100.67
ST16-19A ksp	0.15	0.00	0.02	65.95	19.89	0.07	0.00	0.00	0.00	0.00	10.71	0.12	4.71	0.00	0.00	101.74
ST16-19A ksp	0.05	0.02	0.02	64.67	19.81	0.00	0.00	0.00	0.00	0.00	15.31	0.11	0.95	0.00	0.01	101.34
ST16-19A ksp	0.03	0.00	0.02	64.51	19.58	0.02	0.02	0.00	0.00	0.00	14.93	0.08	1.22	0.00	0.00	100.94
ST16-19A bt	0.02	7.75	2.20	34.69	19.41	22.76	0.06	0.03	0.00	0.57	9.31	0.01	0.06	0.00	0.01	96.85
ST16-19A bt	0.02	7.64	2.20	34.78	18.67	22.69	0.07	0.09	0.00	0.58	9.35	0.00	0.07	0.00	0.01	96.18
ST16-19A bt	0.01	7.79	2.12	35.03	19.10	22.41	0.05	0.04	0.00	0.54	9.27	0.00	0.05	0.00	0.00	96.42
ST16-19A bt	0.02	7.80	1.63	34.21	19.51	22.60	0.04	0.00	0.00	0.66	9.41	0.00	0.07	0.00	0.00	95.81
ST16-19A bt	0.07	7.00	3.46	34.34	18.67	23.49	0.06	0.05	0.01	0.44	9.31	0.00	0.11	0.03	0.00	97.12
ST16-19A cd	0.01	6.27	0.00	48.75	32.18	11.82	0.22	0.00	0.00	0.00	0.00	0.00	0.05	0.00	0.00	99.30
ST16-19A cd	0.06	5.23	0.00	56.67	26.24	9.81	0.17	0.00	0.00	0.00	0.02	0.00	0.05	0.00	0.00	98.25
ST16-19A cd	0.01	6.38	0.01	48.86	32.22	12.09	0.19	0.00	0.00	0.00	0.00	0.00	0.06	0.00	0.00	99.82
ST16-19A cd	0.01	5.98	0.00	48.76	32.24	12.40	0.21	0.00	0.00	0.00	0.00	0.00	0.10	0.00	0.00	99.71
ST16-19A cd	0.02	6.08	0.04	49.12	32.13	12.07	0.19	0.00	0.00	0.00	0.00	0.00	0.09	0.00	0.00	99.74
ST16-19A unkplag	6.25	0.01	0.00	60.46	26.42	0.00	0.00	0.00	0.00	0.00	0.08	0.08	8.48	0.00	0.00	101.78

ST16-19A unkplag	6.92	0.19	0.02	59.34	26.96	0.75	0.02	0.00	0.00	0.00	0.06	0.07	7.71	0.00	0.00	102.04
ST16-19A unkplag	6.99	0.00	0.00	58.91	26.99	0.00	0.00	0.00	0.00	0.00	0.06	0.04	7.85	0.00	0.00	100.84
ST16-19A unkplag	6.89	0.25	0.00	58.74	27.08	0.77	0.01	0.00	0.00	0.00	0.07	0.03	7.51	0.00	0.01	101.37
ST16-19A unkplag	3.92	0.00	0.01	63.63	24.05	0.00	0.01	0.00	0.00	0.00	0.11	0.13	9.84	0.00	0.00	101.72
ST16-09 bt	0.08	6.49	2.82	35.62	20.94	23.59	0.03	0.00	0.02	0.10	9.05	0.00	0.16	0.00	0.00	98.96
ST16-09 bt	0.12	5.78	2.70	33.18	19.17	23.70	0.05	0.00	0.03	0.12	9.02	0.00	0.19	0.00	0.00	94.13
ST16-09 bt	0.05	6.08	2.63	34.05	19.55	23.75	0.01	0.01	0.02	0.14	9.28	0.00	0.16	0.03	0.05	95.85
ST16-09 bt	0.02	6.00	2.97	33.72	19.57	24.66	0.03	0.01	0.01	0.08	9.41	0.01	0.07	0.05	0.00	96.70
ST16-09 bt	0.06	6.10	2.75	33.68	19.10	24.17	0.03	0.03	0.02	0.09	9.05	0.01	0.17	0.01	0.00	95.32
ST16-09 ksp	0.02	0.00	0.00	64.75	19.51	0.02	0.00	0.00	0.00	0.00	15.33	0.10	1.06	0.00	0.02	101.08
ST16-09 ksp	0.01	0.00	0.04	64.42	19.71	0.06	0.00	0.00	0.00	0.01	15.16	0.37	1.08	0.00	0.00	101.15
ST16-09 ksp	0.04	0.07	0.06	63.63	19.81	0.28	0.00	0.00	0.00	0.03	15.00	0.52	1.16	0.00	0.00	100.90
ST16-09 ksp	0.01	0.01	0.00	64.22	19.45	0.00	0.00	0.00	0.00	0.00	15.28	0.32	1.13	0.00	0.00	100.62
ST16-09 ksp	0.03	0.00	0.03	64.99	19.53	0.01	0.01	0.00	0.00	0.00	14.68	0.14	1.47	0.00	0.00	101.20
ST16-09 ox	0.03	0.20	51.81	0.05	0.02	46.07	0.55	0.06	0.02	0.00	0.00	0.01	0.00	0.01	0.01	100.45
ST16-09 ox	0.03	0.21	50.94	0.06	0.04	46.00	0.55	0.03	0.01	0.00	0.02	0.00	0.00	0.08	0.01	99.59
ST16-09 ox	0.02	0.19	50.90	0.04	0.05	45.83	0.58	0.07	0.00	0.00	0.02	0.00	0.01	0.06	0.00	99.24
ST16-09 ox	0.06	0.19	50.44	0.13	0.07	46.12	0.55	0.01	0.00	0.00	0.04	0.00	0.00	0.01	0.00	99.14
ST16-09 ox	0.02	0.18	50.78	0.05	0.04	46.26	0.57	0.07	0.00	0.00	0.02	0.00	0.00	0.03	0.02	99.57
ST16-09 cdactuallyplag?	8.66	0.17	0.02	56.01	28.63	0.43	0.01	0.00	0.00	0.00	0.07	0.17	6.52	0.00	0.04	100.73
ST16-09 cdactuallyplag?	9.08	0.01	0.00	56.33	28.71	0.00	0.00	0.00	0.00	0.00	0.05	0.15	6.57	0.00	0.03	100.92
ST16-09 cdactuallyplag?	5.45	0.11	0.00	60.76	25.73	0.24	0.03	0.00	0.00	0.00	0.13	0.13	8.72	0.00	0.00	101.30
ST16-09 cdactuallyplag?	8.74	0.01	0.02	56.54	28.26	0.00	0.02	0.00	0.00	0.00	0.08	0.15	6.82	0.00	0.00	100.64
ST16-09 cdactuallyplag?	8.81	0.01	0.00	56.45	28.40	0.02	0.02	0.00	0.00	0.00	0.07	0.13	6.67	0.00	0.00	100.58
ST16-09 unknown1	0.15	0.02	0.02	36.01	65.33	0.44	0.00	0.00	0.01	0.15	0.00	0.00	0.01	0.00	0.00	102.10
ST16-09 unknown1	0.01	0.01	0.07	36.22	66.26	0.37	0.00	0.00	0.00	0.00	0.00	0.00	0.01	0.00	0.00	102.95
ST16-09 unknown1	0.00	0.02	0.03	38.08	64.56	0.51	0.00	0.00	0.00	0.00	0.00	0.00	0.02	0.00	0.00	103.23
ST16-09 unknown1	0.01	0.01	0.02	37.60	65.01	0.52	0.00	0.00	0.00	0.00	0.00	0.00	0.00	0.00	0.00	103.16

ST16-09 unknown1	0.01	0.01	0.00	47.85	55.37	0.47	0.00	0.00	0.00	0.00	0.00	0.00	0.00	0.00	0.00	103.72
ST16-09 actualcordierite	0.16	5.58	0.00	46.83	32.74	11.34	0.22	0.00	0.02	0.09	0.00	0.00	0.34	0.00	0.00	97.29
ST16-09 actualcordierite	0.08	5.76	0.00	47.52	33.92	11.50	0.25	0.00	0.00	0.00	0.00	0.00	0.24	0.00	0.00	99.28
ST16-09 actualcordierite	0.02	5.99	0.00	47.30	33.47	11.55	0.27	0.00	0.00	0.00	0.00	0.00	0.15	0.00	0.01	98.75
ST16-09 actualcordierite	0.02	5.80	0.01	47.25	33.24	12.24	0.24	0.00	0.00	0.00	0.00	0.00	0.20	0.00	0.10	99.11
ST16-09 actualcordierite	0.03	5.91	0.01	47.64	33.59	11.96	0.24	0.00	0.00	0.00	0.00	0.00	0.16	0.00	0.00	99.54
STF-10B oxide	0.03	0.15	49.87	0.25	0.19	43.71	0.55	0.04	0.01	0.00	0.04	0.00	0.01	0.01	0.00	95.91
STF-10B oxide	0.22	0.12	48.01	1.98	1.67	42.32	0.58	0.04	0.02	0.00	0.05	0.00	0.25	0.05	0.00	96.34
STF-10B oxide	0.04	0.06	52.07	0.11	0.01	44.81	0.58	0.04	0.01	0.00	0.04	0.00	0.00	0.08	0.00	98.95
STF-10B oxide	0.10	0.12	50.24	0.19	0.44	44.60	0.57	0.06	0.02	0.18	0.04	0.00	0.08	0.00	0.00	97.61
STF-10B oxide	0.04	0.08	51.47	0.11	0.22	44.56	0.57	0.02	0.01	0.00	0.04	0.00	0.06	0.00	0.00	98.29
STF-10B bt	0.02	6.00	3.09	33.07	17.64	22.23	0.07	0.05	0.04	0.53	9.18	0.01	0.13	0.04	0.01	92.07
STF-10B bt	0.07	5.78	3.11	31.25	19.61	22.63	0.06	0.02	0.02	0.44	9.15	0.00	0.22	0.00	0.00	92.28
STF-10B bt	0.10	5.25	2.96	37.17	17.42	21.33	0.03	0.00	0.04	0.51	8.21	0.00	0.20	0.00	0.00	93.06
STF-10B bt	0.07	6.53	2.82	32.43	21.41	21.88	0.05	0.03	0.02	0.50	8.86	0.00	0.19	0.00	0.00	94.68
STF-10B bt	0.10	6.02	2.86	43.39	17.99	19.82	0.03	0.01	0.01	0.35	7.63	0.00	0.13	0.00	0.01	98.31
STF-10B ksp	0.10	0.02	0.01	65.04	19.65	0.01	0.00	0.00	0.01	0.00	10.34	0.08	4.39	0.00	0.00	99.85
STF-10B ksp	0.09	0.00	0.01	64.02	19.24	0.00	0.00	0.00	0.00	0.00	15.35	0.04	0.80	0.00	0.00	99.77
STF-10B ksp	0.04	0.01	0.02	64.20	19.22	0.00	0.00	0.00	0.00	0.00	15.29	0.04	0.99	0.00	0.00	100.00
STF-10B ksp	0.03	0.00	0.01	64.13	19.23	0.00	0.01	0.00	0.00	0.00	15.27	0.03	0.94	0.00	0.00	99.86
STF-10B ksp	0.06	0.01	0.01	64.51	19.09	0.00	0.00	0.00	0.01	0.00	14.72	0.10	1.41	0.00	0.01	100.09
STF-10B plag	8.25	0.01	0.04	56.72	27.40	0.00	0.01	0.00	0.00	0.02	0.06	0.05	6.95	0.00	0.01	99.51
STF-10B plag	8.26	0.01	0.00	57.10	27.56	0.18	0.03	0.00	0.00	0.00	0.07	0.00	6.94	0.00	0.00	100.15
STF-10B plag	8.53	0.00	0.00	56.83	28.46	0.04	0.00	0.00	0.00	0.00	0.04	0.03	6.64	0.00	0.01	100.59
STF-10B plag	8.15	0.01	0.00	56.96	27.80	0.06	0.01	0.00	0.00	0.00	0.07	0.06	6.95	0.00	0.01	100.11
STF-10B plag	8.19	0.00	0.00	56.28	27.23	0.00	0.00	0.00	0.00	0.00	0.06	0.00	6.75	0.00	0.00	98.53
STF-10B cd	0.03	5.52	0.00	46.64	33.20	11.93	0.20	0.00	0.00	0.00	0.00	0.00	0.07	0.00	0.02	97.60
STF-10B cd	0.02	6.00	0.00	47.24	33.52	12.06	0.21	0.00	0.00	0.00	0.00	0.01	0.07	0.00	0.00	99.14

STF-10B cd	0.01	5.77	0.01	46.84	33.21	12.01	0.26	0.00	0.00	0.00	0.00	0.00	0.06	0.00	0.00	98.17
STF-10B cd	0.07	5.68	0.02	47.13	33.31	11.99	0.19	0.00	0.00	0.00	0.01	0.00	0.09	0.00	0.00	98.49
STF-10B cd	0.03	6.05	0.00	47.21	33.19	11.40	0.26	0.00	0.00	0.00	0.00	0.00	0.07	0.00	0.00	98.21
STF-04A musc	0.06	0.81	0.83	46.04	36.07	1.57	0.00	0.00	0.00	0.06	9.29	0.00	0.30	0.00	0.00	95.09
STF-04A musc	0.04	0.86	0.84	46.42	36.22	1.62	0.01	0.00	0.00	0.03	9.07	0.00	0.30	0.00	0.00	95.44
STF-04A musc	0.04	1.07	0.77	46.98	35.49	1.66	0.02	0.00	0.00	0.16	9.88	0.00	0.34	0.00	0.00	96.39
STF-04A musc	0.05	1.33	0.79	50.23	36.72	1.77	0.01	0.00	0.00	0.31	9.58	0.00	0.34	0.00	0.00	101.11
STF-04A musc	0.05	0.80	0.89	45.63	35.14	1.51	0.12	0.00	0.03	0.60	9.79	0.00	0.50	0.00	0.00	94.88
STF-04A bt	0.06	6.86	2.56	34.95	18.50	22.90	0.34	0.03	0.02	0.32	9.23	0.00	0.13	0.00	0.00	95.90
STF-04A bt	0.36	5.35	1.92	45.14	16.46	15.02	0.24	0.02	0.06	0.77	6.92	0.03	0.35	0.00	0.00	92.36
STF-04A bt	0.06	7.06	2.63	35.53	18.60	22.53	0.40	0.00	0.01	0.34	9.27	0.00	0.21	0.03	0.03	96.61
STF-04A bt	0.16	5.46	2.02	35.83	20.64	18.28	0.28	0.00	0.08	0.66	7.28	0.00	0.19	0.04	0.03	90.72
STF-04A bt	0.06	6.89	2.69	35.85	19.05	22.30	0.36	0.01	0.03	0.26	8.98	0.00	0.16	0.06	0.00	96.71
STF-04A ox	0.10	0.03	61.15	1.07	0.25	26.06	3.56	0.00	0.03	0.00	0.04	0.02	0.15	0.12	0.03	93.85
STF-04A ox	0.13	0.06	57.67	1.34	0.72	28.08	3.78	0.02	0.05	0.02	0.05	0.04	0.23	0.09	0.04	93.52
STF-04A ox	0.06	0.04	55.84	0.09	0.06	35.00	5.86	0.02	0.00	0.00	0.01	0.01	0.03	0.16	0.00	98.33
STF-04A ox	0.07	0.06	54.93	0.15	0.07	35.24	7.29	0.01	0.00	0.02	0.02	0.00	0.04	0.17	0.00	99.24
STF-04A ox	0.06	0.03	54.76	0.08	0.01	33.73	6.28	0.05	0.01	0.00	0.03	0.00	0.00	0.13	0.00	96.39
STF-04A ksp	0.01	0.00	0.01	65.01	19.39	0.00	0.00	0.00	0.00	0.00	15.41	0.00	0.75	0.00	0.00	101.03
STF-04A ksp	0.01	0.00	0.00	64.99	19.67	0.00	0.00	0.00	0.00	0.00	15.48	0.00	0.79	0.00	0.00	101.37
STF-04A ksp	0.17	0.00	0.02	64.18	19.32	0.00	0.00	0.00	0.00	0.00	15.53	0.00	0.62	0.00	0.00	100.36
STF-04A ksp	0.03	0.00	0.01	64.68	19.60	0.06	0.00	0.00	0.00	0.00	15.47	0.00	0.80	0.00	0.00	101.25
STF-04A ksp	0.01	0.00	0.03	64.69	19.67	0.00	0.01	0.00	0.00	0.00	15.79	0.00	0.64	0.00	0.00	101.39
STF-26A area3 cd	0.02	6.31	0.00	47.31	33.53	11.50	0.23	0.00	0.00	0.00	0.00	0.00	0.11	0.00	0.00	99.02
STF-26A area3 cd	0.01	6.33	0.00	47.59	33.76	11.49	0.19	0.00	0.00	0.00	0.00	0.00	0.11	0.00	0.00	99.46
STF-26A area3 cd	0.02	6.08	0.02	47.52	34.23	12.13	0.20	0.00	0.00	0.00	0.00	0.00	0.08	0.00	0.00	100.28
STF-26A area3 cd	0.01	6.47	0.02	47.99	33.90	11.17	0.16	0.00	0.00	0.00	0.00	0.00	0.09	0.00	0.00	99.81
STF-26A area3 cd	0.04	6.34	0.00	47.57	34.09	11.22	0.16	0.00	0.00	0.02	0.00	0.00	0.07	0.00	0.02	99.55

STF-26A area3 ksp	0.02	0.00	0.06	64.73	19.28	0.00	0.00	0.00	0.01	0.00	15.46	0.08	1.00	0.00	0.00	100.88
STF-26A area3 ksp	0.03	0.00	0.01	63.89	19.26	0.00	0.00	0.00	0.00	0.01	15.54	0.08	0.83	0.00	0.00	99.93
STF-26A area3 ksp	0.10	0.02	0.00	66.65	20.00	0.12	0.00	0.00	0.00	0.00	6.80	0.04	7.38	0.00	0.02	101.27
STF-26A area3 ksp	0.21	0.00	0.03	64.88	19.36	0.00	0.01	0.00	0.00	0.00	12.64	0.06	2.90	0.00	0.00	100.34
STF-26A area3 ksp	0.01	0.00	0.00	64.96	19.25	0.00	0.00	0.00	0.00	0.00	15.34	0.05	0.98	0.00	0.00	100.87
STF-26A area3 gt	0.24	3.93	0.00	32.54	26.72	36.00	0.49	0.00	0.00	0.00	0.00	0.01	0.02	0.97	0.05	100.98
STF-26A area3 gt	0.23	3.73	0.02	32.66	26.33	35.45	0.50	0.00	0.01	0.00	0.00	0.00	0.00	0.97	0.02	99.94
STF-26A area3 gt	0.38	2.70	0.04	37.90	21.18	37.94	0.65	0.01	0.00	0.00	0.00	0.03	0.03	0.03	0.02	100.95
STF-26A area3 gt	0.33	2.87	0.00	37.79	20.83	38.62	0.68	0.01	0.01	0.00	0.00	0.02	0.01	0.00	0.00	101.17
STF-26A area3 gt	0.36	2.87	0.00	37.48	21.10	38.01	0.76	0.02	0.00	0.00	0.00	0.00	0.00	0.06	0.02	100.67
STF-26A area3 ox	0.11	0.21	52.75	0.05	0.02	45.07	0.09	0.06	0.01	0.00	0.02	0.01	0.00	0.05	0.00	99.62
STF-26A area3 ox	0.05	0.12	51.33	0.12	0.05	45.03	0.63	0.01	0.00	0.00	0.02	0.01	0.00	0.08	0.00	98.57
STF-26A area3 ox	0.02	0.27	52.44	0.02	0.03	45.36	0.18	0.06	0.00	0.00	0.01	0.00	0.00	0.04	0.00	99.60
STF-26A area3 ox	0.02	0.29	52.91	0.08	0.01	45.88	0.09	0.04	0.00	0.00	0.01	0.01	0.02	0.07	0.00	100.56
STF-26A area3 ox	0.02	0.32	52.65	0.00	0.02	45.89	0.10	0.06	0.01	0.00	0.01	0.00	0.02	0.01	0.01	100.19
STF-26A area3 bi	0.05	11.66	4.19	35.54	16.69	17.67	0.01	0.15	0.01	1.16	9.34	0.02	0.16	0.00	0.00	96.61
STF-26A area3 bi	0.03	11.65	4.01	36.21	16.79	18.25	0.02	0.09	0.00	1.19	9.33	0.00	0.11	0.04	0.00	97.69
STF-26A area3 bi	0.02	11.83	3.99	35.88	16.42	16.98	0.03	0.11	0.00	1.23	9.36	0.00	0.13	0.03	0.00	95.94
STF-26A area3 bi	0.07	11.20	4.12	35.22	16.79	17.15	0.01	0.10	0.00	1.14	9.47	0.00	0.10	0.01	0.00	95.30
STF-26A area3 bi	0.05	11.64	3.96	35.76	17.08	17.67	0.02	0.09	0.01	1.13	9.46	0.00	0.11	0.00	0.01	96.93
STF-26A area1 ox	0.01	0.06	51.50	0.09	0.07	44.93	0.80	0.03	0.01	0.00	0.01	0.00	0.00	0.05	0.00	98.68
STF-26A area1 ox	0.00	0.05	51.63	0.10	0.03	45.39	0.80	0.02	0.00	0.00	0.01	0.01	0.00	0.01	0.00	99.20
STF-26A area1 ox	0.11	0.25	65.29	1.85	1.27	23.17	0.32	0.02	0.01	0.00	0.02	0.00	0.03	0.00	0.00	93.76
STF-26A area1 ox	0.01	0.06	71.00	0.08	0.02	21.19	0.06	0.01	0.00	0.00	0.00	0.01	0.06	0.00	0.01	94.07
STF-26A area1 ox	0.01	0.05	52.13	0.08	0.01	45.13	0.90	0.03	0.01	0.03	0.01	0.00	0.06	0.03	0.00	99.55
STF-26A area1 bi	0.01	6.08	3.74	34.40	18.35	23.78	0.08	0.01	0.01	0.60	9.54	0.01	0.07	0.00	0.00	96.78
STF-26A area1 bi	0.02	5.98	3.65	33.77	18.35	23.65	0.09	0.05	0.01	0.55	9.11	0.01	0.09	0.03	0.03	95.46
STF-26A area1 bi	0.01	5.96	3.50	34.12	18.73	23.44	0.08	0.03	0.01	0.57	9.40	0.01	0.10	0.06	0.00	96.11

STF-26A area1 bi	0.02	6.12	3.49	34.78	18.88	23.57	0.08	0.03	0.01	0.60	9.38	0.00	0.08	0.01	0.00	97.14
STF-26A area1 bi	0.00	6.05	4.30	34.69	18.36	23.86	0.07	0.00	0.00	0.55	9.47	0.00	0.06	0.00	0.00	97.54
STF-26A area1 ksp	0.05	0.01	0.03	65.68	18.34	0.00	0.00	0.00	0.00	0.00	15.22	0.10	1.12	0.00	0.00	100.86
STF-26A area1 ksp	0.04	0.00	0.07	64.74	18.15	0.00	0.00	0.00	0.00	0.00	15.45	0.08	0.94	0.00	0.00	99.80
STF-26A area1 ksp	0.03	0.03	0.06	65.33	18.27	0.00	0.00	0.00	0.00	0.00	14.84	0.03	1.26	0.00	0.00	100.22
STF-26A area1 ksp	0.05	0.05	0.02	65.17	18.31	0.02	0.00	0.00	0.00	0.00	14.71	0.10	1.35	0.00	0.04	100.22
STF-26A area1 ksp	0.04	0.00	0.04	65.73	18.44	0.00	0.00	0.00	0.00	0.00	13.93	0.05	2.03	0.00	0.00	100.61
STF-26A area1 cd	0.00	5.95	0.00	48.53	31.69	11.73	0.27	0.00	0.00	0.00	0.00	0.00	0.11	0.00	0.00	98.28
STF-26A area1 cd	0.00	5.94	0.00	48.24	31.99	12.31	0.28	0.00	0.00	0.00	0.00	0.00	0.09	0.00	0.00	98.85
STF-26A area1 cd	0.00	6.01	0.00	48.41	31.62	11.88	0.29	0.00	0.00	0.00	0.00	0.00	0.12	0.00	0.00	98.33
STF-26A area1 cd	0.00	6.05	0.00	48.70	32.03	12.16	0.30	0.00	0.01	0.00	0.00	0.00	0.07	0.00	0.00	99.33
STF-26A area1 cd	0.01	5.92	0.01	47.93	31.49	11.95	0.25	0.00	0.00	0.00	0.00	0.00	0.08	0.00	0.01	97.65
STF-26A area2 gt	0.60	2.91	0.00	37.41	21.01	37.34	1.29	0.00	0.00	0.00	0.00	0.01	0.03	0.03	0.00	100.66
STF-26A area2 gt	0.54	2.70	0.03	36.30	22.13	36.99	1.27	0.01	0.00	0.00	0.00	0.00	0.03	0.05	0.00	100.09
STF-26A area2 gt	0.49	2.74	0.00	36.26	22.61	37.41	1.20	0.00	0.00	0.00	0.00	0.00	0.00	0.06	0.01	100.79
STF-26A area2 gt	0.57	2.83	0.00	37.47	21.16	37.29	1.29	0.02	0.01	0.00	0.00	0.00	0.01	0.00	0.00	100.66
STF-26A area2 gt	0.64	2.51	0.00	37.14	20.89	37.74	1.30	0.00	0.00	0.00	0.01	0.04	0.02	0.00	0.01	100.29
STF-26A area2 ox	0.05	0.07	51.51	0.23	0.23	44.84	0.42	0.03	0.01	0.01	0.02	0.00	0.00	0.00	0.00	98.47
STF-26A area2 ox	0.04	0.08	52.01	0.07	0.09	46.30	0.41	0.00	0.02	0.00	0.02	0.00	0.02	0.10	0.00	100.25
STF-26A area2 ox	0.05	0.12	52.63	0.03	0.05	45.48	0.35	0.02	0.00	0.05	0.02	0.01	0.00	0.05	0.00	99.89
STF-26A area2 ox	0.03	0.10	51.98	0.05	0.00	45.53	0.35	0.03	0.00	0.00	0.01	0.00	0.00	0.05	0.02	99.29
STF-26A area2 ox	0.04	0.07	51.78	0.03	0.02	46.04	0.33	0.02	0.00	0.00	0.01	0.00	0.00	0.04	0.01	99.56
STF-26A area2 bi	0.03	9.93	1.71	35.14	19.98	20.53	0.02	0.00	0.00	0.86	9.19	0.00	0.08	0.00	0.00	97.19
STF-26A area2 bi	0.08	9.27	2.61	33.93	19.35	20.40	0.04	0.00	0.00	0.85	8.80	0.00	0.15	0.00	0.00	95.24
STF-26A area2 bi	0.05	9.49	2.14	34.60	19.15	19.93	0.03	0.00	0.00	0.92	9.41	0.00	0.12	0.01	0.03	95.54
STF-26A area2 bi	0.03	9.53	2.18	34.70	18.96	19.81	0.05	0.00	0.01	1.02	9.58	0.00	0.09	0.02	0.02	95.64
STF-26A area2 bi	0.03	9.79	1.86	34.93	19.59	19.88	0.02	0.00	0.00	1.00	9.24	0.00	0.08	0.00	0.00	96.10
STF-26A area2 spinel	0.01	1.91	0.03	0.02	59.67	36.53	0.14	0.05	0.00	0.00	0.00	0.00	0.00	1.87	0.00	100.30

STF-26A area2 spinel	0.01	1.88	0.04	0.03	59.96	37.59	0.18	0.02	0.01	0.00	0.00	0.00	0.00	1.82	0.00	101.64
STF-26A area2 spinel	0.01	1.97	0.00	0.07	60.38	36.84	0.19	0.05	0.00	0.00	0.00	0.01	0.01	1.90	0.03	101.57
STF-26A area2 spinel	0.02	1.95	0.01	0.52	58.99	36.60	0.18	0.03	0.00	0.00	0.00	0.00	0.03	1.76	0.01	100.18
STF-26A area2 spinel	0.03	1.91	0.02	0.05	60.42	36.91	0.15	0.02	0.00	0.00	0.00	0.00	0.00	1.83	0.00	101.40
STF-26A area2 cd	0.01	6.36	0.01	48.02	33.83	11.37	0.22	0.00	0.00	0.00	0.00	0.00	0.06	0.00	0.00	99.87
STF-26A area2 cd	0.00	6.39	0.01	47.46	33.57	11.46	0.23	0.00	0.00	0.00	0.00	0.00	0.09	0.00	0.00	99.20
STF-26A area2 cd	0.01	6.41	0.02	47.92	33.59	11.42	0.26	0.00	0.00	0.00	0.00	0.00	0.08	0.00	0.02	99.74
STF-26A area2 cd	0.02	6.32	0.01	47.94	33.65	11.19	0.22	0.00	0.00	0.00	0.00	0.00	0.10	0.00	0.03	99.49
STF-26A area2 cd	0.01	6.62	0.02	47.82	33.82	11.60	0.22	0.00	0.01	0.00	0.00	0.00	0.10	0.00	0.00	100.22
STF-26A area2 ksp	0.02	0.00	0.02	65.06	19.22	0.00	0.01	0.00	0.00	0.00	14.33	0.07	1.73	0.00	0.00	100.83
STF-26A area2 ksp	0.03	0.00	0.00	64.76	19.33	0.00	0.00	0.00	0.00	0.00	14.90	0.05	1.32	0.00	0.00	100.72
STF-26A area2 ksp	0.01	0.00	0.01	64.71	18.95	0.00	0.00	0.00	0.00	0.00	15.25	0.08	0.97	0.00	0.00	100.32
STF-26A area2 ksp	0.01	0.00	0.02	64.72	19.30	0.00	0.02	0.00	0.00	0.00	14.04	0.09	2.02	0.00	0.01	100.70
STF-26A area2 ksp	0.02	0.00	0.01	64.38	19.23	0.00	0.00	0.00	0.00	0.00	14.73	0.11	1.41	0.00	0.00	100.26
ST16-03C bi	0.10	7.60	2.79	34.62	19.96	21.39	0.24	0.05	0.21	0.24	9.28	0.01	0.15	0.05	0.00	96.71
ST16-03C bi	0.07	7.43	2.73	34.35	19.88	21.14	0.24	0.04	0.18	0.26	9.29	0.01	0.16	0.03	0.00	95.82
ST16-03C bi	0.09	7.40	2.88	34.29	19.60	21.30	0.24	0.07	0.19	0.17	9.22	0.00	0.17	0.02	0.04	95.74
ST16-03C bi	0.08	7.55	2.66	34.59	19.82	20.74	0.23	0.05	0.18	0.25	9.17	0.02	0.19	0.00	0.00	95.57
ST16-03C bi	0.01	7.52	2.62	34.34	19.95	20.61	0.19	0.06	0.21	0.24	9.47	0.01	0.10	0.00	0.02	95.40
ST16-03C and	0.00	0.02	0.01	35.85	65.49	0.20	0.01	0.00	0.00	0.00	0.00	0.00	0.00	0.00	0.01	101.60
ST16-03C and	0.01	0.03	0.03	35.93	66.01	0.23	0.00	0.00	0.00	0.00	0.00	0.00	0.00	0.00	0.00	102.24
ST16-03C and	0.05	0.04	0.03	35.10	63.72	0.24	0.02	0.00	0.00	0.01	0.00	0.00	0.02	0.00	0.00	99.23
ST16-03C and	0.00	0.03	0.01	35.55	65.35	0.26	0.00	0.00	0.00	0.00	0.00	0.00	0.01	0.00	0.00	101.21
ST16-03C and	0.02	0.02	0.02	36.06	65.38	0.25	0.00	0.00	0.00	0.00	0.00	0.00	0.00	0.00	0.00	101.77
ST16-03C ox	0.06	0.08	52.77	0.04	0.02	42.49	2.79	0.01	0.00	0.04	0.02	0.02	0.01	0.03	0.00	99.45
ST16-03C ox	0.05	0.10	52.65	0.04	0.03	42.24	2.89	0.01	0.01	0.00	0.06	0.02	0.03	0.03	0.01	99.28
ST16-03C ox	0.07	0.08	52.59	0.05	0.04	42.11	2.74	0.00	0.00	0.00	0.04	0.00	0.00	0.09	0.01	98.97
ST16-03C ox	0.17	0.10	52.52	0.06	0.02	42.87	2.83	0.01	0.00	0.00	0.03	0.00	0.00	0.06	0.00	99.77

ST16-03C ox	0.05	0.10	52.43	0.03	0.04	41.61	2.86	0.00	0.01	0.00	0.03	0.00	0.00	0.08	0.00	98.39
ST16-03C plag	4.64	0.00	0.01	62.01	24.27	0.06	0.00	0.00	0.00	0.00	0.11	0.03	8.99	0.00	0.00	100.13
ST16-03C plag	4.65	0.00	0.04	62.00	24.58	0.17	0.00	0.00	0.00	0.00	0.10	0.06	9.16	0.00	0.00	100.77
ST16-03C plag	4.55	0.00	0.01	61.14	24.07	0.08	0.01	0.00	0.00	0.00	0.11	0.10	9.38	0.00	0.00	99.45
ST16-03C plag	4.59	0.00	0.02	61.76	24.53	0.14	0.01	0.00	0.00	0.00	0.08	0.09	9.32	0.00	0.03	100.57
ST16-03C plag	4.74	0.01	0.04	61.85	24.29	0.06	0.00	0.00	0.00	0.00	0.11	0.06	9.18	0.00	0.00	100.34
ST16-03C ksp	0.00	0.00	0.00	63.95	19.27	0.00	0.00	0.00	0.00	0.00	15.38	0.12	0.89	0.00	0.00	100.06
ST16-03C ksp	0.02	0.00	0.04	64.75	19.39	0.01	0.00	0.00	0.00	0.00	14.60	0.06	1.49	0.00	0.00	100.82
ST16-03C ksp	0.02	0.01	0.05	64.32	19.57	0.00	0.00	0.00	0.00	0.00	14.60	0.08	1.47	0.00	0.00	100.60
ST16-03C ksp	0.02	0.01	0.00	64.14	19.65	0.00	0.00	0.00	0.00	0.00	13.77	0.04	2.06	0.00	0.03	100.26
ST16-03C ksp	0.03	0.01	0.02	64.25	19.31	0.00	0.00	0.00	0.00	0.00	13.53	0.07	2.36	0.00	0.01	100.09
ST16-03C musc	0.03	0.45	0.08	45.01	38.10	0.90	0.00	0.00	0.00	0.03	10.34	0.00	0.41	0.00	0.00	95.39
ST16-03C musc	0.01	0.45	0.08	45.70	38.49	0.89	0.00	0.00	0.00	0.00	10.48	0.00	0.40	0.00	0.02	96.52
ST16-03C musc	0.06	0.54	0.54	46.07	38.26	0.91	0.01	0.00	0.00	0.00	10.03	0.01	0.39	0.00	0.00	96.93
ST16-03C musc	0.02	0.39	0.24	45.91	38.87	0.69	0.01	0.00	0.00	0.00	10.47	0.00	0.41	0.00	0.00	97.03
ST16-03C musc	0.02	0.47	0.12	45.33	38.30	0.87	0.02	0.00	0.00	0.00	10.48	0.00	0.40	0.00	0.03	96.14
STF-02B bi	0.05	7.98	2.21	34.40	20.23	20.00	0.16	0.02	0.01	0.28	9.42	0.00	0.20	0.02	0.00	94.94
STF-02B bi	0.03	8.02	2.18	34.90	20.75	20.86	0.18	0.01	0.01	0.24	9.50	0.00	0.23	0.01	0.04	96.94
STF-02B bi	0.11	7.66	2.19	33.45	20.03	20.09	0.16	0.02	0.01	0.27	9.48	0.00	0.17	0.04	0.04	93.67
STF-02B bi	0.06	7.55	2.20	34.07	19.93	20.02	0.16	0.01	0.00	0.27	9.40	0.02	0.20	0.01	0.01	93.84
STF-02B bi	0.04	7.76	2.18	34.52	20.68	19.95	0.14	0.00	0.01	0.28	9.47	0.00	0.22	0.00	0.04	95.27
STF-02B ksp	0.02	0.00	0.00	64.16	19.11	0.07	0.00	0.00	0.01	0.00	14.87	0.06	1.21	0.00	0.01	99.83
STF-02B ksp	0.03	0.00	0.00	64.29	19.11	0.00	0.00	0.00	0.00	0.00	15.03	0.06	1.13	0.00	0.04	100.01
STF-02B ksp	0.03	0.00	0.00	63.47	19.07	0.04	0.01	0.00	0.00	0.00	14.36	0.08	1.66	0.00	0.02	99.08
STF-02B ksp	0.03	0.00	0.00	64.20	19.16	0.02	0.02	0.00	0.00	0.00	14.71	0.06	1.55	0.00	0.00	100.08
STF-02B ksp	0.03	0.00	0.01	63.82	19.09	0.00	0.00	0.00	0.00	0.00	15.28	0.05	0.93	0.00	0.00	99.55
STF-02B and	0.01	0.02	0.03	36.42	65.81	0.17	0.00	0.00	0.00	0.00	0.00	0.01	0.02	0.00	0.01	102.49
STF-02B and	0.31	0.04	0.04	43.16	42.92	0.35	0.00	0.00	0.06	0.00	0.14	0.00	0.07	0.00	0.00	87.09

STF-02B and	0.01	0.02	0.03	35.60	64.74	0.19	0.00	0.00	0.00	0.00	0.00	0.00	0.00	0.00	0.00	100.59
STF-02B and	0.03	0.03	0.00	35.65	65.21	0.19	0.01	0.00	0.00	0.00	0.00	0.00	0.02	0.00	0.00	101.13
STF-02B and	0.05	0.01	0.02	36.05	65.59	0.15	0.00	0.00	0.00	0.00	0.00	0.01	0.01	0.00	0.00	101.89
STF-02B musc	0.29	0.50	0.23	40.06	33.45	1.05	0.00	0.00	0.06	0.09	9.32	0.02	0.41	0.00	0.05	85.48
STF-02B musc	0.08	0.48	0.26	42.82	35.76	1.02	0.00	0.00	0.01	0.02	9.81	0.01	0.43	0.00	0.00	90.75
STF-02B musc	0.09	0.45	0.30	43.20	36.36	1.20	0.01	0.00	0.01	0.00	9.19	0.00	0.37	0.00	0.02	91.24
STF-02B musc	0.09	0.41	0.15	42.94	36.27	1.13	0.00	0.00	0.00	0.00	9.60	0.00	0.44	0.00	0.02	91.08
STF-02B musc	0.08	0.51	0.20	46.17	37.83	1.06	0.01	0.00	0.03	0.06	7.55	0.00	0.37	0.00	0.00	93.89
STF-02B ox	0.22	0.10	57.10	1.97	1.90	25.09	0.61	0.01	0.06	0.69	0.07	0.27	0.26	0.43	0.15	89.88
STF-02B ox	0.26	0.11	51.65	1.53	2.54	33.05	1.50	0.00	0.02	0.58	0.04	0.02	0.13	1.06	0.00	93.41
STF-02B ox	0.29	0.09	54.39	1.79	2.23	27.66	0.96	0.05	0.07	0.66	0.06	0.29	0.18	0.49	0.06	90.19
STF-02B ox	0.27	0.07	58.70	1.59	2.07	24.21	0.26	0.03	0.04	0.32	0.04	0.32	0.16	0.17	0.11	89.56
STF-02B ox	0.13	0.06	55.64	0.87	0.95	30.74	1.42	0.04	0.03	0.25	0.05	0.16	0.13	0.70	0.09	92.39
STF-16A ox	0.07	0.06	56.52	2.47	2.07	33.67	1.34	0.01	0.00	0.03	0.06	0.03	0.02	0.16	0.00	97.62
STF-16A ox	0.10	0.09	52.54	0.29	0.19	43.05	1.44	0.00	0.00	0.00	0.07	0.03	0.03	0.17	0.04	99.12
STF-16A ox	0.05	0.08	52.60	0.03	0.02	42.84	1.52	0.02	0.00	0.00	0.07	0.01	0.00	0.28	0.00	98.61
STF-16A ox	0.04	0.10	52.88	0.01	0.04	42.93	1.60	0.00	0.01	0.00	0.04	0.01	0.00	0.22	0.00	99.05
STF-16A ox	0.06	0.05	52.80	0.07	0.06	42.65	1.52	0.03	0.00	0.00	0.07	0.00	0.00	0.23	0.00	98.66
STF-16A and	0.02	0.02	0.00	76.09	26.16	0.13	0.00	0.00	0.00	0.04	0.02	0.00	0.03	0.00	0.03	102.55
STF-16A and	0.00	0.01	0.01	36.14	65.90	0.24	0.02	0.21	0.00	0.00	0.00	0.00	0.02	0.00	0.00	102.59
STF-16A and	0.07	0.04	0.03	36.16	64.87	0.30	0.00	0.30	0.00	0.00	0.00	0.00	0.02	0.00	0.00	101.88
STF-16A and	0.05	0.01	0.01	34.90	64.08	0.23	0.00	0.05	0.00	0.04	0.00	0.00	0.01	0.00	0.00	99.41
STF-16A and	0.00	0.03	0.05	35.25	64.49	0.20	0.00	0.08	0.00	0.00	0.00	0.00	0.00	0.00	0.00	100.20
STF-16A ksp	0.06	0.01	0.02	64.42	19.41	0.01	0.00	0.00	0.00	0.00	13.25	0.17	2.55	0.00	0.00	100.24
STF-16A ksp	0.03	0.00	0.02	63.44	19.19	0.00	0.00	0.00	0.00	0.00	15.15	0.17	1.06	0.00	0.01	99.37
STF-16A ksp	0.02	0.01	0.02	63.74	19.06	0.00	0.00	0.00	0.00	0.00	15.18	0.14	1.02	0.00	0.03	99.50
STF-16A ksp	0.05	0.00	0.01	64.28	19.36	0.00	0.00	0.00	0.00	0.00	15.24	0.09	0.93	0.00	0.00	100.31
STF-16A ksp	0.02	0.00	0.03	64.58	19.36	0.00	0.00	0.00	0.00	0.00	15.10	0.07	1.07	0.00	0.00	100.56

STF-16A bi	0.04	6.56	2.16	34.37	21.45	21.17	0.17	0.01	0.01	0.30	9.15	0.02	0.14	0.02	0.02	95.58
STF-16A bi	0.09	6.52	2.03	33.73	20.77	20.68	0.14	0.02	0.02	0.38	9.07	0.04	0.21	0.00	0.00	93.59
STF-16A bi	0.05	6.31	2.18	33.43	20.59	21.67	0.13	0.01	0.00	0.21	9.25	0.00	0.15	0.00	0.00	93.97
STF-16A bi	0.02	6.50	2.11	34.08	21.09	21.70	0.13	0.00	0.00	0.21	9.38	0.01	0.17	0.00	0.02	95.40
STF-16A bi	0.11	6.08	2.09	33.45	20.91	20.18	0.14	0.00	0.02	0.29	8.85	0.00	0.17	0.04	0.01	92.29